

The essential roles of Adenosine Triphosphate (ATP) and ATP-associated cellular communication in aerobic granulation

Jiang, Bo

2012

Jiang, B. (2012). The essential roles of Adenosine Triphosphate (ATP) and ATP-associated cellular communication in aerobic granulation. Doctoral thesis, Nanyang Technological University, Singapore.

<https://hdl.handle.net/10356/50938>

<https://doi.org/10.32657/10356/50938>



NANYANG
TECHNOLOGICAL
UNIVERSITY

**THE ESSENTIAL ROLES OF ADENOSINE
TRIPHOSPHATE (ATP) AND ATP-ASSOCIATED
CELLULAR COMMUNICATION IN AEROBIC
GRANULATION**

JIANG BO

SCHOOL OF CIVIL AND ENVIRONMENTAL ENGINEERING

2012

**The Essential Roles of Adenosine Triphosphate (ATP) and
ATP-Associated Cellular Communication in Aerobic
Granulation**

JIANG BO

School of Civil and Environmental Engineering

A thesis submitted to the Nanyang Technological University
in fulfillment of the requirement for the degree of Doctor of Philosophy

2012

ABSTRACT

Aerobic granulation is a process to form dense and spherical aggregates through cell-to-cell self-immobilization without addition of biocarriers. Recently, intensive research efforts have been dedicated to the development of aerobic granules and their applications for wastewater treatment. However, the microbiological origin of this phenomenon is still largely unknown and very little information is currently available regarding the mechanisms of aerobic granulation at levels of energy metabolism and cellular communication. This study, therefore, attempts to address a basic question: Are adenosine triphosphate (ATP) and cellular communication required in the formation and maintenance of aerobic granules?

In the first phase of this study, the possible roles of ATP and cellular communication in the formation of aerobic granules were investigated. For this purpose, three sequencing batch reactors (SBRs) inoculated with synthetic wastewater-acclimated activated sludge were operated in the absence and presence of a chemical uncoupler, 3,3',4',5-tetrachlorosalicylanilide (TCS), which has the ability to dissipate the Proton Motive Force (PMF) and subsequently inhibit ATP synthesis. Results showed that aerobic granules were successfully cultivated in the control reactor free of TCS, while aerobic granulation was completely inhibited with the addition of 2 and 4 mg L⁻¹ TCS. It was found that cellular ATP content in the control reactor increased along granulation process, meanwhile, the increase in the production of signaling molecules, i.e., autoinducer-2 (AI-2) and *N*-acylhomoserine lactones (AHLs), as well as, extracellular polymeric substances (EPS) was also observed. However, in the presence of TCS, the production of AI-2, AHLs and EPS was significantly inhibited due to the suppressed ATP synthesis,

which ultimately resulted in the failure of aerobic granulation. It was, therefore, demonstrated that ATP and cellular communication played important roles in the development of aerobic granules.

In the second phase of this study, two SBRs seeded with mature aerobic granules were run in the absence and presence of chemical uncoupler TCS to look into the possible involvement of ATP and cellular communication in maintaining the structure stability and integrity of aerobic granules. In the control reactor free of TCS, results revealed that cellular ATP, AI-2, AHLs and EPS contents kept nearly constant and the aerobic granules remained stable during the whole operation period. On the contrary, ATP synthesis was dramatically inhibited with the supplement of 2 mg L⁻¹ TCS, which subsequently caused the decrease in AI-2, AHLs and EPS production, and eventually led to the disintegration of aerobic granules. Consequently, it appears that ATP and cellular communication were essential for the maintenance of structure stability and integrity of aerobic granules.

Finally, in the third phase of this study, the relationship between microbial structure in term of biomass density and energy metabolism of aerobic granules was investigated. For this purpose, a series of batch respiratory experiments were carried out using biomasses prepared from mature aerobic granules with different densities, and carbon flows to anabolism and catabolism were measured after 2-h reaction. It was found that aerobic granules had the highest observed CO₂ production yield and the lowest observed growth yield as compared to biomasses with lower densities. In order to maintain their compact three-dimensional structure, aerobic granules would have to produce more AI-2, AHLs and EPS, but at the cost of consuming more non-growth-associated energy, thus, more carbon

was diverted into catabolism for energy production rather than channeled into anabolism for growth, which was responsible for the enhanced CO₂ production yield and lowered growth yield as observed in aerobic granules. These results suggest that energy metabolism of microbial community was structure-related.

ACKNOWLEDGMENTS

Foremost, I would like to express my deep and sincere gratitude to my supervisor, Dr. Liu Yu, whose patience, understanding, as well as, immense academic knowledge and skills, have been invaluable to me. Dr. Liu's steadfast support and continuous encouragement greatly inspired me, especially during those difficult and painful times full of frustration and depression. During the preparation of this thesis, Dr. Liu spent a tremendous amount of time reading through each draft and offered me a great many of illuminating and instructive suggestions. Without his professional guidance and prudent supervision, I would never be able to finish this thesis.

I am deeply grateful to all the technical staff in the Environmental Laboratory for their professional assistance. Without their kind help, my research work would be impossible. My appreciation also goes to School of Civil and Environmental Engineering, Nanyang Technological University for providing me with the research scholarship.

I want to express my special thanks to those faithful friends, for the kind help they have ever offered me and the memorable days we have spent together.

Finally, I am indebted to my parents for their constant emotional support. I acknowledge my husband Dr. Liu Nan, who has been, always, my anchor, my joy and my guiding light. It is your love and care that encourage me to overcome all kinds of difficulties and complete this "marathon journey" towards the PhD degree.

TABLE OF CONTENTS

ABSTRACT.....	I
ACKNOWLEDGMENTS	IV
TABLE OF CONTENTS	V
LIST OF ABBREVIATIONS	IX
LIST OF FIGURES	XII
LIST OF TABLES.....	XVIII
PUBLICATIONS	XIX
CHAPTER 1 INTRODUCTION.....	1
1.1 BACKGROUND	1
1.2 OBJECTIVES AND SCOPE OF THIS STUDY	2
1.3 ORGANIZATION OF THE THESIS	3
CHAPTER 2 LITERATURE REVIEW	4
2.1 INTRODUCTION	4
2.2 DEVELOPMENT OF AEROBIC GRANULES UNDER VARIOUS CONDITIONS	5
2.3 MECHANISMS OF AEROBIC GRANULATION.....	12
2.3.1 A General Model for Aerobic Granulation.....	13
2.3.2 Selection Pressure-Driven Aerobic Granulation.....	18
2.3.3 Energy Metabolism in Aerobic Granulation	22
2.4 APPLICATIONS OF AEROBIC GRANULATION.....	23

2.4.1 Treatment of Organics and Nutrients	23
2.4.2 Treatment of Phenolic Compounds.....	27
2.4.3 Treatment of Other Toxic Organic Compounds.....	29
2.4.4 Treatment of Heavy Metals.....	31
2.4.5 Treatment of Dyestuffs.....	33
2.5 SUMMARY	34
CHAPTER 3 DEPENDENCE OF AEROBIC GRANULATION ON ATP AND CELLULAR COMMUNICATION.....	35
3.1 INTRODUCTION	35
3.2 MATERIALS AND METHODS	37
3.2.1 Experimental Setup and Operation	37
3.2.2 Determination of EPS	38
3.2.3 Determination of Cellular ATP	39
3.2.4 Determination of AI-2 by Bioluminescence Assay.....	40
3.2.5 Determination of AHLs by Bioluminescence Assay	41
3.2.6 β -galactosidase Bioassay of AHLs.....	42
3.2.7 Identification of AHLs by TLC Analysis.....	43
3.2.8 SEM Observation.....	44
3.2.9 Biofilm Formation Assay in 96-well Plates	45
3.2.10 Other Methods	46
3.3 RESULTS.....	46
3.3.1 Effect of TCS on Biomass Density and Morphology	46

3.3.2 Effect of TCS on Substrate Removal	50
3.3.3 Effect of TCS on EPS Content.....	51
3.3.4 Effect of TCS on Cellular ATP Content	53
3.3.5 Effect of TCS on Relative AI-2 Content	54
3.3.6 Effect of TCS on Relative AHL Content	55
3.3.7 Effect of TCS on Biofilm Formation	58
3.4 DISCUSSION	59
3.5 SUMMARY	68
CHAPTER 4 DEPENDENCE OF STRUCTURE STABILITY AND INTEGRITY OF AEROBIC GRANULES ON ATP AND CELLULAR COMMUNICATION	70
4.1 INTRODUCTION	70
4.2 MATERIALS AND METHODS	71
4.2.1 Experimental Setup and Operation	71
4.2.2 EPS Staining and Imaging	71
4.2.3 HPSEC Analysis of EPS	72
4.2.4 Biofilm Detachment Assay in 96-well Plates	73
4.2.5 Other Methods	74
4.3 RESULTS.....	74
4.3.1 Effect of TCS on Substrate Removal.....	74
4.3.2 Effect of TCS on Granule Morphology and Structure	75
4.3.3 Effect of TCS on EPS	79

4.3.4 Effect of TCS on Cellular ATP Content	82
4.3.5 Effect of TCS on Relative AI-2 and AHL Contents	84
4.3.6 Effect of TCS on Biofilm Stability	87
4.4 DISCUSSION	88
4.5 SUMMARY	94
CHAPTER 5 ANALYSIS OF CARBON FLOWS IN AEROBIC GRANULES	95
5.1 INTRODUCTION	95
5.2 MATERIALS AND METHODS	96
5.3 RESULTS	99
5.3.1 Elemental Composition of Aerobic Granules	99
5.3.2 Biomass Density and Substrate Removal	100
5.3.3 EPS Production and Distribution	101
5.3.4 Production of AI-2 and AHLs	104
5.3.5 Carbon Flows	106
5.4 DISCUSSION	109
5.5 SUMMARY	117
CHAPTER 6 CONCLUSIONS AND RECOMMENDATIONS.....	118
6.1 CONCLUSIONS.....	118
6.2 RECOMMENDATIONS	120
REFERENCES.....	122

LIST OF ABBREVIATIONS

AB medium	Autoinducer bioassay medium
AHLs	<i>N</i> -acylhomoserine lactones
AI-2	Autoinducer-2
ANOVA	Analysis of variance
APHA	American Public Health Association
ATCC	American Type Culture Collection
ATP	Adenosine triphosphate
BHL	<i>N</i> -butyryl-L-homoserine lactone
CCCP	Carbonyl cyanide <i>m</i> -chlorophenyl hydrazone
CFB	Cytophaga-Flavobacteria-Bacteroides
CIA	Chloroaniline
CLSM	Confocal Laser Scanning Microscopy
COD	Chemical oxygen demand
Con A	Concanavalin A tetramethylrhodamine conjugate
DCP	Dichlorophenol
DMP	Dimethyl phthalate
DNP	2,4-Dinitrophenol
DO	Dissolved oxygen
DOC	Dissolved organic carbon
DPD	4,5-Dihydroxy-2,3-pentanedione
EPA	Environmental Protection Agency
EPS	Extracellular polymeric substances
FITC	Fluorescein isothiocyanate
GAO	Glycogen Accumulating Organism

HHL	<i>N</i> -hexanoyl-L-homoserine lactone
HPLC	High Performance Liquid Chromatography
HPSEC	High Performance Size Exclusion Chromatography
HRT	Hydraulic retention time
ICP	Inductively Coupled Plasma
MB	Methylene blue
MBR	Membrane bioreactor
MG	Malachite green
MLSS	Mixed liquor suspended solids
MLVSS	Mixed liquor volatile suspended solids
MTBE	Methyl <i>tert</i> -butyl ether
NTA	Nitrilotriacetic acid
OD	Optical Density
OHL	<i>N</i> -octanoyl-L-homoserine lactone
OLR	Organic loading rate
OP	Octylphenol
PA	Phthalic acid
PAE	Phthalic acid ester
PAO	Phosphate Accumulating Organism
PBS	Phosphate-buffered saline
PMF	Proton Motive Force
PN	Extracellular proteins
PNP	<i>p</i> -nitrophenol
PS	Extracellular polysaccharides
RND	Resistance-nodulation-division
SABR	Sequencing airlift bioreactor
SBR	Sequencing batch reactor

SDS	Sodium dodecyl sulfate
SEM	Scanning Electron Microscopy
SOUR	Specific oxygen utilization (or uptake) rate
SVI	Sludge volume index
TAE	Tris-Acetic acid-EDTA
TBA	<i>tert</i> -butyl alcohol
TCP	2,4,6-Trichlorophenol
TCS	3,3',4',5-Tetrachlorosalicylanilide
TIC	Total inorganic carbon
TLC	Thin-layer Chromatography
TOC	Total organic carbon
UASB	Upflow anaerobic sludge blanket
X-Gal	5-Bromo-4-chloro-3-indolyl- β -D-galactopyranoside

LIST OF FIGURES

Figure 2.1	The pathways for the production of three types of quorum sensing signaling molecules in bacteria. a: Biosynthesis of oligopeptides; b: biosynthesis of AHLs; c: biosynthesis of AI-2 (Keller and Surette 2006).	16
Figure 2.2	Quorum sensing-mediated biofilm formation (Fuqua and Greenberg 2002).	16
Figure 2.3	Schematic representation of extracellular polymeric substances (EPS)-bonding aerobic granulation (Liu et al. 2004c).	17
Figure 3.1	Schematic diagram of the SBR. 1: Influent pump; 2: gas flow meter; 3: air pump; 4: effluent pump; 5: air bubble; 6: granule/floc; 7: air diffuser.	38
Figure 3.2	The coupled bioluminescent reactions of the Beta-Glo [®] assay system. 6-O- β -galactopyranosyl-luciferin is cleaved by β -galactosidase into D-luciferin which in turn serves as the substrate for luciferase to produce light in the presence of cofactors.	42
Figure 3.3	Profiles of biomass density in R1 to R3 during 30-d operation. ■: R1 free of TCS; □: R2 with 2 mg L ⁻¹ TCS; ▲: R3 with 4 mg L ⁻¹ TCS.	47
Figure 3.4	Morphologies of sludge in R1 to R3. a: Seed activated sludge; b: R1 free of TCS on day 30; c: R2 with 2 mg L ⁻¹ TCS on day 30; d: R3 with 4 mg L ⁻¹ TCS on day 14. Bar: 1 mm.	48
Figure 3.5	Size profiles of biomass with and without exposure to TCS during 40-d operation (SBRs fed with ethanol as the carbon	

	source). ●: SBR free of TCS; ○: SBR added with 1 mg L ⁻¹ TCS; ▲: SBR added with 2 mg L ⁻¹ TCS; △: SBR added with 4 mg L ⁻¹ TCS.	49
Figure 3.6	SEM images of R1- to R3-biomass. a: Seed activated sludge; b: R1 free of TCS on day 30; c: R2 with 2 mg L ⁻¹ TCS on day 30; d: R3 with 4 mg L ⁻¹ TCS on day 14. Bar: 2 μm.	50
Figure 3.7	Profiles of COD removal efficiency in R1 to R3 during 30-d operation. ■: R1 free of TCS; □: R2 with 2 mg L ⁻¹ TCS; ▲: R3 with 4 mg L ⁻¹ TCS.	51
Figure 3.8	Changes of extracellular PS content in R1- to R3-biomass during 30-d operation. ■: R1 free of TCS; □: R2 with 2 mg L ⁻¹ TCS; ▲: R3 with 4 mg L ⁻¹ TCS.	52
Figure 3.9	Changes of extracellular PN content in R1- to R3-biomass during 30-d operation. ■: R1 free of TCS; □: R2 with 2 mg L ⁻¹ TCS; ▲: R3 with 4 mg L ⁻¹ TCS.	53
Figure 3.10	Profiles of cellular ATP content in R1- to R3-biomass during 30-d operation. ■: R1 free of TCS; □: R2 with 2 mg L ⁻¹ TCS; ▲: R3 with 4 mg L ⁻¹ TCS.	54
Figure 3.11	Changes of relative AI-2 content in R1- to R3-biomass during 30-d operation. ■: R1 free of TCS; □: R2 with 2 mg L ⁻¹ TCS; ▲: R3 with 4 mg L ⁻¹ TCS.	55
Figure 3.12	Gram-stained image of biomass. Red color indicates Gram-negative bacteria. Bar: 10 μm.	56
Figure 3.13	Changes of relative AHL content in R1- to R3-biomass during 30-d operation. ■: R1 free of TCS; □: R2 with 2 mg L ⁻¹ TCS; ▲: R3 with 4 mg L ⁻¹ TCS.	57

Figure 3.14 β -galactosidase bioassay of AHLs in R1- and R2-biomass on day 30. Blue color indicates the presence of AHLs.	57
Figure 3.15 TLC analysis of AHLs. AHL sample was extracted from aerobic granules in R1, chromatographed on C18 reverse-phase thin-layer plates, developed with methanol/water (60:40, v/v) and the spots were visualized with the indicator of <i>A. tumefaciens</i> NT1 (<i>traR</i> ; <i>tra::lacZ749</i>).	58
Figure 3.16 Effect of TCS on biofilm formation in flat-bottom 96-well tissue culture polystyrene microtiter plates. Each data point is the mean value of triplicate analyses and error bars represent one standard deviation.	59
Figure 3.17 Relationship between biomass density and relative AI-2 content in R1.	63
Figure 3.18 Relationship between biomass density and relative AHL content in R1.	64
Figure 3.19 Effect of DPD and OHL on biofilm formation in flat-bottom 96-well tissue culture polystyrene microtiter plates. Each data point is the mean value of triplicate analyses and error bars represent one standard deviation.	65
Figure 3.20 Relationship between cellular ATP and relative AI-2 contents. ■: R1 free of TCS; □: R2 with 2 mg L ⁻¹ TCS; ▲: R3 with 4 mg L ⁻¹ TCS.	67
Figure 3.21 Relationship between cellular ATP and relative AHL contents. ■: R1 free of TCS; □: R2 with 2 mg L ⁻¹ TCS; ▲: R3 with 4 mg L ⁻¹ TCS.	67
Figure 4.1 Profiles of COD removal efficiency in G1 and G2 during 30-d operation. ■: G1 free of TCS; □: G2 with 2 mg L ⁻¹ TCS.	75

Figure 4.2	Profiles of biomass mean size in G1 and G2 during 30-d operation. ■: G1 free of TCS; □: G2 with 2 mg L ⁻¹ TCS.	76
Figure 4.3	Profiles of biomass density in G1 and G2 during 30-d operation. ■: G1 free of TCS; □: G2 with 2 mg L ⁻¹ TCS.	76
Figure 4.4	Sludge morphologies in G1 and G2. a: Seed aerobic granules; b: G1 free of TCS on day 30; c: G2 with 2 mg L ⁻¹ TCS on day 4; d: G2 with 2 mg L ⁻¹ TCS on day 30. Bar: 1 mm.	78
Figure 4.5	SEM images of biomass in G1 and G2 on day 30. a: G1 free of TCS; b: G2 with 2 mg L ⁻¹ TCS. Bar: 2 μm.	78
Figure 4.6	Changes of EPS content in G1- and G2-biomass during 30-d operation. ■: PS in G1; □: PS in G2; ●: PN in G1; ○: PN in G2.	79
Figure 4.7	HPSEC chromatograms of EPS extracted from biomass in G1 (line) and G2 (dash) on day 30.	80
Figure 4.8	CLSM images of stained EPS in G1 and G2 on day 30. a: Extracellular PS in G1; b: extracellular PS in G2; c: extracellular PN in G1; d: extracellular PN in G2. Orange: α-polysaccharides stained by Con A. Blue: β-polysaccharides stained by calcofluor white. Yellow: proteins stained by FITC. Bar: 200 μm.	81
Figure 4.9	Profiles of cellular ATP content in G1- and G2-biomass during 30-d operation. ■: G1 free of TCS; □: G2 with 2 mg L ⁻¹ TCS.	83
Figure 4.10	Cycle profiles of cellular ATP content in two SBRs inoculated with ethanol-fed aerobic granules. ●: SBR free of TCS; ○: SBR fed with 4 mg L ⁻¹ TCS.	84
Figure 4.11	Gram-stained image of biomass. Red color represents Gram-negative bacteria. Bar: 10 μm.	85
Figure 4.12	Changes of relative AI-2 content in G1- and G2-biomass during 30-d operation. ■: G1 free of TCS; □: G2 with 2 mg L ⁻¹ TCS.	86

Figure 4.13 Changes of relative AHL content in G1- and G2-biomass during 30-d operation. ■: G1 free of TCS; □: G2 with 2 mg L ⁻¹ TCS.	86
Figure 4.14 β-galactosidase bioassay of AHLs on day 30. a: G1 free of TCS; b: G2 with 2 mg L ⁻¹ TCS. Blue color indicates the presence of AHLs.	87
Figure 4.15 Effect of TCS on biofilm detachment from flat-bottom 96-well tissue culture polystyrene microtiter plates. Black: control wells free of TCS; grey: wells containing 2 mg L ⁻¹ TCS. Each data point is the mean value of triplicate analyses and error bars represent one standard deviation.	88
Figure 4.16 Relationship between cellular ATP and relative AI-2 contents. ■: G1 free of TCS; □: G2 with 2 mg L ⁻¹ TCS.	91
Figure 4.17 Relationship between cellular ATP and relative AHL contents. ■: G1 free of TCS; □: G2 with 2 mg L ⁻¹ TCS.	92
Figure 5.1 Schematic diagram of the respirometric system.	97
Figure 5.2 Biomass morphologies of (a) intact granules and (b) ground granules. Bar: 1 mm.	97
Figure 5.3 Respective densities of S1- to S5-biomass.	100
Figure 5.4 Profiles of TOC utilization by S1 to S5.	101
Figure 5.5 Production of extracellular PS by S1 to S5.	102
Figure 5.6 Production of extracellular PN by S1 to S5.	102
Figure 5.7 CLSM images of EPS distribution in intact and ground granules. a: Extracellular PS in intact granule; b: extracellular PS in ground granule; c: extracellular PN in intact granule; d: extracellular PN in ground granule. α-polysaccharides: orange (stained by Con A); β-polysaccharides: blue (stained by calcofluor white); proteins: yellow (stained by FITC). Bar: 200 μm.	103

Figure 5.8	Production of AI-2 by S1 to S5.	105
Figure 5.9	Production of AHLs by S1 to S5.	105
Figure 5.10	Carbon flows in the batch cultures of S1 to S5. ■: The observed growth yield (Y_{obs}); □: the observed CO_2 production yield (Y_{CO_2}).	108
Figure 5.11	Relationship between biomass density and the observed CO_2 production yield.	110
Figure 5.12	Dependence of extracellular PS production on the observed CO_2 production yield.	112
Figure 5.13	Dependence of extracellular PN production on the observed CO_2 production yield.	113
Figure 5.14	Dependence of AI-2 production on the observed CO_2 production yield.	116
Figure 5.15	Dependence of AHL production on the observed CO_2 production yield.	116

LIST OF TABLES

Table 3.1	Variations of COD concentration in one cycle in R1 to R3 (mg L^{-1}) ..	51
Table 5.1	The composition of synthetic substrate	98
Table 5.2	Elemental compositions of intact and ground granules	99
Table 5.3	Carbon flows in batch respiratory experiments	108

PUBLICATIONS

I: Journal Papers

1. **Jiang, B.** and Liu, Y. (2012) Dependence of structure stability and integrity of aerobic granules on ATP and cell communication. *Applied Microbiology and Biotechnology*. DOI: 10.1007/s00253-012-4315-6.
2. **Jiang, B.** and Liu, Y. (2012) Roles of ATP-dependent *N*-acylhomoserine lactones (AHLs) and extracellular polymeric substances (EPSs) in aerobic granulation. *Chemosphere* **88**(9): 1058-1064.
3. **Jiang, B.** and Liu, Y. (2010) Energy uncoupling inhibits aerobic granulation. *Applied Microbiology and Biotechnology* **85**(3): 589-595.

II: Book Chapters

1. **Jiang, B.,** Liu, Y. and Paul, E. (2012) Energy uncoupling for sludge minimization: Pros and cons. In: Paul, E. and Liu, Y. (Ed.), *Biological Sludge Minimization and Biomaterials/Bioenergy Recovery Technologies*. John Wiley & Sons, Inc.
2. **Jiang, B.,** Liu, Y., Chen, G. H. and Paul, E. (2009) Uncoupled energy metabolism for sludge reduction in the activated sludge process. In: Dumont, F. E. and Sacco, J. A. (Ed.), *Biochemical Engineering*. Nova Science Publisher, New York.

CHAPTER 1

INTRODUCTION

1.1 BACKGROUND

In aerobic wastewater treatment, the activated sludge process is the predominant system and has been employed extensively for municipal and industrial wastewater purification. Though this process has been modified and optimized, its limits have been reached and the solid-liquid separation efficiency still remains a point of attention. Recently, research efforts have shifted to exploiting aerobic granulation technology for wastewater bioremediation. As compared to the conventional activated sludge, aerobic granules exhibit unique advantages of regular, dense and heterogeneous structure; excellent settling properties; high biomass retention; tolerance to high loading rates and toxicity; etc. (Liu and Tay 2004; Adav et al. 2008a). Because of such characteristics, aerobic granulation appears to be a promising biotechnology for treatment of wastewater containing various contaminants, e.g., organics, nitrogen, phosphorus, xenobiotic compounds, heavy metals, dyestuffs (Jiang et al. 2002; Liu et al. 2002; Lin et al. 2003; Yang et al. 2003; Sun et al. 2008).

So far, almost all research on aerobic granulation was carried out with focus on exploring the factors that may influence aerobic granulation in sequencing batch reactors (SBRs), such as: substrate composition, organic loading rate, hydrodynamic shear forces, settling time, cycle time, volumetric exchange ratio, dissolved oxygen, temperature, etc. as reviewed in Chapter 2. In order to develop

the strategies for expediting the formation of aerobic granules and boost their industrial applications for wastewater treatment, a sound understanding of the mechanisms behind aerobic granulation is essential. At present, several mechanisms and models have been proposed to explain aerobic granulation in SBR, such as the selection pressure theory (Liu et al. 2005c; Adav et al. 2008a). However, little information is currently available in the literature with regard to the possible involvement of adenosine triphosphate (ATP) and cellular communication in aerobic granulation and sustaining the structure stability and integrity of aerobic granules. This study almost for the first time provided direct experimental evidence showing the roles of ATP and cellular communication in aerobic granulation, as well as, in maintaining the structure stability and integrity of aerobic granules, which is highly beneficial to get full understanding of the fundamentals of aerobic granulation at levels of energy metabolism and cellular communication.

1.2 OBJECTIVES AND SCOPE OF THIS STUDY

The aim of this study is to investigate fundamentals of the development of aerobic granules and the maintenance of their structure stability and integrity at levels of energy metabolism and cellular communication. The specific objectives of this study include the following aspects:

- To explore the possible roles of ATP and cellular communication in the development of aerobic granules; to investigate the effect of energy uncoupling by chemical uncoupler, 3,3',4',5-tetrachlorosalicylanilide (TCS),

on the physiological behaviors of microorganisms, i.e., quorum sensing, extracellular polymeric substances (EPS).

- To look into the possible involvement of ATP and cellular communication in maintaining the structure stability and integrity of mature aerobic granules; to examine the responses of aerobic granules to energy dissipation by chemical uncoupler TCS in terms of the production of autoinducer-2 (AI-2), *N*-acylhomoserine lactones (AHLs) and EPS, etc.
- To analyze the relationship between microbial structure (in term of biomass density) and energy metabolism of aerobic granules through understanding the carbon flows to anabolism and catabolism, as well as structure-related signaling molecules and EPS production.

1.3 ORGANIZATION OF THE THESIS

This thesis consists of six chapters. Chapter 1 is a brief introduction over the subject. Chapter 2 presents a comprehensive literature review of aerobic granulation. Chapter 3 investigates the roles of ATP and cellular communication in the formation of aerobic granules. Chapter 4 looks into the possible involvement of ATP and cellular communication in maintaining the structure stability and integrity of aerobic granules. Chapter 5 particularly focuses on the relationship between microbial structure in term of biomass density and energy metabolism of aerobic granules. The final conclusions and recommendations for future studies are presented in Chapter 6.

CHAPTER 2

LITERATURE REVIEW

2.1 INTRODUCTION

Biogranulation is a cell-to-cell self-immobilization process in which biological, physical and chemical phenomena are involved. Biogranulation can be divided into anaerobic and aerobic granulation. So far, anaerobic granules mostly form in upflow anaerobic sludge blanket (UASB) reactors for the treatment of high-strength organic wastewater. However, the anaerobic granulation technology has several drawbacks, including (i) a long start-up period; (ii) a relatively high operational temperature; (iii) strong sensitivity to the characteristics of wastewater; (iv) unsuitability for low-strength organic wastewater treatment; (v) low efficiency in the removal of nutrients (nitrogen and phosphorus) and (vi) the requirement of adequate post-treatment (Liu et al. 2004c; Adav et al. 2008a). As a novel environmental biotechnology, the aerobic granulation technology can overcome the above shortcomings and is increasingly attracting the interests of numerous researchers and engineers.

Aerobic granules are dense and round-shape microbial aggregates embedded with different bacterial species that can perform different roles in degrading complex wastewater. The formation of aerobic granules was first reported by Mishima and Nakamura (1991) in a continuous aerobic upflow sludge blanket reactor and, afterwards, was frequently observed in SBRs. To date, studies on aerobic

granulation have been conducted by research groups around the world and hundreds of papers related to aerobic granules have been published.

This chapter aims to review the major progresses and developments in aerobic granulation technology during the past two decades. The essential cultivation conditions, mechanisms and models of aerobic granulation, as well as, their potential applications for wastewater treatment are delineated. It is expected that this review can provide useful information to facilitate the understanding, engineering and optimizing of aerobic granulation.

2.2 DEVELOPMENT OF AEROBIC GRANULES UNDER VARIOUS CONDITIONS

Basically, bacteria would prefer dispersed, rather than aggregated state under normal culture conditions because of the repulsive electrostatic forces and hydration interactions among them (Liu et al. 2003d; Liu and Tay 2004). Consequently, aerobic granulation is not a spontaneous process and a number of operational and environmental conditions have to be fulfilled to achieve successful granulation. The main factors and parameters that may influence or control the development of aerobic granules are discussed in this section.

Substrate composition

A great variety of substrates have been applied for cultivation of aerobic granules, including glucose, acetate, ethanol, starch, molasses, sucrose, phenol, as well as,

real wastewater (Jiang et al. 2002; Tay et al. 2002a; Arrojo et al. 2004; Zheng et al. 2005). Moreover, inorganic carbon source has also been successfully used to develop nitrifying granules (Tay et al. 2002c). It appears that the type of substrate carbon source had insignificant effect on aerobic granulation. However, bacterial structure and species diversity of mature aerobic granules were closely related to the nature of carbon source. For example, the glucose-fed aerobic granules had a fluffy outer surface predominated by filamentous bacteria, while the acetate-fed aerobic granules exhibited a compact microbial structure predominated by rod-like species (Tay et al. 2001c). When cultivated with phenol as the carbon and energy source, aerobic granules were predominated by *Proteobacterium*, which had significant contribution to phenol degradation process (Whiteley and Bailey 2000; Jiang et al. 2004).

The positive, divalent and trivalent ions, such as Ca^{2+} , Mg^{2+} , Fe^{2+} and Fe^{3+} , have been proved to enhance aerobic granulation in SBR (Mahoney et al. 1987; Ren et al. 2008; Li et al. 2009). Jiang et al. (2003) reported that augmentation with $100 \text{ mg Ca}^{2+} \text{ L}^{-1}$ significantly decreased the granulation period from 32 d to 16 d. It was also found that the Ca^{2+} -fed aerobic granules were more compact with improved settling and strength characteristics, and had higher polysaccharide content. So far, three mechanisms of the enhancement of aerobic granulation by metal ions have been proposed: (i) metal ions combine with negatively charged moieties on bacterial surface to neutralize negative charges; (ii) metal ions form precipitates to serve as the microbial nuclei which would promote aggregation; (iii) metal ions form ionic bonds on the surface of bacteria to bridge individual cells and further accelerate granulation (Gao et al. 2011a).

Organic loading rate

It has been demonstrated that aerobic granules can form in a wide range of organic loading rates (OLR) varying from 2.5 to 15 kg COD m⁻³ d⁻¹ (Moy et al. 2002; Tay et al. 2002b; Tay et al. 2004b), indicating that OLR would not determine the development of aerobic granules. However, the characteristics of aerobic granules were closely associated with the OLR applied. Chen et al. (2008) pointed out that a relatively higher OLR led to the formation of larger and denser aerobic granules with decreased bioactivity in terms of specific oxygen utilization rate (SOUR) and specific growth rate, which would help to maintain granule stability and improve reactor operation. In a study of microbial population dynamics during aerobic granulation, Li et al. (2008) found that the reactor with the highest OLR (4.5 kg COD m⁻³ d⁻¹) had the lowest species diversity, while the reactor with the lowest OLR (1.5 kg COD m⁻³ d⁻¹) had the highest species diversity. In addition, Liu et al. (2003a) reported that the strength of aerobic granules decreased with the increase in OLR, which could be reasonably due to the raised biomass production rate at a higher OLR. Hence, OLR plays an important role in maintaining the structure stability of aerobic granules, though it is not a governing factor of aerobic granulation.

Hydrodynamic shear force

Previous studies showed that hydrodynamic shear force was an essential role in aerobic granulation in SBRs and aerobic granules with more compact structure were developed at higher hydrodynamic shear force (Tay et al. 2001b). Chen et al. (2007b) operated four SBRs at different hydrodynamic shear forces in terms of superficial upflow air velocities of 0.8, 1.6, 2.4 and 3.2 cm s⁻¹, respectively. It was

found that aerobic granules could maintain a stable structure and had the potential of long-term operation at high hydrodynamic shear forces (2.4 and 3.2 cm s⁻¹). However, aerobic granules developed at low hydrodynamic shear forces (0.8 and 1.6 cm s⁻¹) had filamentous and loose structure with irregular shape, and poor performance and operation instability were also observed. Adav et al. (2007a) explored the effect of air aeration intensities (1-3 L air min⁻¹) on aerobic granulation in three identical SBRs fed with phenol-containing wastewater. At low aeration intensity (1 L min⁻¹), sludge flocs were structurally compacted but no granules were formed. At high aeration rate (3 L min⁻¹), mature granules (1-1.5 mm) with smooth outer surface and a compact interior structure were formed. At intermediate intensity (2 L min⁻¹), large granules were found but eventually failed with overgrowth of filaments. These observations suggest that hydrodynamic shear force could impact on the structure of aerobic granules. Moreover, the metabolism of microorganisms was also found to be influenced by hydrodynamic shear force. Tay et al. (2001b) observed that the ratio of extracellular polysaccharides (PS) to extracellular proteins (PN) increased with the increase in superficial upflow air velocity, i.e., higher hydrodynamic shear force would stimulate bacteria to produce more extracellular PS, which can mediate the cohesion and adhesion of microorganisms, and plays a key role in the maintenance of the structure stability and integrity of aerobic granules. Furthermore, it was found that hydrodynamic shear force had a positive effect on cell surface hydrophobicity. As a result, the enhanced production of extracellular PS and increased cell surface hydrophobicity at higher hydrodynamic shear force would contribute to the formation and maintenance of compact and strong aerobic granules. Hydrodynamic shear force is not a leading stimulator of aerobic granulation in SBR. However, accumulated evidence has demonstrated that the structure of aerobic granules is hydrodynamic shear force-associated (Liu and Tay 2002).

Settling time

Settling time acts as a major hydraulic selection pressure controlling aerobic granulation. Qin et al. (2004a) and Qin et al. (2004b) reported that aerobic granules were successfully cultivated and became dominant only at a settling time of 5 min, while mixtures of aerobic granules and suspended sludge were observed in SBRs run at settling times of 20, 15 and 10 min. The production of extracellular PS was induced and cell surface hydrophobicity was improved significantly at short settling times, which would result in a strong interaction among microorganisms and further lead to the formation of dense and stable aerobic granules. Similarly, in study of McSwain et al. (2004), aerobic granules formed in SBR at a settling time of 2 min, while flocs co-existed with aerobic granules in the reactor with 10 min settling. At a short settling time, suspended biomass with poor settleability will be washed out, and only good settling bioparticles will be preferentially selected and retained in the reactor. By contrast, at a long settling time, sludge flocs with poor settling property cannot be withdrawn effectively, and may ultimately outcompete aerobic granules (Qin et al. 2004b; Liu et al. 2005c), as the specific growth rate and growth yield of aerobic granules are much lower than those of suspended activated sludge (Tay et al. 2004a; Yang et al. 2004a). These findings demonstrate that settling time is a decisive factor in the development of aerobic granules in SBR and short settling time could enhance aerobic granulation.

Cycle time

The SBR cycle usually consists of filling, aeration, settling and discharging. The SBR cycle time is interrelated to the hydraulic retention time (HRT) at a given volumetric exchange ratio, describing the frequency of solids discharge through

effluent withdrawal. If the SBR is run at an extremely short cycle time, microbial growth would be suppressed due to insufficient reaction time and frequent washout. Conversely, if the cycle time is set much longer than that required for substrate oxidation reactions, biomass hydrolysis would occur to cause failure in aerobic granulation eventually (Liu et al. 2005c). As a result, the SBR cycle time should be kept in a proper range that is short to inhibit biomass hydrolysis, but long enough for biomass growth and accumulation in the reactor (Liu et al. 2005c). Pan et al. (2004) studied the effect of HRT on the development of aerobic granules and found that HRT between 2 and 12 h would provide adequate hydraulic selection in the reactors, which was favorable for the formation and maintenance of stable aerobic granules with good settleability, high cell surface hydrophobicity and high ratio of extracellular PS to extracellular PN. Tay et al. (2002c) investigated the effect of cycle time on the formation of nitrifying granules in SBR. No nitrifying granulation was observed in the SBR operated at the longest cycle time of 24 h due to a very weak hydraulic selection pressure, while the washout of nitrifying sludge was found in the SBR run at the shortest cycle time of 3 h, leading to the failure in nitrifying granulation. Excellent nitrifying granules were developed in SBRs operated at respective cycle times of 6 and 12 h. A short cycle time would stimulate microbial activity and the production of extracellular PS, as well as improve the cell surface hydrophobicity. These microbial changes would favor the formation of nitrifying granules.

Volumetric exchange ratio

The volumetric exchange ratio of an SBR is defined as the discharged effluent volume at the end of the settling period divided by the total working volume of the

reactor. Wang et al. (2006b) run four SBRs at a settling time of 5 min, while at different volumetric exchange ratios in the range of 20-80%. Results showed that a rapid granulation could be achieved in SBR operated at high volumetric exchange ratios, and the fraction of aerobic granules to total biomass was found to be closely related to the volumetric exchange ratio applied to SBR, e.g., aerobic granules dominated the SBR run at higher volumetric exchange ratios of 60% and 80%, while a mixture of aerobic granules and suspended bioflocs developed at smaller volumetric exchange ratios of 20% and 40%. It was also found that the production of EPS was stimulated significantly by higher volumetric exchange ratios, which was associated with substantial accumulation of calcium that formed EPS-Ca²⁺-EPS bridges in aerobic granulation. It appears that volumetric exchange ratio of SBR plays a vital role in aerobic granulation.

Dissolved oxygen

The effect of dissolved oxygen (DO) concentration on aerobic granulation in SBR remains unclear nowadays. Aerobic granules can be successfully cultivated at DO concentrations of above 2 mg L⁻¹ (Yang et al. 2003). However, they also can form at low DO concentrations in the range of 0.7-1.0 mg L⁻¹ (Peng et al. 1999). McSwain and Irvine (2008) operated two SBRs with identical shear force, but at two different DO concentrations. It was found that aerobic granules could not form at a DO concentration of less than 5 mg L⁻¹. Generally, DO concentration is not a decisive parameter in aerobic granulation if the reactor is provided with sufficient aeration.

Temperature

Aerobic granules are usually cultivated at room temperature (20-25 °C). Song et al. (2009) developed aerobic granules in sequencing batch airlift reactors at 25, 30 and 35 °C. Results showed that 30 °C was the optimum temperature for matured granule cultivation, at which the aerobic granules had a more compact structure, better settling ability and higher bioactivity. de Kreuk et al. (2005) observed that a start-up at 20 °C and lowering the temperature to 15 °C and 8 °C, the granule stability was not affected. However, a start-up at 8 °C resulted in irregular granule structure and the outgrowth of filamentous microorganisms in aerobic granules, which caused severe biomass washout and unstable operation. Zitomer et al. (2007) developed thermophilic aerobic granules at 55 °C in SBR co-existed with flocculent particles. The average granule diameter was as high as 1.2-1.9 mm and granule resistance to disintegration was comparable to mesophilic aerobic granules. Thermophilic aerobic granulation has potential advantages when treating hot wastes from industries, such as pulp and paper production. However, considering the poor solubility of oxygen at high temperature, it would not be a suitable or cost-effective technology for municipal wastewater treatment (Gao et al. 2011a). These observations demonstrate that temperature is not a determining factor in aerobic granulation.

2.3 MECHANISMS OF AEROBIC GRANULATION

Aerobic granulation is a complicated biological phenomenon of cell assembly without carrier support, and the mechanisms of this microbial aggregation process

remain a topic of considerable discussion. This section attempts to provide a comprehensive review on the existing mechanisms and models of aerobic granulation in SBR.

2.3.1 A General Model for Aerobic Granulation

Aerobic granules form through microbial self-immobilization in the absence of biocarriers, in which physicochemical and biological interactions would make significant contributions. It has been known that aerobic granulation is a gradual multiple-step process consisting of the progression from seed sludge to compact aggregates, further to granular sludge and finally to mature granules. Based on this understanding, a general four-step model for aerobic granulation was proposed by Liu and Tay (2002):

Step 1: Physical movement to initiate bacterium-to-bacterium contact. The following forces are generally involved in this step: hydrodynamic force; diffusion force; gravity force; thermodynamic forces (e.g., Brownian movement) and cell mobility.

Existing evidence has been shown that cell mobility by means of flagella, cilia or pseudopods is important not only for initial attachment but also for translocation along the surface in the biofilm formation (Kogure et al. 1998; Lemon et al. 2007). As aerobic granulation requires direct contact between or among microorganisms, it is possible that cell mobility would also be involved in this bacterial self-aggregation process. Once the initial contact is established, cells are thought to

move on top of the surface, leading to the development of typical three-dimensional architecture of aerobic granules.

Step 2: Initial attraction to keep stable multi-cellular contacts. The attractive forces are as follows:

- physical forces: Van der Waals forces; opposite charge attraction; thermodynamic forces (e.g., free energy of surface, surface tension); hydrophobicity and linkage/bridge by filamentous bacteria.
- chemical forces: hydrogen liaison; ionic pairs; ionic triplets and inter-particulate bridge; etc.
- biochemical forces: cellular surface dehydration; cellular membrane fusion and cellular communication.

Cell surface hydrophobicity is an important affinity force in the initiation of aerobic granulation (Liu et al. 2003d; Liu et al. 2004b). It has been established that cell surface hydrophobicity is inversely correlated to the quantity of surface charge of microorganisms (Liao et al. 2001). With the increase in cell surface hydrophobicity, the negative charges on bacterial surface will decrease, thus, repulsive forces among particles will become weaker, which in turn favors the cell-to-cell approach and finally lead to the formation of aerobic granules (Liu et al. 2003d). On the other hand, according to the thermodynamic theory, increase in cell surface hydrophobicity would cause a corresponding decrease in the excess Gibbs energy of the surface, which would promote the self-aggregation of bacteria out of the hydrophilic liquid phase (Liu et al. 2004b). Tay et al. (2000) proposed the

proton translocation-dehydration theory to describe the molecular mechanism of anaerobic granulation, suggesting that the bacterial surface dehydration caused by proton translocating activity would initiate the sludge granulation. Consequently, a high cell surface hydrophobicity would result in a strong interaction among microorganisms and further serves as a driving force for aerobic granulation.

Cellular communication (also termed as “quorum sensing”) by the production, release, detection of and subsequent response to accumulated signaling molecules has been known as an effective way for microorganisms to coordinate communal behaviors (Bassler 2002). So far, three types of signaling molecules have been identified, i.e., oligopeptides and *N*-acylhomoserine lactones (AHLs) are used by Gram-positive and Gram-negative bacteria, respectively, while autoinducer-2 (AI-2) produced by both Gram-positive and Gram-negative bacteria enables interspecies communication (Figure 2.1) (Camilli and Bassler 2006; Keller and Surette 2006). Recent research has shown that cellular communication plays a prominent role in the development of biofilms and the spatial distribution of biofilm-associated bacteria (Figure 2.2) (Davies et al. 1998; Fuqua and Greenberg 2002; Hardie and Hurlier 2008; Asahi et al. 2010). Considering that aerobic granules can be regarded as a special form of biofilms with highly organized three-dimensional structure, it is reasonable to predict that quorum sensing would also be essentially involved in aerobic granulation and in the spatial organization of bacteria in the granule matrix. Up to now, research on this topic is very limited. Consequently, quorum sensing-mediated mechanism of aerobic granulation need to be further studied.

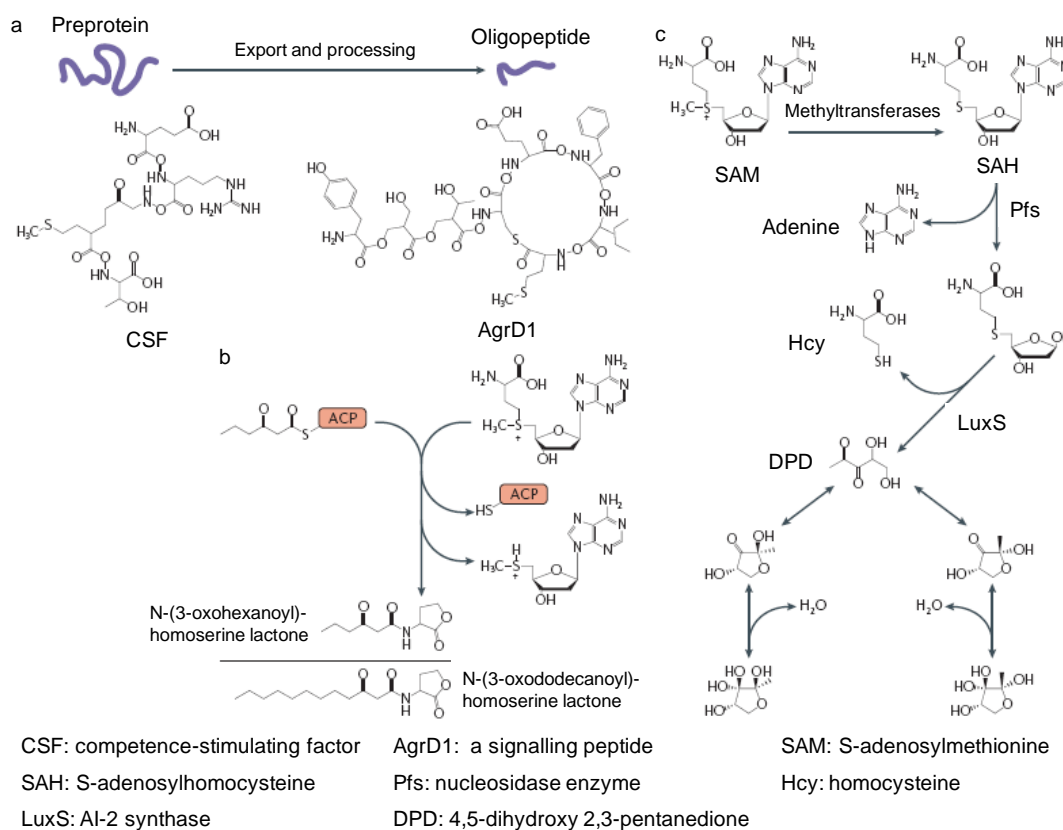


Figure 2.1 The pathways for the production of three types of quorum sensing signaling molecules in bacteria. a: Biosynthesis of oligopeptides; b: biosynthesis of AHLs; c: biosynthesis of AI-2 (Keller and Surette 2006).

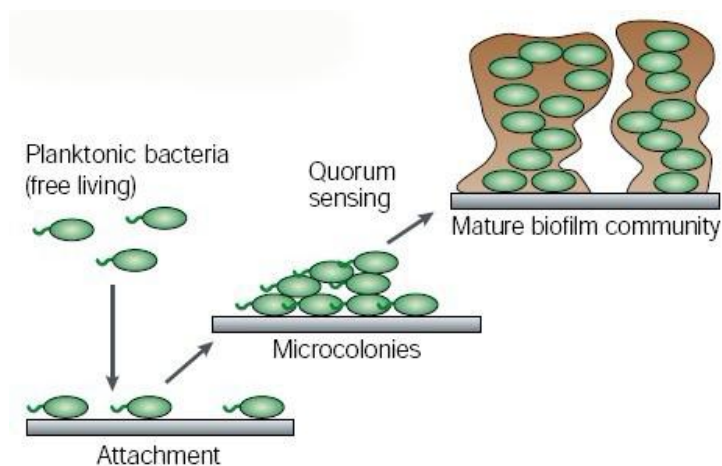


Figure 2.2 Quorum sensing-mediated biofilm formation (Fuqua and Greenberg 2002).

Step 3: Microbial forces to make cell aggregates mature by extracellular polymer production, cellular cluster growth, environment-induced metabolic changes and genetic competence.

Extracellular polymeric substances (EPS) are sticky materials mainly comprising polysaccharides, proteins, nucleic acids, humic acids and lipids (Liu et al. 2004c). EPS forms a three-dimensional and highly hydrated matrix in which bacteria and other particles are embedded and kept in close proximity, allowing for synergistic interactions (Liu et al. 2004c; Flemming and Wingender 2010). EPS is believed to be highly involved in biological adhesion and microbial aggregation processes. High EPS content has been shown to facilitate the formation and maintenance of granular structure (Tay et al. 2001a; Zhang et al. 2007), while weakened structure of aerobic granules or failed aerobic granulation due to metabolic blocking of EPS production has also been reported (Yang et al. 2004c; Jiang and Liu 2010). Restated, EPS would not only simply link individual cells together, but also serve as a protective barrier for the bacterial community, which contributes to long-term stability.

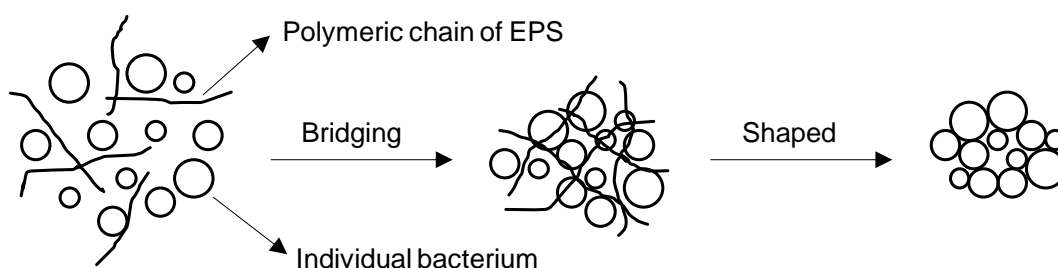


Figure 2.3 Schematic representation of extracellular polymeric substances (EPS)-bonding aerobic granulation (Liu et al. 2004c).

Step 4: Hydrodynamic shear force to stabilize the three-dimensional structure of microbial aggregates.

This four-step granulation model took into account the evolution of aerobic granules from both engineering and microbiological aspects, which provided a comprehensive understanding of the mechanisms of aerobic granulation. However, it should be noted that the phenomenon at molecular or genetic levels still requires further investigation.

2.3.2 Selection Pressure-Driven Aerobic Granulation

Different microbial species, mixed or single, such as aerobic activated sludge, nitrifying bacteria, *Acinetobacter calcoaceticus*, have been observed to form aerobic granules, which indicates that aerobic granulation might be species-independent (Liu and Tay 2002). On the other hand, as discussed above, many factors have been identified to affect the development of aerobic granules, suggesting that aerobic granulation should be governed by operational conditions. In fact, the essence of aerobic granulation can be regarded as the periodic selection of sludge bioparticles in SBR, that is, light and suspended bioflocs with poor settleability will be washed out, while only heavy aggregates with the ability to adapt to the “selection pressure” can survive and be retained in the system. This selection pressure-driven theory suggests that aerobic granulation in SBR may be an effective defensive or protective strategy of microbial community against external stresses, which is reasonable from the standpoint of biological evolution theory or survival of the fittest.

In SBR, hydrodynamic shear force generally created by aeration and described by superficial upflow air velocity has been recognized as a driving force towards successful aerobic granulation. Relatively high superficial upflow air velocity would be in favor of fast formation of aerobic granules, while absence of aerobic granulation was observed when the superficial upflow air velocity was very low (Tay et al. 2001b; Adav et al. 2007a). Tay et al. (2001b) also reported that the superficial upflow air velocity had a significant positive effect on the production of polysaccharides, SOUR, cell surface hydrophobicity and specific gravity of aerobic granules. The SBR cycle time can also exert a selection pressure on sludge bioparticles. In study of nitrifying granulation, Tay et al. (2002c) noted that nitrifying granules could only form under strong selection pressures in term of SBR cycle time, and a short cycle time would enhance microbial activity and polysaccharides production, as well as, improve cell surface hydrophobicity. These observations imply that aerobic granulation is an operational condition-induced microbial phenomenon, which is achieved by altering the surface properties and metabolic behaviors of microorganisms.

The settling time and volumetric exchange ratio are two vital selection pressures on aerobic granulation. Failures in aerobic granulation in SBR due to improper control of settling time and volumetric exchange ratio have been reported (Liu et al. 2005c). Based on the empirical Vesilind equation and the Stokes formula, Liu et al. (2005b) proposed an equation to describe the settling velocity of bioparticles shown as follows:

$$V_s = \alpha \frac{d_p^2}{SVI} e^{-\beta X} \quad (2.1)$$

where V_s is settling velocity of a bioparticle, d_p is the diameter of a bioparticle, SVI is the sludge volume index, X is biomass concentration, α and β are constant coefficients. Equation 2.1 suggests that the settling velocity of aerobic granules is determined by SVI, mean size of granules and biomass concentration of granules. If the distance for bioparticles to travel to the discharge port is L , which is proportionally correlated to the volumetric exchange ratio of SBR, the corresponding traveling time of bioparticles can be calculated as follows:

$$\text{Traveling time to the discharge port} = \frac{L}{V_s} \quad (2.2)$$

Equation 2.2 indicates that high V_s would lead to short traveling time to discharge port. Consequently, bioparticles with a traveling time shorter than the designed settling time will be retained in the SBR, otherwise, they will be withdrawn out of the reactor.

Liu et al. (2005d) further combined three major selection pressures, i.e., settling time, volumetric exchange ratio or discharge depth, and discharge time into one, the minimum settling velocity of bioparticles, and proposed a unified model to describe these three selection pressures for aerobic granulation in SBR:

$$(V_s)_{\min} = \frac{L}{t_s + \frac{(t_d - t_{d,\min})^2}{t_d}} \quad (2.3)$$

where $(V_s)_{\min}$ is the minimum settling velocity of bioparticles, L is the depth of the discharge port, t_s is the designed settling time, t_d is the preset discharge time, $t_{d,\min}$

is the minimum discharge time, at which the fraction of aerobic granules in the SBR is close to 100%. Equation 2.3 implies that proper adjustments of settling time, discharge time and the volumetric exchange ratio could enhance selection of bioparticles for rapid aerobic granulation in SBR. This model has been verified by experimental data from laboratory-scale aerobic granular sludge SBR by Liu et al. (2005c). This unified selection pressure model offers a guideline for manipulating and optimizing aerobic granulation process in SBR, as well as, provides a single engineering basis for successfully scaling up aerobic granular sludge SBR to obtain stable aerobic granulation.

Li and Li (2009) conducted numerical simulation and laboratory experiments to investigate the determining factor and the underlying mechanism in aerobic granulation in SBR. The simulation results fit in well with the experimental data obtained from SBRs using different sludge discharge methods, indicating that the selective discharge of loose and slow settling sludge flocs was a crucial controlling factor for aerobic granulation. The main mechanism of the selective sludge discharge for aerobic granulation was that loose and suspended sludge flocs must be eliminated from the reactor to avoid competing with aerobic granules for substrates uptake and utilization, i.e., the substrates feeding to aerobic granules would be enhanced. Consequently, more growth and accumulation of aerobic granules would occur in SBR, leading to complete aerobic granulation. In fact, the selective sludge discharge in their study also serves as a selection pressure.

2.3.3 Energy Metabolism in Aerobic Granulation

In aerobic oxidation process, microorganisms generate ATP by coupling electron transport and oxidative phosphorylation, during which electrons are transferred from an electron donor (substrate) to a final electron acceptor (oxygen) (Mitchell 1961; Wolfe 1993). It has been reported that aerobic granules have a lower growth yield and a higher carbon dioxide production yield than activated sludge, i.e., more dissolved organic carbon would be converted into carbon dioxide for energy production rather than for biosynthesis, which implies that the energy metabolism of aerobic granules is dissociated to some extent (Liu et al. 2005a). Moreover, selection pressure-induced energy spilling has also been observed in aerobic granules. Under a stronger shear force or a shorter settling time, more energy produced from substrate oxidation would be applied to non-growth-associated activities, such as the production of polysaccharides and the improvement of cell surface hydrophobicity, which may help maintain a balance with the external forces and favor the structure stability of aerobic granules (Qin et al. 2004b). It has been suggested that energy spilling is probably a mechanism for protecting bacteria from stressful environmental conditions and potentially toxic schemes of substrate metabolism (Russell and Cook 1995). In addition, Liu and Tay (2001) hypothesized that energy spilling might be associated with a stimulated proton translocation across the cellular membrane, which would favor the formation of a stronger granule structure. Although energy metabolism in aerobic granulation has been described, it is not yet completely understood and may not provide a comprehensive picture for this process. Thus, the effect of energy metabolism on aerobic granulation need to be further studied.

2.4 APPLICATIONS OF AEROBIC GRANULATION

Aerobic granulation is desirable in biological treatment processes because of many advantages, e.g., excellent settleability, high and stable contaminant transformation rate, high tolerance to toxicity, efficient biomass separation. This section attempts to review the main applications of aerobic granulation technology in the treatment of organics, nutrients (nitrogen and phosphorus), toxic organic compounds, heavy metals and dyestuffs.

2.4.1 Treatment of Organics and Nutrients

Aerobic granules are densely packed microbial aggregates with good settling capability, thus leading to high biomass retention in the reactor. Due to such unique attributes, aerobic granules have been developed for treating high-strength organic wastewater. The first attempt was started by Moy et al. (2002), who investigated the ability of aerobic granules to sustain high OLR by a step-up increase in organic loading from 6 to 15 kg COD m⁻³ d⁻¹. Increases in OLR were implemented after the reactor had reached steady state, i.e., COD removal efficiencies stabilized at values greater than 89% for at least two weeks. The aerobic granules could sustain the maximum OLR of 15 kg COD m⁻³ d⁻¹ with COD removal rate more than 92%. Schwarzenbeck et al. (2005) cultivated aerobic granules using wastewater from an industrial dairy plant with a total COD of 2,800 mg L⁻¹ and a soluble COD of 1,500 mg L⁻¹. After complete granulation and the separation of biomass from the effluent, COD removal efficiency of 90% was achieved at a volumetric exchange ratio of 50% and a cycle duration of 8 h. Aerobic granules were also developed in SBR fed with brewery wastewater by Wang et al. (2007b). High and stable COD

removal efficiency of 88.7% was obtained after granulation at a volumetric exchange ratio of 50% and a cycle time of 6 h. Moreover, Schwarzenbeck et al. (2004) developed aerobic granules in SBR treating wastewater from malting process which had a high content of particulate organic matter (0.9 g TSS L⁻¹). It was found that particles with a diameter lower than 25-50 µm could be removed at the efficiency of 80%, whereas particles bigger than 50 µm were only removed at the efficiency of 40%. The authors proposed two different mechanisms for particulate organic matter removal, i.e., during initial granule formation and growth, particles were incorporated into the biofilm matrix of the granules; for mature granules, particulate organic matter was removed due to the metabolic activity of protozoa population covering the surface of the granules.

Nitrification and denitrification are two interrelated processes to completely remove nitrogen in the wastewater. In nitrification, ammonium converts into nitrite and nitrate, and they are subsequently reduced to gaseous nitrogen by denitrifiers. Yang et al. (2003, 2004b, 2005) noted the simultaneous removal of organics and nitrogen by aerobic granules due to the coexistence of heterotrophic, nitrifying and denitrifying populations. The nitrifying and denitrifying activities were significantly enhanced with the increase in the substrate N/COD ratio, while the heterotrophic activity tended to decrease. It was also demonstrated that DO concentration played an important role in nitrification and denitrification processes. Low DO concentration would result in a low nitrification rate and a high denitrification rate. Meanwhile, results indicated that a certain mixing power was required to ensure sufficient mass transfer between the liquid and the granules. Jang et al. (2003) also observed alternate nitrification and denitrification in aerobic granules with nitrification efficiency of up to 97% and COD removal efficiency of up to 95%. Ammonia oxidizing bacteria were found to exist primarily in the upper

and middle layers of the granule and most of the nitrification was likely to occur from the surface to 300 μm into the granular thickness.

Lin et al. (2003) cultivated phosphorus-accumulating microbial granules at different substrate P/COD ratios varying from 1/100 to 10/100 by weight in SBRs. The granules had typical P-accumulating characteristics, i.e., they would release phosphate with concomitant uptake of soluble organic carbon in the anaerobic stage, followed by rapid phosphate assimilation in the aerobic stage. The P uptake fell within the range of 1.9 to 9.3% by weight. With the increase in substrate P/COD ratio, the size of P-accumulating granules showed a decreasing trend, while the compactness and density increased. Dulekgurgen et al. (2003) also developed aerobic granules in an SBR with activated sludge as the seed for enhanced biological phosphorus removal. The concentrations of phosphorus in the influent and effluent were 20.8 and 0.1 mg L^{-1} , respectively, indicating a removal rate of up to 99.6%.

Simultaneous nitrification, denitrification and phosphorus removal by aerobic granules have been studied in a laboratory-scale SBR (Lemaire et al. 2008). Good nitrification and phosphorus removal were observed throughout the SBR operation, but denitrification and full nutrient removal were completed only when granules were formed. Phosphate accumulating organism (PAO) *Accumulibacter* spp. and glycogen non-polyphosphate-accumulating organism (GAO) *Competibacter* spp. were found to be the most abundant microbial community members. However, *Accumulibacter* spp. dominated in the outermost 200 μm region of the granule, while *Competibacter* spp. dominated in the granule central anoxic zone. In a study of treating abattoir wastewater by aerobic granules in SBR, Cassidy and Belia

(2005) found that the removal of COD and P was over 98%, and the removal of N and VSS was over 97%.

de Kreuk et al. (2007) presented a mathematical model to describe an aerobic granular SBR for simultaneous removal of COD, nitrogen and phosphate. Simulation results indicated that oxygen penetration depth into the granules and the ratio of anoxic and aerobic biomass played crucial roles in overall nutrient removal. The optimum granule diameter for maximum N- and P-removal at a DO concentration of 2 mg L^{-1} and a temperature of $20 \text{ }^{\circ}\text{C}$ was between 1.2 and 1.4 mm with an optimum COD loading rate of $1.9 \text{ kg m}^{-3} \text{ d}^{-1}$. This model would help for process understanding, as well as, for optimization of the nutrient removal efficiency. Xavier et al. (2007) established a multi-scale model of aerobic granular sludge SBR to describe the complex dynamics of populations and nutrient removal by considering two-dimensional spatial distributions of four bacterial groups, i.e., heterotrophs, ammonium oxidizers, nitrite oxidizers and PAO. The simulations provided a good insight into the bioconversion processes occurring while describing both short-term dynamics and long-term reactor operation. This model incorporated dynamics of microbial metabolism, granule-scale diffusion-reaction with 2-D spatial arrangement and larger scale SBR operation. Another mathematical model was proposed by Ni et al. (2008) to describe the simultaneous autotrophic and heterotrophic growth in granule-based SBR. According to the model, the autotrophs were mainly located in the outer layer of granules for DO consumption, whereas the heterotrophs were present in the center of granules, or in the outer layer of granules. Simulation results also demonstrated that the influent substrate and $\text{NH}_4^+\text{-N}$ had significant effect on the composition of heterotrophic and autotrophic biomass in granules.

2.4.2 Treatment of Phenolic Compounds

Phenol, a major xenobiotic pollutant widely present in industrial effluents, is considered to be toxic to aquatic species even at a concentration as low as 1 mg L^{-1} (Brown et al. 1967). Phenol in wastewater is difficult to remove by conventional activated sludge systems because of its inherently toxic and inhibitory effect on microorganisms by denaturing proteins and disrupting the cytoplasmic membrane (Keweloh et al. 1989; Watanabe et al. 1999). To overcome such difficulties, research has been devoted to degradation of phenol with aerobic granules. Jiang et al. (2002) first reported the successful cultivation of aerobic granules fed with phenol as the sole carbon source at a phenol loading rate of $1.5 \text{ g L}^{-1} \text{ d}^{-1}$. The granules possessed a good tolerance towards phenol and a higher degree of microbial activity compared with their activated sludge origin, indicating their potential for the treatment of phenol-containing industrial wastewater. Tay et al. (2005a) compared activated sludge and acetate-fed aerobic granules as microbial inocula for phenol biodegradation at a phenol loading of $1.8 \text{ kg m}^{-3} \text{ d}^{-1}$ in SBRs. Results revealed that activated sludge failed to remove phenol and system failure occurred within 4 days. In contrast, aerobic granules acclimated rapidly and nearly complete phenol removal was achieved after a slight lag time. Upon exposure to phenol, filamentous bacteria with sheaths started to emerge and eventually dominated in granules, which might serve as a protective shield against phenol toxicity. Recent study by Ho et al. (2010) showed that aerobic granules could degrade phenol at a concentration of up to $5,000 \text{ mg L}^{-1}$ without severe inhibitory effect. The aerobic granules after acidic (pH 3) or alkaline (pH 12) treatment still effectively degraded $3,000 \text{ mg L}^{-1}$ of phenol. Moreover, Adav and Lee (2008b) cultivated aerobic granules with a single bacterial strain, *Acinetobacter calcoaceticus*, which was found to be a good phenol reducer and an efficient

autoaggregator. The single-culture aerobic granules exhibited long-term structure stability and high phenol degrading capacity.

Chlorinated phenolic compounds, highly recalcitrant contaminants with toxic and carcinogenic properties, are considered a critical environmental problem. Some of the chlorophenols have been listed as priority pollutants by the US Environmental Protection Agency (EPA) (Ghisalba 1983). There is, therefore, urgency to effectively remediate industrial wastewater that is contaminated with chlorophenols and aerobic granulation can be a viable alternative. Wang et al. (2007a) developed aerobic granules for the biological degradation of 2,4-dichlorophenol (2,4-DCP) in an SBR with glucose as the co-substrate. With a step-up increase in influent 2,4-DCP concentration, stable granules with a diameter range of 1-2 mm were obtained after 39-d operation. After granulation, the removal efficiencies of 2,4-DCP and COD were 94% and 95%, respectively. The specific 2,4-DCP biodegradation rate in the granules followed the Haldane model and peaked at $39.6 \text{ mg } 2,4\text{-DCP g}^{-1} \text{ VSS}^{-1} \text{ h}^{-1}$ at a 2,4-DCP concentration of 105 mg L^{-1} . Aerobic granules were also cultivated for the degradation of 4-chlorophenol (4CP) and 2,4,6-trichlorophenol (TCP) with sodium acetate as the co-substrate (Carucci et al. 2008, 2009). It was found that acetate-fed aerobic granules showed good resistance to high 4CP concentrations in the influent, and complete removal of 4CP was achieved after adaption. The presence of TCP did not irreversibly inhibit biomass activity, and complete TCP degradation was also obtained after acclimation.

Moreover, Yi et al. (2006) successfully cultivated p-nitrophenol (PNP)-degrading aerobic granules in SBR at a PNP loading rate of $0.6 \text{ kg m}^{-3} \text{ d}^{-1}$ with glucose as the co-substrate. The specific PNP degradation rate increased with corresponding

increase in PNP concentration from 0 to 40.1 mg L⁻¹ with a peak rate at 19.3 mg PNP g⁻¹ VSS⁻¹ h⁻¹, and decreased as the PNP concentration increased further. The SOUR at 100 mg L⁻¹ PNP was found to increase with the evolution of small granules to large granules, indicating that the granulation process would enhance metabolic efficiency toward biodegradation of PNP. The PNP-degrading aerobic granules could also degrade other phenolic compounds, such as hydroquinone, p-nitrocatechol, phenol, 2,4-dichlorophenol and 2,6-dichlorophenol. Liu et al. (2008) investigated the aerobic and anaerobic degradation of 4-*t*-octylphenol (4-*t*-OP) using aerobic granules and found that the aerobic degradation rate was much higher than anaerobic degradation rate. The optimal pH values for 4-*t*-OP degradation were 9 and 7 under aerobic and anaerobic conditions, respectively, and the degradation rate decreased with an increase in the initial 4-*t*-OP concentration. Wastewater from fossil fuel refining, pharmaceuticals and pesticides contains various phenolic compounds which are often more toxic than phenol. Farooqi et al. (2008) looked into the treatment of mixtures of phenol and m-cresol in SBR. Results showed that the maximum phenol and m-cresol up to 800:700 mg L⁻¹ was removed with efficiency of 95%, indicating that aerobic treatment by SBR can be successfully used for phenol/m-cresol mixtures, a representative of major components in chemical and petrochemical wastewater. In addition, an acclimatization period was required for the degradation of phenol and m-cresol.

2.4.3 Treatment of Other Toxic Organic Compounds

Except for phenolic compounds, aerobic granules could also be applied for biological remediation and removal of other recalcitrant organic compounds from industrial wastewater. In study of Adav et al. (2007b), aerobic granules cultivated

with 500 mg L⁻¹ phenol as the co-substrate could effectively degrade pyridine in the concentration range of 250-2500 mg L⁻¹. At initial pyridine concentrations of 250 and 500 mg L⁻¹, degradation obeyed closely a zero-order kinetics with no time delay. The specific degradation rate of pyridine was 73.0 and 66.8 mg g⁻¹ VSS⁻¹ h⁻¹ at 250 and 500 mg L⁻¹ pyridine, respectively. Aerobic granules for biodegradation of *tert*-butyl alcohol (TBA) were developed in SBR by step-wise increase in TBA concentrations in the influent (Tay et al. 2005b; Zhuang et al. 2005). The adapted granules were capable of complete TBA removal and contained a highly stable microbial population with low phylogenetic diversity belonging to Proteobacteria and the Cytophaga-Flavobacteria-Bacteroides (CFB) group. Zhang et al. (2008a) and Zhang et al. (2008b) successfully developed aerobic granules in SBR targeting for methyl *tert*-butyl ether (MTBE) removal with or without ethanol as the co-substrate. It was found that the removal efficiency of MTBE exceeded 99% after the reactor stabilized. Zhu et al. (2008) developed chloroanilines (CIA)-degrading aerobic granules in a sequencing airlift bioreactor (SABR) by decreasing settling time and gradually increasing CIA loading up to 0.8 kg m⁻³ d⁻¹. The steady-state granules had constant CIA removal efficiency of 99.9% and specific CIA degradation rate of 0.181 g g⁻¹ VSS⁻¹ d⁻¹. Nancharaiah et al. (2008) examined the development of aerobic granules in the presence of nitrilotriacetic acid (NTA) in SBR. Results showed that aerobic granulation was significantly enhanced by this chelating agent and complete removal of NTA was accomplished during the SBR cycle. In a study of Zeng et al. (2007), phthalic acid (PA)-degrading aerobic granules were pre-cultured in SBR using acclimated activated sludge as inocula and collected on day 180 and stored at 4°C for 8 weeks. It was shown that the size, settling ability and structure integrity of the granules remained stable during the storage period. After 7-d reviving operation, the PA-degrading aerobic granules recovered their bioactivities to the levels before storage. Zeng et al. (2008) further

successfully isolated a strain PA-02 from PA-degrading aerobic granules, which possessed phthalic acid ester (PAE)-degrading ability without acclimation. Based on 16S ribosomal DNA sequence, the isolate belonged to *Sphingomonas* genus with 100% similarity to *Sphingomonas* sp. strain D84532. Results showed that strain PA-02 could also degrade dimethyl phthalate (DMP), dibutyl phthalate and diethylhexyl phthalate.

2.4.4 Treatment of Heavy Metals

Heavy metals are toxic and non-biodegradable agents often found in industrial wastewater from mining, electroplating, smelting, tannery, textile, pharmaceuticals, etc. (Srivastava and Majumder 2008). Recent research showed that a variety of biomaterials including marine algae, fungi, bacteria and yeast had the potential to adsorb heavy metals (Sheng et al. 2004; García et al. 2005; Göksungur et al. 2005; Kang et al. 2007). However, several weaknesses such as post-separation, stability of biosorbents and regeneration after use have limited their practical use. In view of the physical characteristics of aerobic granules with porous structure, large surface area and excellent settleability, they would be good biosorbent candidates for heavy metals. The removal of Cd^{2+} , Zn^{2+} and Cu^{2+} by aerobic granules has been documented (Liu et al. 2002; Liu et al. 2003c; Liu et al. 2003e), and three biosorption mechanisms, i.e., ion exchange, binding to extracellular polymers and chemical precipitation, were demonstrated (Xu and Liu 2008). According to the thermodynamics of the biosorption process, a theoretical initial condition-dependent isotherm model was developed to describe the biosorption of three heavy metals, i.e., Cd^{2+} , Zn^{2+} and Cu^{2+} by aerobic granules. The biosorption capacities of Cd^{2+} , Zn^{2+} and Cu^{2+} were 625, 204 and 52.9 mg g^{-1} , respectively. This

model implied that aerobic granule-based biosorption would be an innovative and effective technology for the removal of heavy metals from industrial wastewater (Liu et al. 2004a). Xu et al. (2006) reported that Ni^{2+} biosorption by aerobic granules was pH-dependent. The biosorption capacity increased with the increase in pH in the range of 2-6 and the maximum capacity reached at the pH value of 6. It was also found that some light metals, such as K^+ , Mg^{2+} and Ca^{2+} were released into the bulk solution during Ni^{2+} uptake on the aerobic granules, indicating that the mechanism of ion exchange was involved in Ni^{2+} biosorption. The similar pH-dependent biosorption of Cu^{2+} onto aerobic granules was revealed by Gai et al. (2008). In study of Zhang et al. (2005a), rare earth metal cerium (Ce) was adsorbed by aerobic granules and the biosorption conformed to a first-order kinetics model. The biosorption ability of aerobic granules was related to both initial Ce ion and granule concentrations. The maximum biosorption capacity of Ce by aerobic granules was 357 mg g^{-1} granules. Aerobic granules have also been applied by Nancharaiah et al. (2006) for radionuclide uranium removal. They investigated the biosorption of uranium at different initial pH values (1 to 8) and different initial uranium concentrations (6 to 750 mg L^{-1}). Results indicated that biosorption was rapid ($< 1 \text{ h}$) in acidic pH range (1 to 6) compared to that at pH 7.0 or above and almost complete removal of uranium was achieved in the range of $6\text{-}100 \text{ mg L}^{-1}$ in less than 1 h. Redlich-Peterson model gave the best fit when the experimental data were analyzed using different adsorption isotherm equations. The maximum biosorption capacity of uranium was determined to be $218 \pm 2 \text{ mg g}^{-1}$ dry granular biomass. This study suggests that aerobic granules can be used to recover/remove uranium (and probably other radionuclides) from dilute nuclear wastewater and is potentially cost-effective.

2.4.5 Treatment of Dyestuffs

Many dyes known as carcinogens and mutagens are major environmental pollutants commonly present in industrial wastewater from textile and tannery manufacturing, paper and pulp processing, etc. (Gupta et al. 2003). Aerobic granules have been employed for adsorption and degradation of dyes due to their superior settling capability, strong structure and high bioactivity. Sun et al. (2008) conducted batch experiments to study the feasibility of malachite green (MG) biosorption by aerobic granules and noted that the biosorption of MG was highly dependent on initial concentration, adsorbent dosage, pH and temperature. Studies indicated that MG biosorption on aerobic granules obeyed pseudo-second order kinetics and the Langmuir isotherm. The monolayer biosorption (saturation) capacity was determined to be 56.8 mg of MG per gram of aerobic granules at 30°C. Thermodynamic studies confirmed that biosorption process was spontaneous and endothermic. Gao et al. (2011b) examined the contributions of EPS, residual sludge (the sludge left after EPS extraction) and functional groups (e.g., amine, carboxyl, phosphate and lipid) on aerobic granules on biosorption of four different dyes. Results revealed that the contribution of residual sludge to dye biosorption was greater than that related to EPS. The biosorption mechanisms were dependent on the chemical structure of dyes and functional groups on biosorbents. Recently, aerobic granules for treatment of methylene blue (MB)-containing wastewater were successfully developed in SBR using activated sludge as inocula (Ma et al. 2011). The stable aerobic granules had regular, smooth surface and compact structure with diameters ranging from 2 to 4 mm. After granulation, the removal efficiencies of MB and COD reached to 56% and 93%, respectively. Specific MB biodegradation rate followed the Haldane model.

2.5 SUMMARY

Aerobic granulation through cell-to-cell self-immobilization in SBR appears to be a promising biotechnology for handling a wide spectrum of wastewater. Aerobic granules have a denser and more compact structure which enables excellent settleability, higher biomass retention, higher tolerance to large loads and multiple toxic pollutants, a more stable operation with better quality effluent, thus making them superior than any other conventional systems. This review highlights the main factors influencing aerobic granulation, mechanisms and models of aerobic granulation, as well as, their applications for wastewater bioremediation. It seems that the knowledge about the mechanisms of aerobic granulation at levels of energy metabolism and cellular communication still remains unclear and some fundamental questions with regard to aerobic granulation still stay unanswered, i.e., (1) Are ATP and cellular communication essentially involved in the formation of aerobic granules? (2) Does the maintenance of structure stability and integrity of aerobic granules require ATP and cellular communication? and (3) What is the relationship between microbial structure and energy metabolism of aerobic granules? This study aims to address these questions and provide a better understanding of the mechanisms of aerobic granulation at levels of energy metabolism and cellular communication.

CHAPTER 3

DEPENDENCE OF AEROBIC GRANULATION ON ATP AND CELLULAR COMMUNICATION

3.1 INTRODUCTION

Aerobic granulation as a novel environmental biotechnology has been sparked enormous interest in the past two decades. Most of the studies have been carried out in laboratory-scale sequencing batch reactors (SBRs) with focus on granulation under various conditions and a number of factors have been identified as triggering forces, such as hydraulic selection pressures, extracellular polymeric substances (EPS), cell surface hydrophobicity (Tay et al. 2001b; Liu et al. 2003d; Adav and Lee 2008a). However, little information is currently available about the fundamentals of aerobic granulation at the level of energy metabolism. According to the chemiosmotic theory (Mitchell 1961), adenosine triphosphate (ATP), which serves as a primary bioenergy currency of microorganisms is synthesized via Proton Motive Force (PMF) created by coupling electron transport and oxidative phosphorylation. Under normal culture conditions, electron transport and oxidative phosphorylation are tightly coupled and the physiological behaviors of microorganisms are closely associated with the interaction between these two reactions.

Uncoupling of electron transport and oxidative phosphorylation would be an effective way to inhibit energy production, which can be achieved by using

chemical uncouplers. Uncouplers of oxidative phosphorylation are typical weak acids with substantial lipid solubility and can carry protons across the cellular membrane. Once inside the membrane matrix, the higher pH causes the uncoupler to deprotonate. As a result, the uncoupler has the effect of transporting hydrogen ion back into the matrix, bypassing the F_o proton channel, and thereby preventing ATP synthesis (Mathews et al. 1999).

Cellular communication (also known as “quorum sensing”) mediated by signaling molecules (autoinducers) has been shown to regulate diverse phenotypic traits (Schauder and Bassler 2001; Daniels et al. 2004; Liu et al. 2007). Autoinducer-2 (AI-2) produced by both Gram-positive and Gram-negative bacteria is a universal signaling molecule mediating intra- and inter-species communication, whereas *N*-acylhomoserine lactones (AHLs) are typical conserved signaling molecules present in many Gram-negative bacteria. AI-2 and AHLs have been reported to regulate biofilm formation of many bacterial species (Davies et al. 1998; Hardie and Heurlier 2008; Asahi et al. 2010). However, their bona fide roles in aerobic granulation are still ambiguous.

The aim of this chapter is therefore to investigate the possible roles of ATP and cellular communication in the development of aerobic granules. For this purpose, a typical chemical uncoupler, 3,3',4',5-tetrachlorosalicylanilide (TCS), which can effectively disrupt the PMF and further inhibit ATP generation, was used. It is expected that this chapter would offer deeper insights into the mechanisms of aerobic granulation at levels of energy metabolism and cellular communication.

3.2 MATERIALS AND METHODS

3.2.1 Experimental Setup and Operation

Three identical columns (150 cm in height, 5 cm in inner diameter) with a working volume of 2 L were used as SBRs, namely R1, R2 and R3 (Figure 3.1), housed in a temperature-controlled room at 25°C. The reactors were operated sequentially in 4-h cycles comprising 5 min of feeding, 220 min of aeration, 10 min of settling and 5 min of effluent withdrawal. The effluent was drained off from the middle port of the column (50 cm above the reactor bottom), giving a volumetric exchange ratio of 50% and an HRT of 8 h. Fine air bubbles for aeration and mixing were introduced by an air pump through an air diffuser equipped at the bottom of each reactor. Air flow rate was kept constant at 3 L min⁻¹ controlled by a gas-flow controller. R1 to R3 were inoculated with 2 g L⁻¹ of pre-acclimated activated sludge originally taken from a local municipal wastewater treatment plant (Ulu Pandan Water Reclamation Plant, Singapore). The influent synthetic wastewater consisted of ethanol and sodium acetate as mixed carbon source (equivalent to 1,120 mg L⁻¹ of chemical oxygen demand, COD), 200 mg L⁻¹ of NH₄Cl, 30 mg L⁻¹ of K₂HPO₄, 30 mg L⁻¹ of KH₂PO₄, 30 mg L⁻¹ of CaCl₂·2H₂O, 25 mg L⁻¹ of MgSO₄·7H₂O and 20 mg L⁻¹ of FeSO₄·7H₂O. In order to explore the roles of ATP and cellular communication in the development of aerobic granules, chemical uncoupler TCS (Sigma-Aldrich) was added into R2 and R3 at respective concentrations of 2 and 4 mg L⁻¹ from day one onwards, while R1 was used as the control free of TCS. Sampling was conducted in aeration period (30 min after the feeding stage started) in specific cycles.

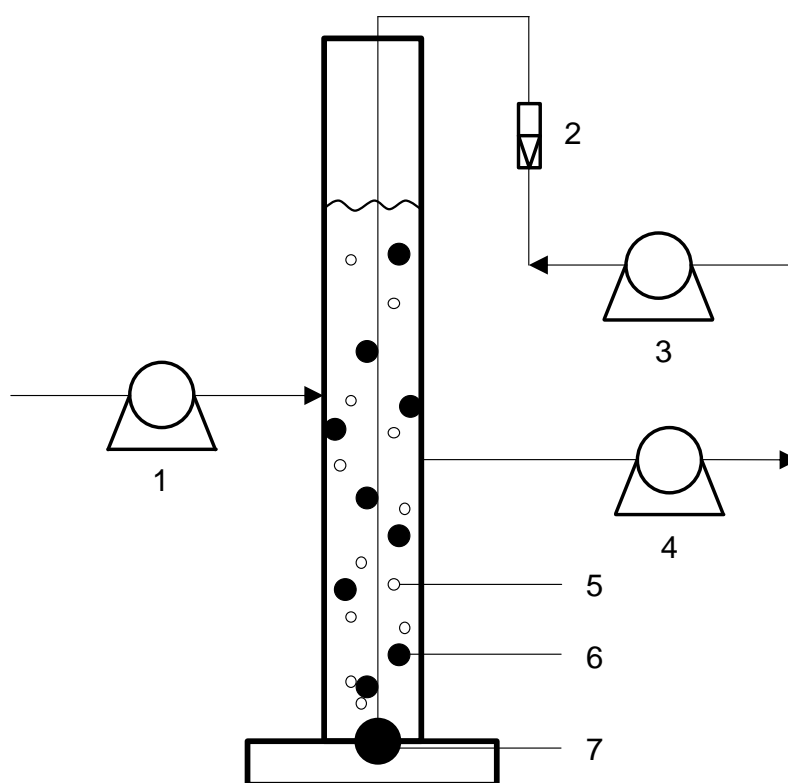


Figure 3.1 Schematic diagram of the SBR. 1: Influent pump; 2: gas flow meter; 3: air pump; 4: effluent pump; 5: air bubble; 6: granule/floc; 7: air diffuser.

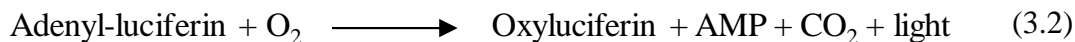
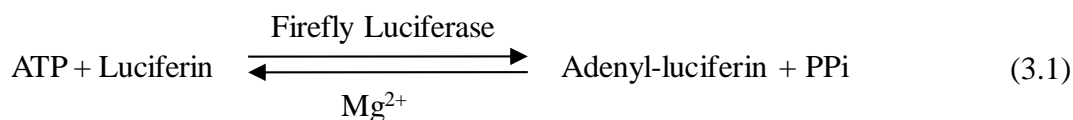
3.2.2 Determination of EPS

Extracellular polysaccharides (PS) and proteins (PN) in biosamples were extracted by modified cold aqueous extraction method (Jia et al. 1996), i.e., 10 mL of fresh biomass was centrifuged at 3,500 rpm for 5 min (KUBATO, Japan) to remove supernatant and washed twice with de-ionized water. The recovered biomass was ground and re-suspended in 10 mL of 8.5% NaCl solution containing 0.22% formaldehyde. This mixture was subsequently homogenized by an ultrasonic homogenizer (Sonics & Materials, CT, USA), chilled and agitated with a vortex mixer (Vortex-Genie[®] 2T w/Timer, Scientific Industries Inc., USA) for 3 min, during which time the extracellular PS and PN were extracted into the solution.

The suspension was further centrifuged at 10,000 rpm for 30 min and the supernatant was filtered through a 0.20- μ m syringe filter (Minisart[®] NY 25, Germany) to remove residual solids before analysis. Extracellular PS and PN contents were determined by a UV/Visible spectrophotometer (UV/Vis PharmaSpec UV-1700, Shimadzu, Japan) using the phenol-sulfuric method (Dubois et al. 1956) and the folin method (Lowry et al. 1951), respectively. The calibration standards were glucose (Sigma-Aldrich) for extracellular PS and bovine serum albumin (Sigma-Aldrich) for extracellular PN. Three replicates were done for each sample.

3.2.3 Determination of Cellular ATP

Cellular ATP was extracted according to the modified method by Chen and Leung (2000), that is, 2.5 mL of trichloroacetic acid solution (5%, w/v) was added into 2.5 mL of fresh sample and homogenized by an ultrasonic homogenizer for 3 min in an ice-water bath. Subsequently, 0.5 mL of the homogenate was added into 4.5 mL of 1 \times TAE buffer (Tris-Acetic acid-EDTA buffer: 40 mM Tris, 20 mM acetic acid, 1 mM EDTA) to make a 5-mL solution with a final pH of 7.75 and was then filtered through a 0.20- μ m syringe filter to remove any suspended solids. The filtrate was collected in a sterilized 2-mL centrifuge tube (Eppendorf, Hamburg, Germany) and stored at -20°C before analysis. The cellular ATP content was measured by a microplate reader (Biotek, Synergy 2, Winooski, VT) with FLAA Adenosine 5'-triphosphate (ATP) Bioluminescent Assay Kit (Sigma-Aldrich). The quantitative determination of cellular ATP is based on the firefly luciferin-luciferase bioluminescent reactions shown in the following equations. Each sample was assayed in triplicate and all values were expressed on the basis of dry biomass.



3.2.4 Determination of AI-2 by Bioluminescence Assay

Cell-free culture fluids for determination of relative AI-2 content were obtained as follows. A fraction of fresh sludge sample (equivalent to 10 mg dry biomass) was harvested by centrifugation, washed twice with de-ionized water and re-suspended in 5 mL of sterile autoinducer bioassay (AB) medium (Bassler et al. 1994). This mixed suspension was thoroughly homogenized by an ultrasonic homogenizer and followed by centrifugation at 10,000 rpm for 10 min. The supernatant was collected by filtration through a 0.20- μm syringe filter and stored at -20°C before analysis. The bioluminescence assay of relative AI-2 content was performed according to the techniques by Surette and Bassler (1998). Briefly, the reporter strain *Vibrio harveyi* BB170 (ATCC BAA 1117, Manassas, VA) was propagated aerobically in batch cultures of AB medium in a rotary shaker (INFORS HT) for 12-16 h (150 rpm, 30°C) and diluted 1/5,000 (v/v) into fresh sterile AB medium. Afterwards, 180 μL of the diluted culture was placed into 96-well plates (Greiner, Germany), each well containing 20 μL of cell-free sample fluids or 20 μL of sterile AB medium for blank wells. The plates covered with lids were agitated at 150 rpm and 30°C in the rotary shaker and the light production was monitored by a microplate reader at a 30-min interval in luminescence mode at a constant temperature of 30°C . Bioluminescence of sample over that of the blank was calculated as the fold induction indicating relative AI-2 content. Each sample was measured in quadruplicate.

3.2.5 Determination of AHLs by Bioluminescence Assay

Cell-free culture fluids to be tested for relative AHL content were extracted as described below. A certain amount of fresh biosample (equivalent to 10 mg dry biomass) was recovered by centrifugation, washed twice with de-ionized water and re-suspended in 5 mL of sterile minimal medium (per liter contains 2 g glucose, 10.5 g K_2HPO_4 , 4.5 g KH_2PO_4 , 2 g $(NH_4)_2SO_4$, 0.2 g $MgSO_4 \cdot 7H_2O$, 15 mg $CaCl_2 \cdot 2H_2O$, 10 mg $FeSO_4 \cdot 7H_2O$ and 3 mg $MnSO_4 \cdot H_2O$; adjust pH to 6.8) (Hu et al. 2003). This mixture was homogenized by an ultrasonic homogenizer and subsequently centrifuged at 10,000 rpm for 10 min. The supernatant was passed through a 0.20- μm syringe filter to ensure that the sample was free of cells and then stored at $-20^\circ C$ until analysis was conducted. The bioluminescence assay of relative AHL content was carried out based on the method of Singh and Greenstein (2006) with some modifications. The reporter strain *Agrobacterium tumefaciens* NT1 (*traR*; *tra::lacZ749*) used as the biosensor to detect AHL signals was cultivated to late exponential phase in a rotary shaker at 150 rpm and $30^\circ C$ in minimal medium supplemented with $50 \mu g mL^{-1}$ of streptomycin and $5 \mu g mL^{-1}$ of tetracycline. This bacterial culture was diluted in fresh minimal medium containing no antibiotics to an OD_{600} of 0.1 and dispensed in $50 \mu L$ per well of 96-well plates which contained $25 \mu L$ of cell-free sample fluids in each well. The sterile minimal medium and cell-free sample fluid on day 0 were used as blank and the sample control, respectively. The plates were incubated at $30^\circ C$ with agitation for 16-18 h. Subsequently, $75 \mu L$ of Beta-Glo[®] (Promega) was added into each well, followed by 90-min incubation in the dark and the luminescence was measured using a microplate reader at the end of incubation period. The amount of luminescence produced correlated with the amount of reporter protein β -galactosidase expressed which further corresponded to AHL content. The luminescence produced by

sample higher than that of blank was considered active. The relative AHL content was quantified as the fold of the net luminescence of sample (luminescence of sample subtract luminescence of blank) over the net luminescence of sample control (luminescence of sample on day 0 subtract luminescence of blank). All assays were repeated at least three times in parallel. The coupled bioluminescent reactions of the Beta-Glo[®] assay system were shown in Figure 3.2.

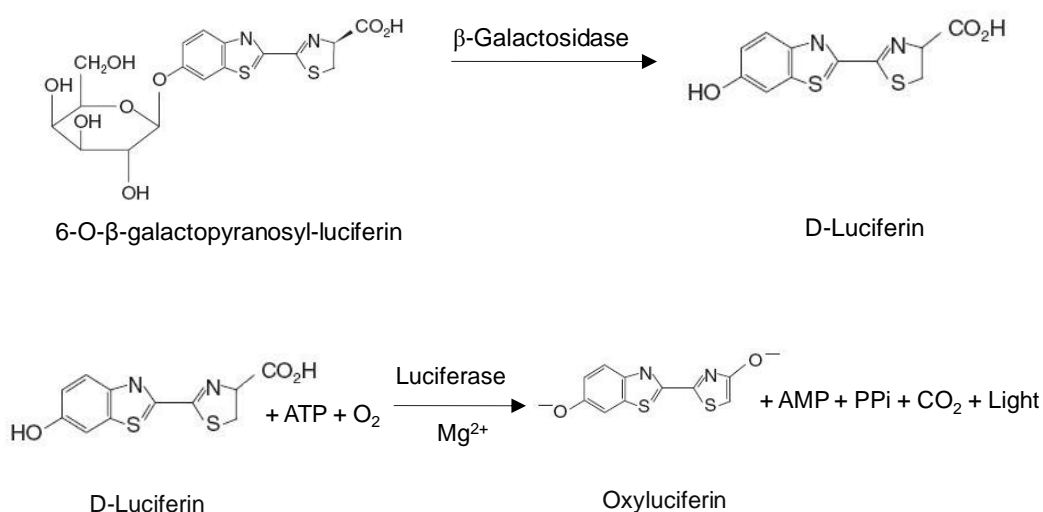


Figure 3.2 The coupled bioluminescent reactions of the Beta-Glo[®] assay system. 6-O-β-galactopyranosyl-luciferin is cleaved by β-galactosidase into D-luciferin which in turn serves as the substrate for luciferase to produce light in the presence of cofactors.

3.2.6 β-galactosidase Bioassay of AHLs

The reporter strain *A. tumefaciens* NT1 (*traR*; *tra::lacZ749*) was cultivated aerobically in minimal medium to late exponential phase as described above. This bacterial culture was diluted with an equal volume of fresh minimal medium which also contained two antibiotics. This broth was poured into melted agar (2%, w/v,

maintained at 45°C) in the ratio of 1:1, mixed thoroughly and immediately dispensed in 10 mL aliquots to 60 mm×15 mm cell culture dishes (Corning, NY, USA). After the agar had solidified, the plate surface was spread over by 10 µL of 5-bromo-4-chloro-3-indolyl-β-D-galactopyranoside (X-Gal, 20 mg mL⁻¹ in dimethyl sulphoxide) and covered by a sterilized 0.2-µm Sartolon membranefilter (Sartorius, polyamid, 25007-25-N, Germany). A portion of biosample (equivalent to 6 mg dry biomass) was recovered by centrifugation, washed twice with de-ionized water and loaded onto the top of the membranefilter. The cell culture dishes were incubated at 30°C for 24 h (Precision Scientific, India). The blue pigmentation development due to X-Gal hydrolysis by induced expression of β-galactosidase indicated the positive identification of AHLs in the sample. Images were recorded by a digital camera (Canon IXUS 130, Japan). A minimum of three replications were performed for each sample to confirm reproducibility.

3.2.7 Identification of AHLs by TLC Analysis

AHLs in aerobic granules in R1 were extracted according to the modified method of Yeon et al. (2008), i.e., gently rinsed aerobic granules were placed in ethyl acetate and homogenized by an ultrasonic homogenizer. This mixture was centrifuged at 10,000 rpm for 10 min and the supernatant was transferred to a clean tube. These extraction steps were repeated three times and the supernatant was combined together. Afterwards, the supernatant containing AHLs was dried over anhydrous magnesium sulphate, filtered and completely evaporated to dryness by a rotary evaporator (Heidolph, Germany) at 30°C. The residue of AHL extracts was finally dissolved in 250 µL of HPLC-grade acetonitrile and stored at -20°C before analysis. For thin-layer chromatography (TLC) analysis, aliquots of 5-µL AHL

sample were applied to C18 reverse-phase TLC plates and the chromatograms were developed with the mobile phase of methanol/water (60:40, v/v) following the procedure described by Shaw et al. (1997). The plates were then put in a fume hood to evaporate any moisture at room temperature and overlaid with a thin uniform film (about 3 mm) of minimal medium agar (1%, w/v, maintained at 45°C) containing overnight culture of *A. tumefaciens* NT1 (*traR*; *tra::lacZ749*) (in the ratio of 10:1) and 40 µg mL⁻¹ of X-Gal. The plates were solidified and incubated in a sterilized closed plastic container at 30°C for 18-20 h. Tentative identification of AHLs in aerobic granules was performed by comparing the R_f values of the sample spots with those of AHL standards purchased from Sigma-Aldrich. Images were taken by a digital camera.

3.2.8 SEM Observation

Flocs or granules were washed with 1× phosphate-buffered saline (PBS) buffer (pH 7.2) and immersed in a 2% glutaraldehyde solution for 4 h. The fixed biomass was then rinsed with 0.1 M sodium cacodylate buffer for three times (each with 20 min). Afterwards, biosamples were dehydrated in graded ethanol series for 10 min each (once in 50%, 70%, 85%, 95%; twice in 100%) and subjected to drying with a CO₂ critical point drier (E3000, VG microtech, England). Finally, biosamples were sputter-coated with gold at a current of around 20 mA for 60 s (SC7620 Mini Sputter Coater, UK) and observed by a scanning electron microscopy (SEM, ZEISS EVO 50, Germany).

3.2.9 Biofilm Formation Assay in 96-well Plates

Acclimated activated sludge was firstly filtered through a 45- μm sieve (Fritsch, Germany) to remove large cell aggregates or clumps and then centrifuged at 3,500 rpm for 5 min to remove supernatant. The harvested sludge was rinsed twice with de-ionized water and re-suspended in de-ionized water with a biomass concentration of around 1 g L^{-1} . This activated sludge suspension was subsequently mixed with equal volume of fresh substrate (the composition of the substrate was the same as described in 3.2.1 Experimental Setup and Operation) and ready for inoculation. For study of TCS inhibition to biofilm development, a total of 150 μL of the sludge suspension supplemented with 2 and 4 mg L^{-1} TCS was inoculated into each well of flat-bottom 96-well tissue culture polystyrene microtiter plates (Iwaki, Japan), while control wells received 150 μL of sludge suspension without TCS. The plates were incubated at 30°C with shake (150 rpm) for 12 h. At the end of incubation, each well of the plates was gently washed with $1\times$ PBS buffer for three times to remove planktonic or unattached cells. The remaining fixed biomass was then stained with 175 μL of 1% (v/v) Gram's crystal violet (Fluka) for 2 min and three wash cycles with 250 μL of $1\times$ PBS buffer were performed subsequently to remove excess crystal violet. The stained plates were dried in a fume hood at room temperature and each well was decolorized with 175 μL of 95% ethanol for 2 min. The eluted solution was transferred into 1-mL cuvette and the absorbance at 600 nm (A_{600}) was measured with a UV-Vis spectrophotometer (UVmini-1240, Shimadzu, Japan) which indirectly indicated the amount of biofilm biomass.

3.2.10 Other Methods

Mixed liquor suspended solids (MLSS) and mixed liquor volatile suspended solids (MLVSS) were measured according to Standard Method (APHA 2005). Biomass density (as weight per volume of biomass) was determined following guidelines of APHA (2005) and Liu and Wang (2007). COD in the influent and effluent was analyzed using COD digestion vials (HACH, USA). Gram staining was performed with the method developed by Black (1993). The morphology of biomass was observed by an image analyzer (SZX-ILLK2000, Olympus) with Image Pro Plus software (Media Cybernetics, L.P.; version 4.0).

3.3 RESULTS

3.3.1 Effect of TCS on Biomass Density and Morphology

Biomass density is an important indicator of aerobic granulation which reflects the compactness of clustered biomass (Kim et al. 2008). Figure 3.3 shows the respective changes in biomass density with and without exposure to TCS in R1 to R3 over 30-d operation. In R1 free of TCS, the biomass density gradually increased from 1.0083 g mL^{-1} for seed activated sludge to 1.0195 g mL^{-1} on day 14, and remained almost stable afterwards. On the contrary, the densities of biomass in R2 and R3 supplemented with 2 and 4 mg L^{-1} TCS tended to decrease in the first 4 d, and were gradually restored to their initial levels, but much lower than that in R1 with successful granulation. It should be noted that the biomass concentration in R3 dropped to less than 200 mg L^{-1} after two weeks of operation, thus, R3 was terminated due to such low biomass concentration.

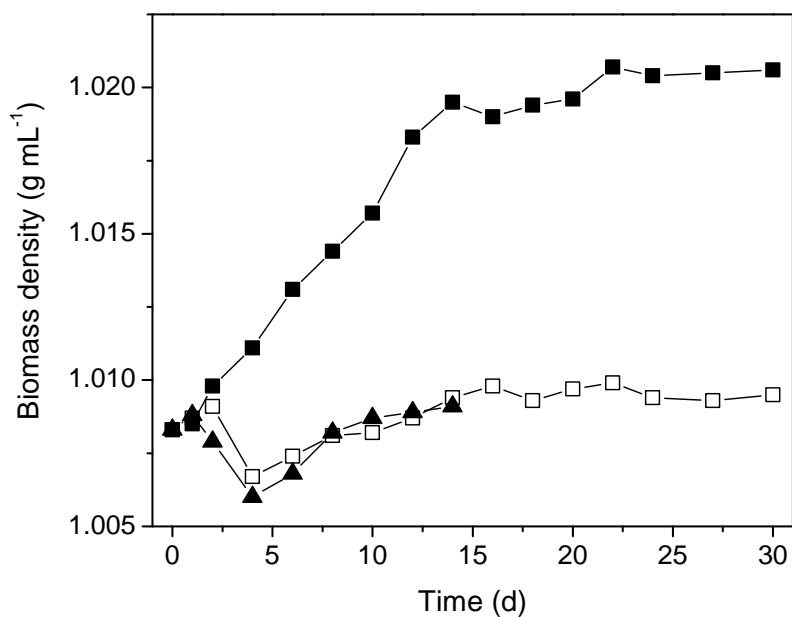


Figure 3.3 Profiles of biomass density in R1 to R3 during 30-d operation. ■: R1 free of TCS; □: R2 with 2 mg L⁻¹ TCS; ▲: R3 with 4 mg L⁻¹ TCS.

The morphological evolution of sludge in R1 to R3 was observed by an image analyzer (Figure 3.4). In R1 free of TCS, tiny aggregates first appeared on day 8, and then gradually developed into large-size and round-shape aerobic granules. However, only loose bioflocs were observed in R2 and R3 supplemented respectively with 2 and 4 mg L⁻¹ TCS, indicating unsuccessful aerobic granulation. These observations indeed are consistent with the profiles of biomass density presented in Figure 3.3. Consequently, TCS at the concentrations studied appeared to inhibit aerobic granulation.

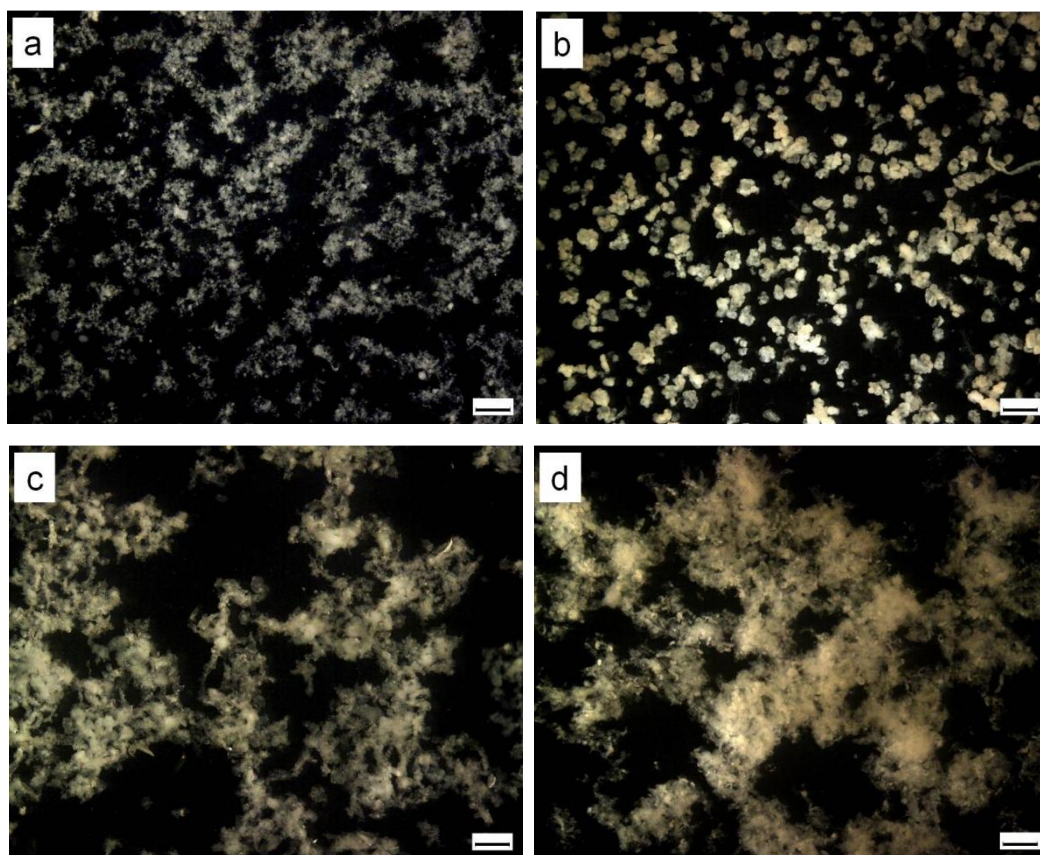


Figure 3.4 Morphologies of sludge in R1 to R3. a: Seed activated sludge; b: R1 free of TCS on day 30; c: R2 with 2 mg L⁻¹ TCS on day 30; d: R3 with 4 mg L⁻¹ TCS on day 14. Bar: 1 mm.

In fact, unsuccessful aerobic granulation has also been observed in ethanol-fed SBRs with the addition of TCS at respective concentrations of 1, 2 and 4 mg L⁻¹ (data not shown). It can be seen in Figure 3.5 that the mean size of biomass in the control reactor free of TCS gradually increased to a stable value of 2.5 mm, while the mean sizes of biomass subjected to different TCS concentrations of 1 to 4 mg L⁻¹ remained unchanged over 40 d of operation, which are comparable with that of the seed activated sludge. After 40-d operation, the settleability of the sludge with the addition of 2 and 4 mg L⁻¹ TCS became worse and worse, and complete sludge

washout occurred in these two reactors ultimately. Once again these clearly showed that TCS can seriously inhibit the formation of aerobic granules.

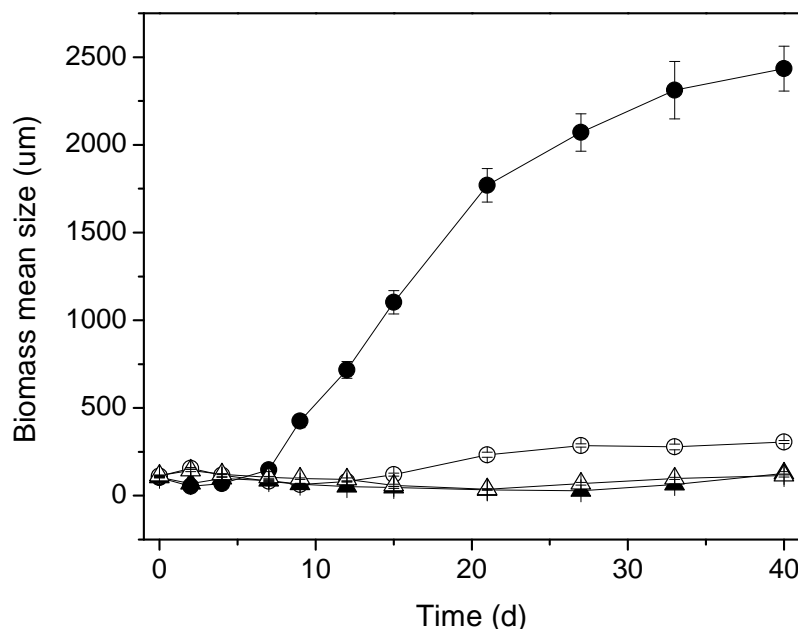


Figure 3.5 Size profiles of biomass with and without exposure to TCS during 40-d operation (SBRs fed with ethanol as the carbon source). ●: SBR free of TCS; ○: SBR added with 1 mg L⁻¹ TCS; ▲: SBR added with 2 mg L⁻¹ TCS; △: SBR added with 4 mg L⁻¹ TCS.

Figure 3.6 illustrates the SEM images of seed activated sludge and biomasses taken from R1 to R3. It can be seen that the seed activated sludge consisted of a wide variety of rod- and cocci-type species with a small amount of filamentous bacteria. After 30-d operation, mature granules formed in R1 free of TCS and bacteria in such granules were tightly associated to form the structural backbones and embedded in the EPS matrix. This observation is in accordance with the high density of R1-biomass as shown in Figure 3.3. By contrast, the phenotype of biomasses in R2 and R3 fed with respective TCS concentrations of 2 and 4 mg L⁻¹ were similar, i.e., bacilli were predominant and no clear EPS matrix was observed.

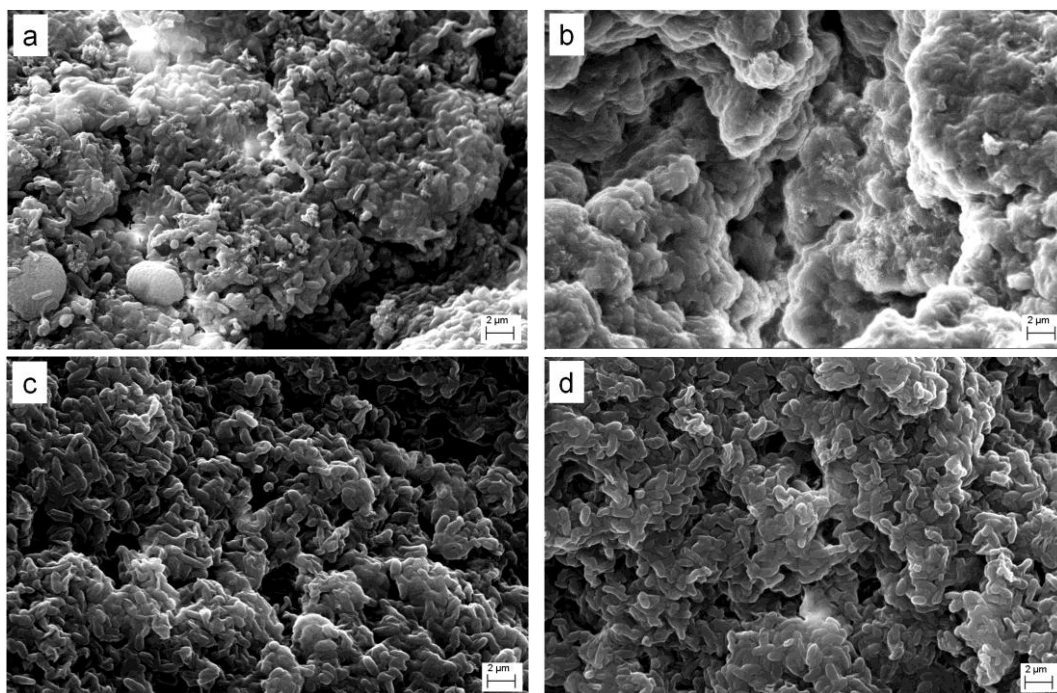


Figure 3.6 SEM images of R1- to R3-biomass. a: Seed activated sludge; b: R1 free of TCS on day 30; c: R2 with 2 mg L⁻¹ TCS on day 30; d: R3 with 4 mg L⁻¹ TCS on day 14. Bar: 2 μm.

3.3.2 Effect of TCS on Substrate Removal

Figure 3.7 shows the COD removal efficiencies in R1 to R3 during 30-d operation. It reveals that the substrate removal efficiencies in R2 and R3 with the addition of 2 and 4 mg L⁻¹ TCS were almost not affected. Table 3.1 further displays the variations of COD concentration observed in one cycle of R1 to R3. It appears that nearly all influent COD was removed in the first 30 min in three reactors. These results suggest that the effect of TCS on the substrate removal was not significant, which is in good agreement with the current understanding of that chemical uncouplers would not inhibit electron transport system by which substrate continues to be oxidized.

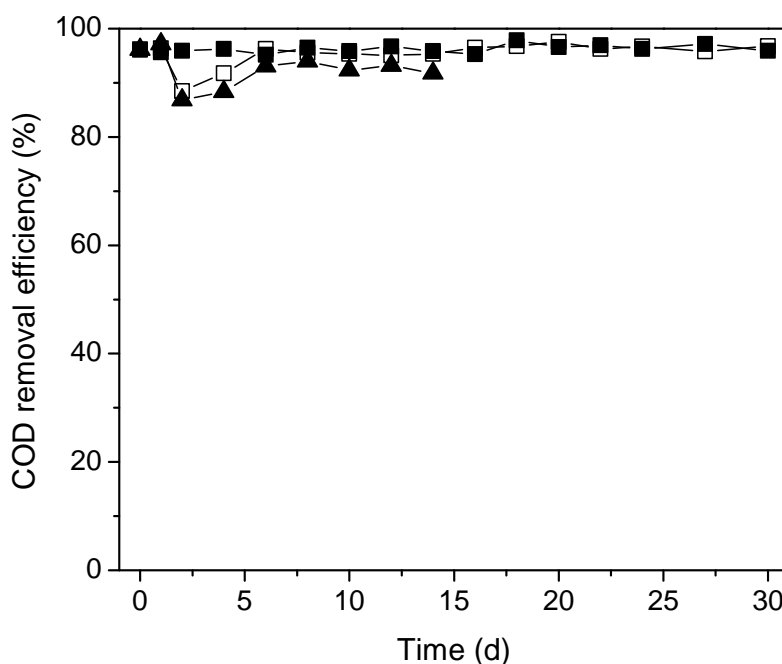


Figure 3.7 Profiles of COD removal efficiency in R1 to R3 during 30-d operation.

■: R1 free of TCS; □: R2 with 2 mg L⁻¹ TCS; ▲: R3 with 4 mg L⁻¹ TCS.

Table 3.1 Variations of COD concentration in one cycle in R1 to R3 (mg L⁻¹)

	0 h	0.5 h	1 h	2 h	3 h	4 h
R1	560	30.2	29.7	26.8	25.3	24.5
R2	560	25.3	23.6	22.2	21.1	20.4
R3	560	20.5	18.2	16.9	15.5	15.9

3.3.3 Effect of TCS on EPS Content

EPS, a conglomeration of biopolymers with major components of extracellular PS and PN, has been believed to build the scaffold for microorganisms and play a vital role in the formation of biofilms and biogranules (Sutherland 2001; Liu et al. 2004c; Flemming and Wingender 2010). Figures 3.8 and 3.9 show the profiles of

extracellular PS and PN contents in R1- to R3-biomass during 30-d operation. In R1 free of TCS, both extracellular PS and PN contents increased over time and finally stabilized at around 25 and 50 mg g⁻¹ MLVSS, respectively, while declining trends were observed in R2 and R3 with the addition of 2 and 4 mg L⁻¹ TCS. For example, at the end of operation, the extracellular PS and PN contents in R2 were 4.7- and 2.9-fold lower than those in the control reactor, which were even lower than those of seed activated sludge. These results imply that TCS at the concentrations studied can inhibit the production of both extracellular PS and PN, and in turn may cause the failure of aerobic granulation. In the study of the effect of uncoupler 2,4-dinitrophenol (DNP) on the cell surface properties of marine bacteria, Jain et al. (2007) also reported reduced EPS production by three marine isolates in the presence of DNP.

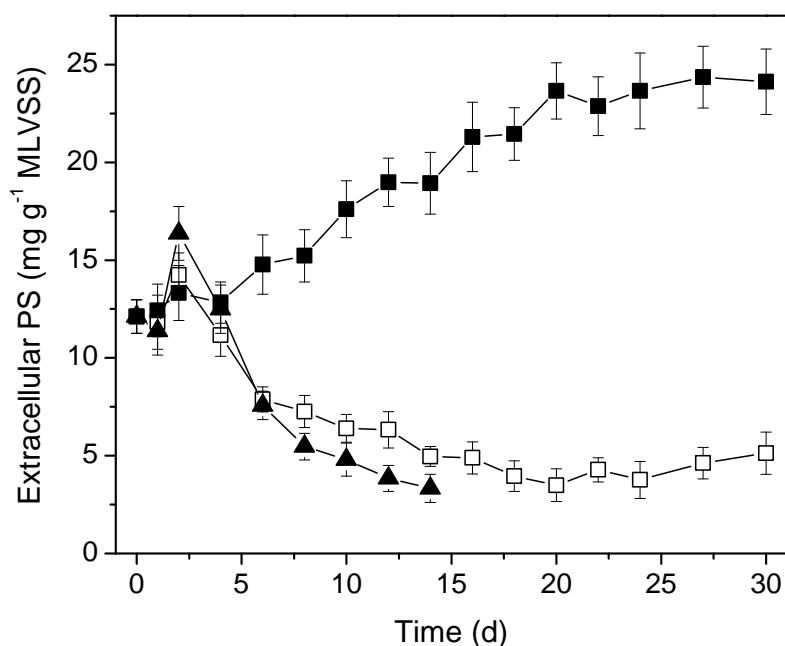


Figure 3.8 Changes of extracellular PS content in R1- to R3-biomass during 30-d operation. ■: R1 free of TCS; □: R2 with 2 mg L⁻¹ TCS; ▲: R3 with 4 mg L⁻¹ TCS.

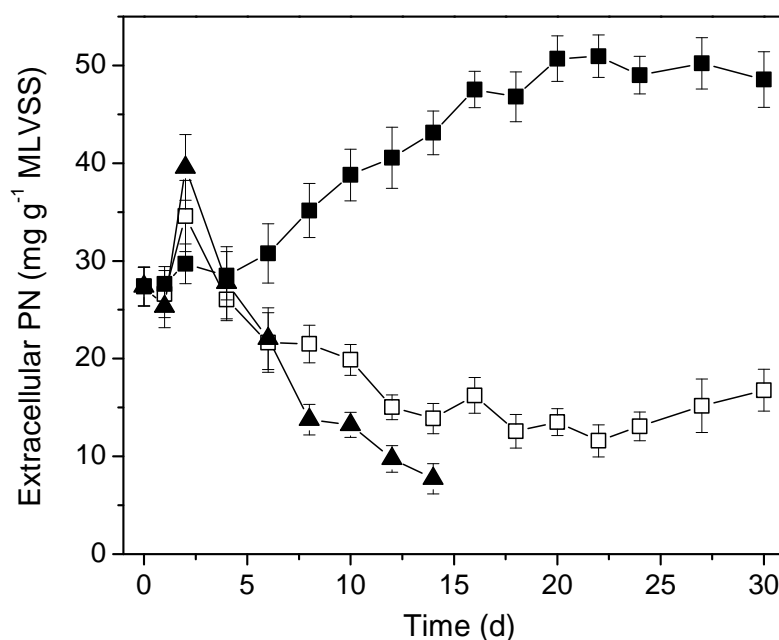


Figure 3.9 Changes of extracellular PN content in R1- to R3-biomass during 30-d operation. ■: R1 free of TCS; □: R2 with 2 mg L⁻¹ TCS; ▲: R3 with 4 mg L⁻¹ TCS.

3.3.4 Effect of TCS on Cellular ATP Content

As a typical chemical uncoupler, TCS is able to dissipate the proton gradient created through respiratory chain across the inner cellular membrane, as a consequence, ATP synthesis comes to a halt. Figure 3.10 shows the variations of cellular ATP content in R1- to R3-biomass with and without exposure to TCS during 30-d operation. It can be seen that the cellular ATP content in R1-biomass increased from 9.12×10^{-7} mol g⁻¹ MLVSS for seed activated sludge to a stable level of 1.71×10^{-6} mol g⁻¹ MLVSS for aerobic granules. Meanwhile, decreased cellular ATP contents were obtained in R2- and R3-biomass with the addition of 2 and 4 mg L⁻¹ TCS, e.g., the cellular ATP content in R2-biomass was only half of that in R1-biomass at the end of operation. These results clearly indicate that TCS can effectively suppress cellular ATP synthesis.

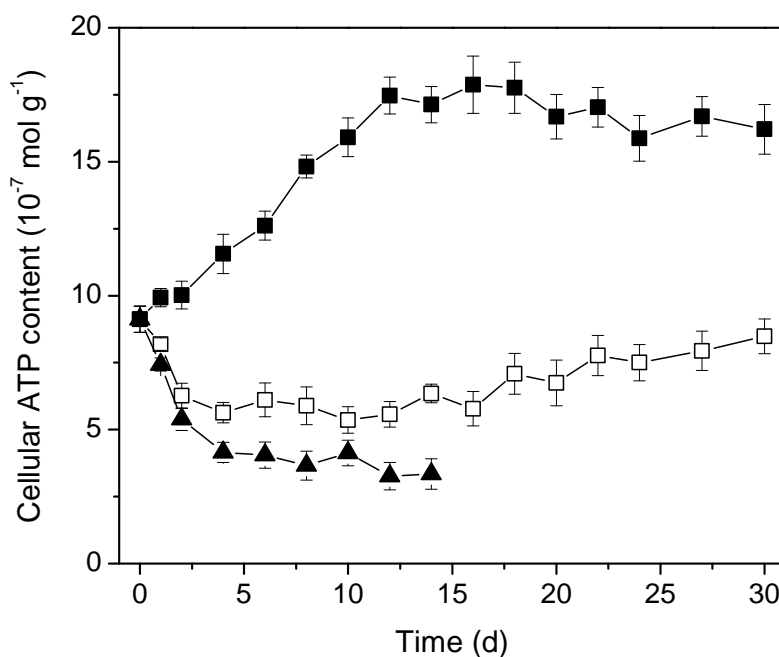


Figure 3.10 Profiles of cellular ATP content in R1- to R3-biomass during 30-d operation. ■: R1 free of TCS; □: R2 with 2 mg L⁻¹ TCS; ▲: R3 with 4 mg L⁻¹ TCS.

3.3.5 Effect of TCS on Relative AI-2 Content

AI-2-mediated quorum sensing has been believed to regulate both intra- and inter-species communication and play an important role in microbial aggregation and biofilm formation (Yoshida et al. 2005; Shao et al. 2007). The changes of relative AI-2 content in R1- to R3-biomass are presented in Figure 3.11. It is obvious that the relative AI-2 content in R1-biomass free of TCS changed insignificantly until day 8, that is, it remained at the level of the seed activated sludge before day 8. Afterwards, the relative AI-2 content increased rapidly and finally stabilized at the fold induction of around 4.5. However, the relative AI-2 contents in R2- and R3-biomass remained at lower levels over the entire operation period. For instance, the relative AI-2 content in R2-biomass was nearly two-time lower than that of the

control at the end of operation. These results suggest that TCS at the concentrations studied would inhibit the production of AI-2, which is essential for coordinating microbial group behaviors during aerobic granulation.

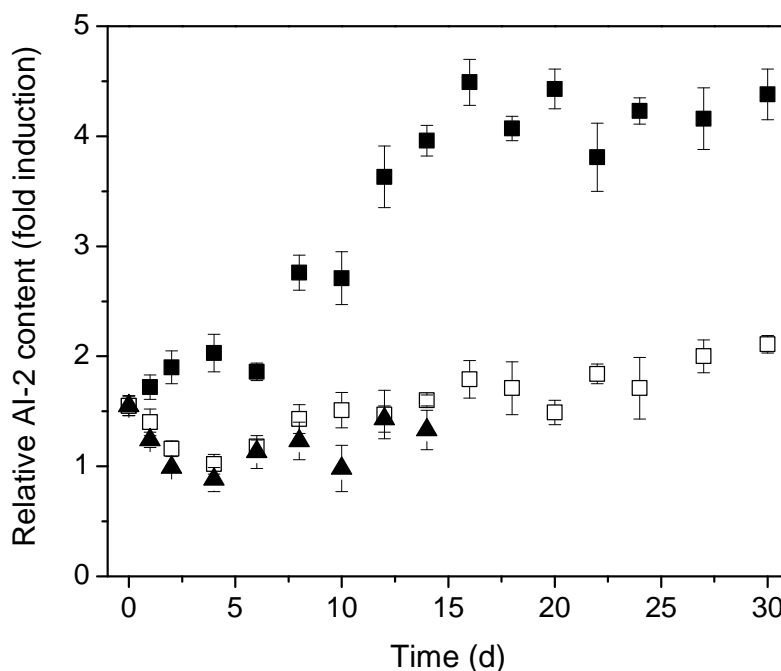


Figure 3.11 Changes of relative AI-2 content in R1- to R3-biomass during 30-d operation. ■: R1 free of TCS; □: R2 with 2 mg L⁻¹ TCS; ▲: R3 with 4 mg L⁻¹ TCS.

3.3.6 Effect of TCS on Relative AHL Content

AHLs are signaling molecules that have been identified in many Gram-negative bacteria, and are known to regulate diverse biological functions including biofilm formation (Zhang et al. 2002). It can be seen in Figure 3.12 that Gram-negative bacteria were predominant in R1 to R3, thus, relative AHL contents in R1- to R3-biomass were measured. Figure 3.13 shows that the relative AHL content increased with aerobic granulation in R1 free of TCS. Conversely, they dropped significantly

in the first 4 d in R2 and R3, and then stabilized at their initial levels. Compared to R1, the relative AHL contents in R2- and R3-biomass were lower over the entire operation period. These findings were further supported by β -galactosidase bioassay presented in Figure 3.14, suggesting that AHLs were abundant in aerobic granules indicated by intensive blue coloration, while AHLs were negligible in R2-biomass exposed to TCS. To further identify the types of AHLs in aerobic granules, TLC analysis was performed with extracts from R1 granules, followed by revelation with *A. tumefaciens* NT1 (*traR*; *tra::lacZ749*) as the indicator. Comparison of the R_f values of blue spots developed by AHL sample with those of known AHL standards suggests that *N*-hexanoyl-L-homoserine lactone (HHL) and *N*-octanoyl-L-homoserine lactone (OHL) were primarily present in aerobic granules (Figure 3.15).

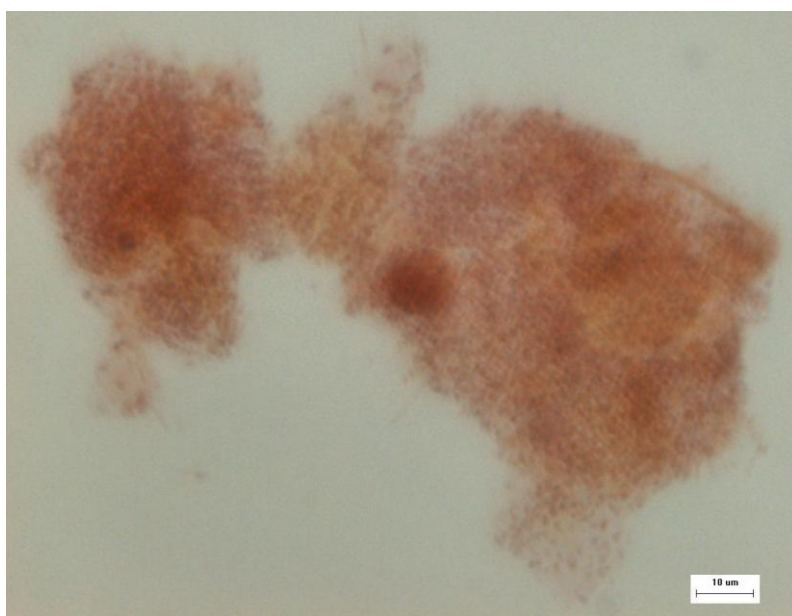


Figure 3.12 Gram-stained image of biomass. Red color indicates Gram-negative bacteria. Bar: 10 μ m.

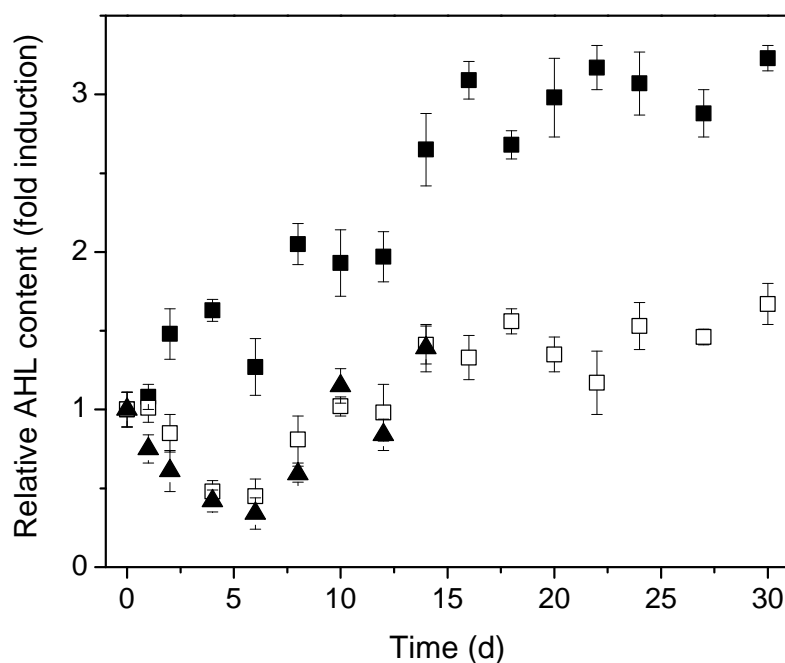


Figure 3.13 Changes of relative AHL content in R1- to R3-biomass during 30-d operation. ■: R1 free of TCS; □: R2 with 2 mg L⁻¹ TCS; ▲: R3 with 4 mg L⁻¹ TCS.

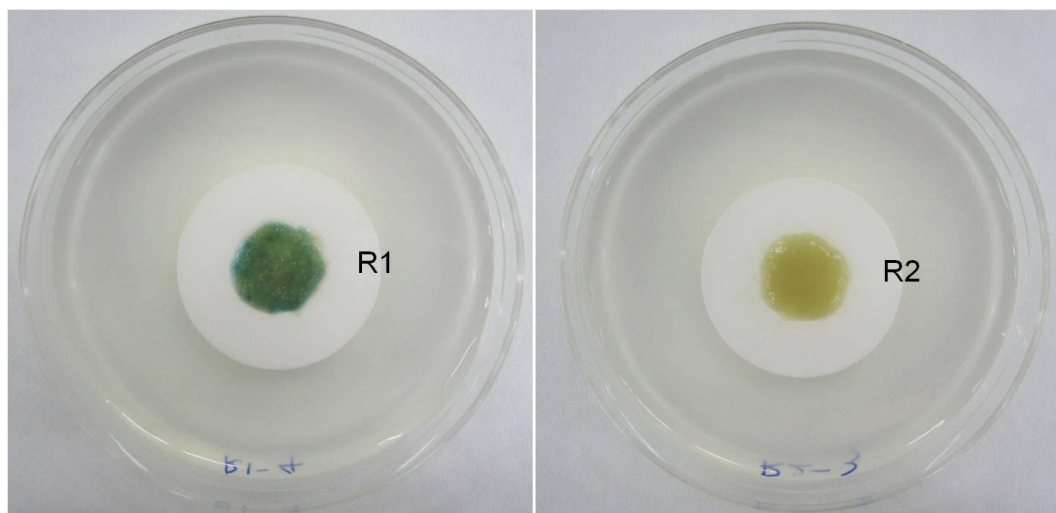


Figure 3.14 β -galactosidase bioassay of AHLs in R1- and R2-biomass on day 30. Blue color indicates the presence of AHLs.

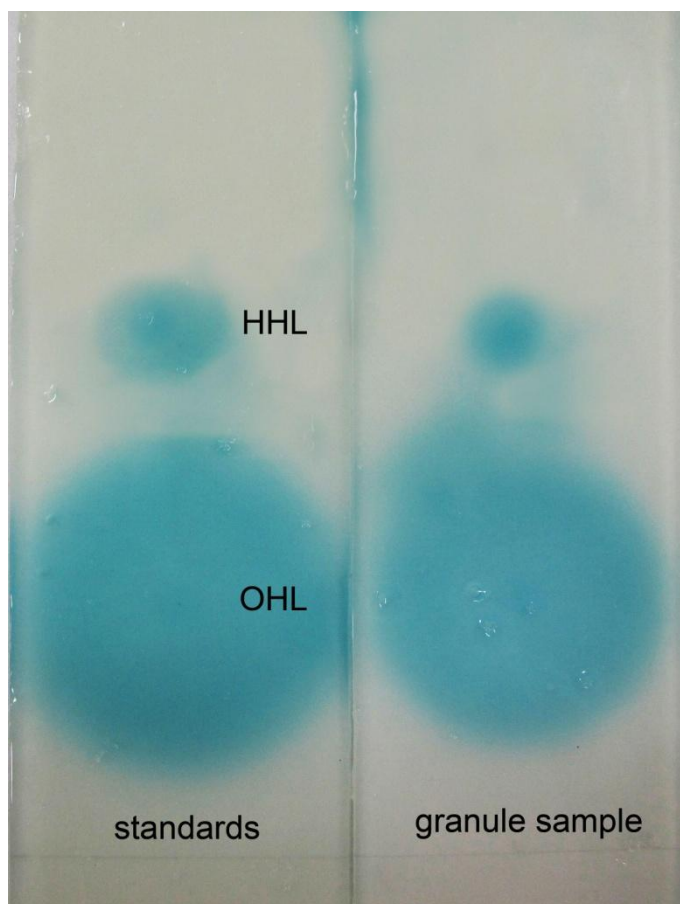


Figure 3.15 TLC analysis of AHLs. AHL sample was extracted from aerobic granules in R1, chromatographed on C18 reverse-phase thin-layer plates, developed with methanol/water (60:40, v/v) and the spots were visualized with the indicator of *A. tumefaciens* NT1 (*traR*; *tra::lacZ749*).

3.3.7 Effect of TCS on Biofilm Formation

Aerobic granules can be regarded as a special case of biofilms forming through bacterium-to-bacterium adhesion without addition of artificial biocarriers. In order to further confirm the findings reported above, the effect of TCS on biofilm formation was studied by *in vitro* adhesion assay conducted in flat-bottom 96-well tissue culture polystyrene microtiter plates. The attached cells after 12-h incubation

were stained with crystal violet followed by solubilization with 95% ethanol and the absorbance at 600 nm was recorded. This assay provides an indirect and semi-quantitative measurement of the adherent cell mass. It can be seen in Figure 3.16 that about 89% and 97% of inhibition of bacterial attachment were achieved when TCS was added into the culture medium at respective concentrations of 2 and 4 mg L⁻¹ as compared with control wells. These results suggest that the supplement of TCS in the culture medium can effectively block biofilm formation.

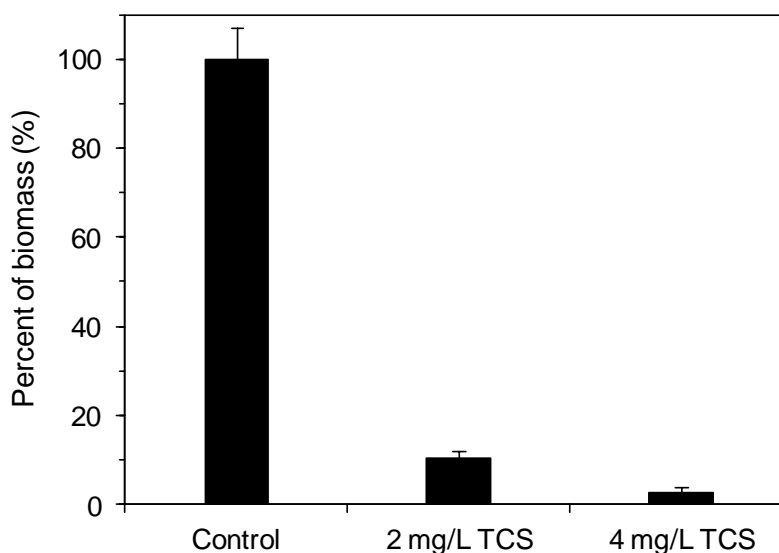


Figure 3.16 Effect of TCS on biofilm formation in flat-bottom 96-well tissue culture polystyrene microtiter plates. Each data point is the mean value of triplicate analyses and error bars represent one standard deviation.

3.4 DISCUSSION

It has been known that TCS as a typical chemical uncoupler can block the oxidative phosphorylation reaction for ATP synthesis due to its ability to collapse the proton gradient across the cellular membrane (Cook and Russell 1994;

Mathews et al. 1999). On the other hand, TCS at the concentrations studied had negligible effect on substrate removal efficiency (Figure 3.7 and Table 3.1), which is consistent with the commonly accepted understanding of that chemical uncouplers would not suppress the electron transport-associated substrate oxidation. Compared to the control reactor (R1), addition of 2 and 4 mg L⁻¹ TCS to R2 and R3 led to a significant drop in the cellular ATP content (Figure 3.10). Meanwhile, no aerobic granulation was observed in R2 and R3 (Figure 3.4). These suggest that aerobic granulation is favored by a high ATP content, while inhibited ATP synthesis by TCS can effectively suppress granulation, that is, the development of aerobic granules is ATP-dependent. Such conclusion is supported by the results obtained from biofilm formation assay in 96-well plates, showing that the addition of TCS can also effectively block biofilm development (Figure 3.16).

Klebensberger et al. (2006) investigated the response of *Pseudomonas aeruginosa* strain PAO1 to sodium dodecyl sulfate (SDS) and found that the cells started to form macroscopic aggregates at high energy supply, while no aggregates could be observed if the energy supply was reduced by inhibiting respiration with KCN or carbonyl cyanide *m*-chlorophenyl hydrazone (CCCP). Moreover, inhibition of the energy-generating function has been found to prevent the development of competence for cell aggregation in many systems (Calleja 1984; O'Toole et al. 2000). In fact, aerobic granulation is a bacterium-to-bacterium self-immobilization process, requiring aggregation of microorganisms. Once cells approach and interact with their neighbors, localized PMF and ATP on the cell surface will tend to increase, which would be the driving force for the adhering process (Ellwood et al. 1982; Hong and Brown 2009). This and previous studies demonstrate that an energized state of cells is essential for microbial aggregation, while energy deficiency would cause the failure of granule formation.

EPS has been known to contribute to cell-to-cell interaction and can further strengthen microbial structure through forming the polymeric matrix (Liu et al. 2004c; Flemming and Wingender 2010). Compared with the control reactor, both extracellular PS and PN contents in R2- and R3-biomass subjected to TCS were strikingly reduced and even less than those of seed activated sludge at the end of operation (Figures 3.8 and 3.9). It has been believed that EPS production is a metabolic strategy of cells to facilitate survival, but at the cost of consuming non-growth-associated energy. For example, the energy required for synthesis of polysaccharides and proteins is 12.6 and 36.4 mmol ATP g⁻¹, respectively (Robinson et al. 1984; Russell 2007). These seem to suggest that the decreased ATP level due to the presence of TCS would result in a reduced EPS pool, which, in part, was responsible for the failure of aerobic granulation in R2 and R3. Failed microbial attachment and/or aggregation due to inhibited EPS synthesis has also been reported in other studies. For example, in the study of free ammonia inhibition to aerobic granulation, Yang et al. (2004c) found that microbial respiratory activity was seriously inhibited at elevated free ammonia concentrations; as a result, the total amount of extracellular PS and PN was reduced accordingly, which led to the failure of aerobic granulation. Cammarota and Sant'Anna Jr. (1998) also reported that microbial adhesion and biofilm formation were significantly reduced by DNP-induced EPS inhibition. As a typical chemical uncoupler, TCS can disrupt PMF essential for ATP synthesis, hence, it is a reasonable consideration that under energy deprivation conditions, microorganisms would satisfy their basic metabolic requirements prior to synthesis and secretion of “luxury” macromolecules, such as EPS, thus compromising microbial self-aggregation as observed in Figure 3.4.

In addition, it was found that extracellular PN content was twice of extracellular PS content in R1 granules (Figures 3.8 and 3.9), i.e., extracellular PN may play an essential role in aerobic granulation. Through in situ EPS staining of aerobic granules grown on a mixed substrate of glucose and peptone, McSwain et al. (2005) revealed that the formation of aerobic granules was dependent on a noncellular protein core. In the study of the influence of cell surface properties of thermophilic streptococci on attachment to stainless steel, Flint et al. (1997) reported that treating the cells with sodium metaperiodate, lysozyme or trichloroacetic acid to disrupt cell surface polysaccharides had no effect on attachment, whereas treatment with trypsin or SDS to remove cell surface proteins resulted in a 100-fold reduction in the number of bacteria attaching. Dufrene et al. (1996) investigated the adhesion of *Azospirillum brasilense* to glass and polystyrene, and observed the correlation between protein concentration at the cell surface or at the support surface and adhesion density under different experimental conditions, which demonstrated the involvement of extracellular PN in the adhesion of *A. brasilense* to inert surfaces. Moreover, Allison and Sutherland (1987) found that a non-polysaccharide-producing mutant, as well as, the polysaccharide-producing wild type both adhered to glass surface. It is apparent that specific contributions of extracellular PS and PN to microbial adhesion and granulation are subject to further study.

Many bacterial species can employ extracellular signaling molecules as their language to coordinate self-aggregation, adhesion and biofilm formation (Riedel et al. 2001; McNab et al. 2003). In R1 free of TCS, small aggregates first appeared on day 8, before which the relative AI-2 and AHL contents were very low. Afterwards, they increased rapidly and ultimately reached to a relatively high level (Figures 3.11 and 3.13). The relationships between biomass density and relative

AI-2/AHL contents were further presented in Figures 3.17 and 3.18. It appears that both relative AI-2 and AHL contents in R1 only started to rise when a critical biomass density of around 1.0131 g mL^{-1} was achieved. Such finding is consistent with the existing understanding of density-dependent quorum sensing. At low biomass density, basal-level production of autoinducers would be rapidly diluted in the surrounding environment and eventually led to the inappreciable amount of autoinducers in biomass. As the density of biomass increased, the concentration of autoinducers increased concomitantly. Once certain biomass density or “quorum” was reached, the autoinducers would accumulate to a threshold level sufficient to be sensed and began to regulate aerobic granulation. The close correlations between biomass density and relative AI-2/AHL contents clearly suggest that AI-2- and AHL-mediated quorum sensing would be involved in the development of aerobic granules.

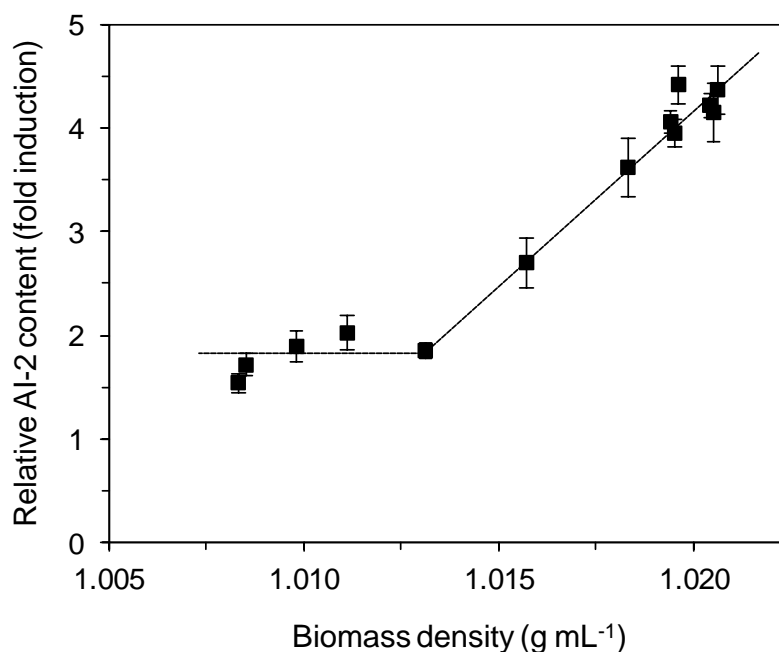


Figure 3.17 Relationship between biomass density and relative AI-2 content in R1.

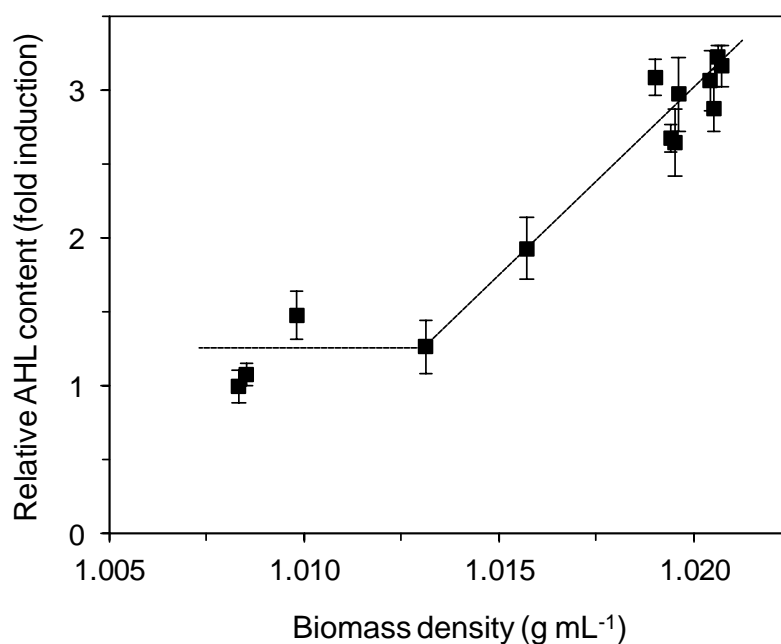


Figure 3.18 Relationship between biomass density and relative AHL content in R1.

Gram-negative bacteria can produce a variety of AHL molecules which differ only in the length of the acyl-chain moiety and the substitution at position C3 (Camilli and Bassler 2006). In order to identify the types of AHLs detected in aerobic granules, AHL extracts obtained from R1 granules were separated by TLC coupled with biodetection by a thin film of minimal medium agar seeded with the biosensor of *A. tumefaciens* NT1 (*traR*; *tra::lacZ749*). As can be seen in Figure 3.15, two intensive pigment spots were observed in TLC chromatograms. Comparison of their R_f values with those of known AHL standards showed that these AHLs preliminarily belonged to HHL and OHL, respectively. This suggests that HHL and OHL were two predominant AHLs in mature aerobic granules, i.e., they may play a more important role in aerobic granulation.

It appears from the above discussion that AI-2- and AHL-mediated quorum sensing would be essentially involved in aerobic granulation. In order to further confirm this conclusion, batch experiments in flat-bottom 96-well tissue culture polystyrene

microtiter plates with and without the addition of exogenous autoinducers were carried out. It was found that the addition of 4,5-dihydroxy-2,3-pentanedione (DPD, precursor of AI-2) and/or OHL (one of the primary AHLs in aerobic granules in R1) substantially enhanced biofilm formation (Figure 3.19). For example, the addition of 1 μ M DPD together with 4 μ M OHL resulted in 67% increase in fixed biomass as compared with the control.

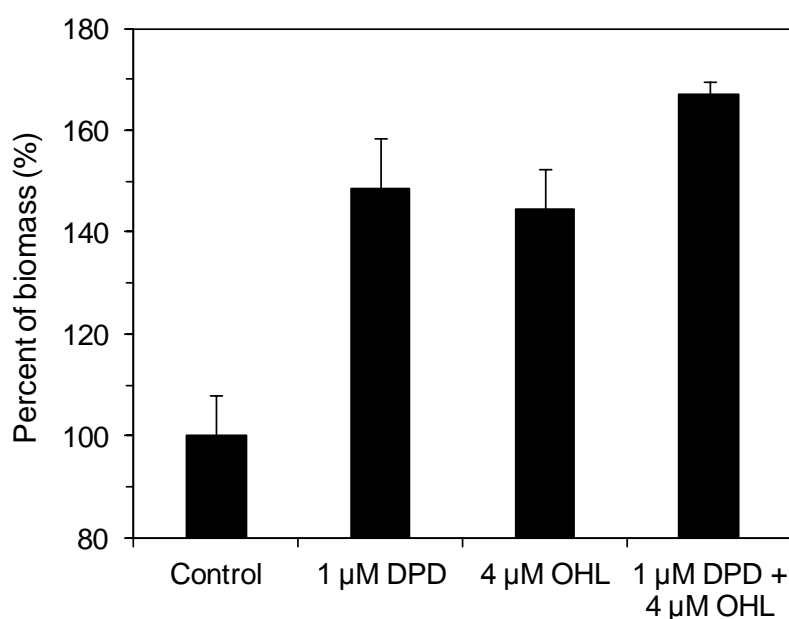


Figure 3.19 Effect of DPD and OHL on biofilm formation in flat-bottom 96-well tissue culture polystyrene microtiter plates. Each data point is the mean value of triplicate analyses and error bars represent one standard deviation.

Furthermore, luminescence and β -galactosidase bioassays revealed that AI-2 and AHL production by microorganisms exposed to TCS was significantly inhibited as compared to the control free of TCS (Figures 3.11, 3.13 and 3.14). Figures 3.20 and 3.21 illustrate the close dependence of relative AI-2 and AHL contents on cellular ATP level with and without exposure to TCS. These results indicate that the production of signaling molecules is energy-dependent, i.e., decreased ATP

content would result in reduced synthesis of AI-2 and AHLs. In fact, both AI-2 and AHLs are derived from biosynthesis pathway of S-adenosylmethionine which is made from methionine and ATP by methionine adenosyltransferase (Bassler 2002; Chen et al. 2002; Dong et al. 2007), that is, the synthesis of AI-2 and AHLs is associated with ATP. Therefore, inhibited ATP generation by TCS would be responsible for the observed reduction of AI-2 and AHLs. On the other hand, the export of signaling molecules highly depends on PMF-driven resistance-nodulation-division (RND) efflux pumps (Pumbwe et al. 2008). Under PMF dissipation conditions, the activity and expression of RND efflux pumps would be repressed, leading to the intracellular accumulation of signaling molecules rather than transporting them out of cells. For example, Pearson et al. (1999) reported that sodium azide or CCCP, both of which can de-energize cells, caused the cellular concentration of autoinducers to rise. In the study of *Pseudomonas aeruginosa* biofilm development, Ikonomidis et al. (2008) also observed the enhanced intracellular accumulation of autoinducers by inhibiting MexAB-OprM efflux system in the presence of CCCP. Similarly, TCS as a typical chemical uncoupler can effectively dissipate the PMF, and would eventually result in less export of signaling molecules out of the cell membrane. This in turn may partially explain the reduced AI-2 and AHL contents observed in R2 and R3 with the addition of TCS.

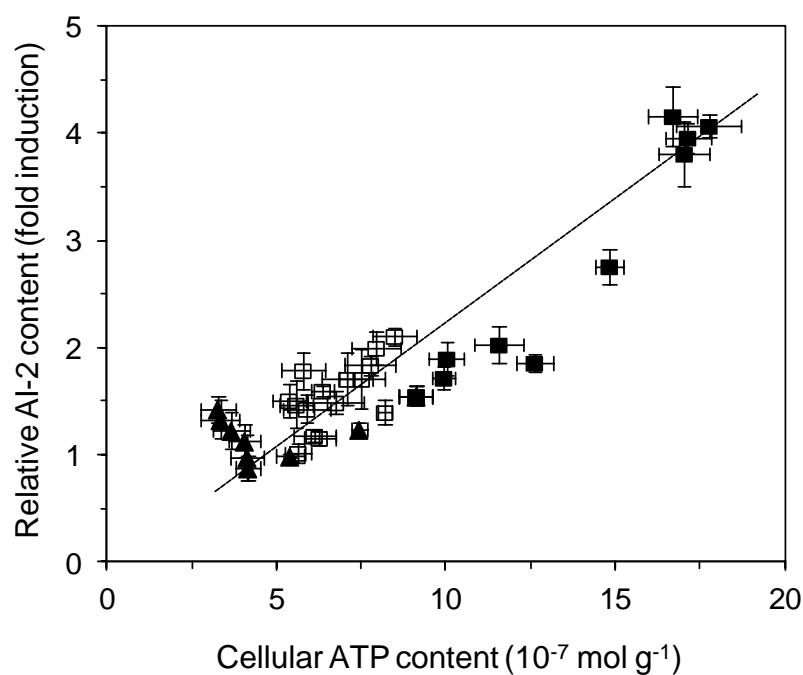


Figure 3.20 Relationship between cellular ATP and relative AI-2 contents. ■: R1 free of TCS; □: R2 with 2 mg L^{-1} TCS; ▲: R3 with 4 mg L^{-1} TCS.

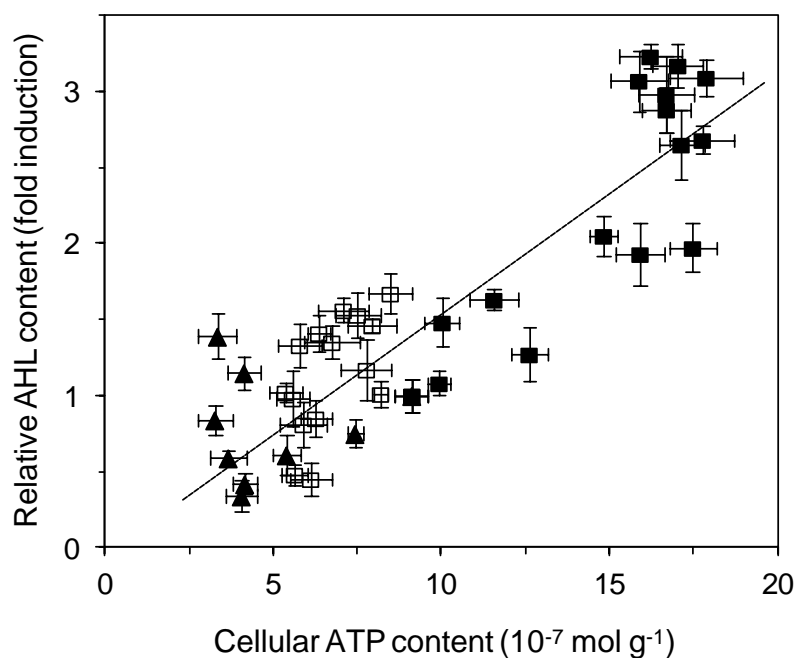


Figure 3.21 Relationship between cellular ATP and relative AHL contents. ■: R1 free of TCS; □: R2 with 2 mg L^{-1} TCS; ▲: R3 with 4 mg L^{-1} TCS.

The profiles of biomass density in R2 and R3 (Figure 3.3) imply the failure of aerobic granulation, which was evidenced by image analysis shown in Figure 3.4c and 3.4d. These together with Figures 3.11, 3.13 and 3.14 indicate that the deficiency of AI-2 and AHLs in R2 and R3 would be partially responsible for the unsuccessful aerobic granulation. In fact, failed microbial attachment or aggregation due to the inhibition of quorum sensing systems has been reported. In the study of quorum sensing and self-aggregation, Chandler et al. (2009) found that wild-type strain *Burkholderia thailandensis* would self-aggregate and form macroscopic clumps in a minimal medium, while the AHL synthase-deficient mutant strain could not. Furthermore, inactivation of *luxS* based on gene interruption in *Streptococcus anginosus* resulted in a mutant deficient in AI-2 activity and ultimately inhibited biofilm formation (Petersen et al. 2006).

3.5 SUMMARY

In this chapter, a typical chemical uncoupler TCS was employed to investigate the roles of ATP and cellular communication in the formation of aerobic granules. TCS can effectively disrupt the tight linkage between electron transport and oxidative phosphorylation, thus dissipating PMF and subsequently inhibiting ATP synthesis. Aerobic granules were successfully developed in the control reactor free of TCS, but no aerobic granulation was observed with the addition of 2 and 4 mg L⁻¹ TCS. In the presence of TCS, the ATP-dependent signaling molecules (AI-2 and AHLs) and EPS production was strongly inhibited, which resulted in the failure of aerobic granulation. Therefore, the formation of aerobic granules appears to require ATP and ATP-associated cellular communication. Furthermore, two types of AHL

molecules, i.e., HHL and OHL, were indentified in mature aerobic granules from the control reactor, indicating their essential roles in aerobic granulation. In addition, TCS at the concentrations studied did not exhibit significant influence on substrate removal efficiency.

CHAPTER 4

DEPENDENCE OF STRUCTURE STABILITY AND INTEGRITY OF AEROBIC GRANULES ON ATP AND CELLULAR COMMUNICATION

4.1 INTRODUCTION

It appears from Chapter 3 that ATP and ATP-associated cellular communication are essentially involved in the formation of aerobic granules. However, Chapter 3 did not address another fundamental question of if the maintenance of structure stability and integrity of mature aerobic granules also need ATP and cellular communication. So far, very limited information is available in the literature with regard to the possible involvement of ATP and cellular communication in maintaining the three-dimensional architecture of aerobic granules. Therefore, this chapter attempts to provide direct experimental evidence showing the possible roles of ATP and cellular communication in maintaining the structure stability and integrity of aerobic granules. For this purpose, the chemical uncoupler TCS (also used in Chapter 3) which can effectively collapse the PMF across the cellular membrane and further inhibit ATP synthesis, was employed. It is expected that this chapter would deepen the current understanding of the sustaining structure stability and integrity of aerobic granules at levels of energy metabolism and cellular communication.

4.2 MATERIALS AND METHODS

4.2.1 Experimental Setup and Operation

The same experimental setup (Figure 3.1) and operational conditions as presented in Chapter 3 were adopted in this chapter. In order to look into the possible roles of ATP and cellular communication in maintaining the structure stability and integrity of aerobic granules, mature aerobic granules pre-cultivated in the control reactor (R1) described in Chapter 3 were inoculated into two SBRs, namely G1 and G2, at the initial biomass concentration of 2 g L^{-1} . The seed aerobic granules had a mean size of $725 \text{ }\mu\text{m}$ and a biomass density of 1.017 g mL^{-1} . G1 served as the control free of TCS, while G2 was supplemented with 2 mg L^{-1} TCS. The synthetic wastewater fed to G1 and G2 was also the same as used in Chapter 3.

4.2.2 EPS Staining and Imaging

EPS staining was carried out according to the modified procedure of Chen et al. (2007a). Biosamples were centrifuged at 3,500 rpm for 5 min (KUBATO, Japan) to remove supernatant, washed twice with $1 \times$ PBS buffer (pH 7.2) and kept fully hydrated in 2-mL centrifuge tubes (Eppendorf, Hamburg, Germany) covered with aluminum foil. In extracellular PS staining, 100 μL of concanavalin A conjugated with tetramethylrhodamine (Con A, 250 mg L^{-1} , Molecular Probes, Carlsbad, CA, USA) was first dripped onto the sample and incubated for 30 min on a orbital shaker (OS-20 Boeco, Germany) at 100 rpm to stain α -mannopyranosyl and α -glucopyranosyl residues. Afterwards, 100 μL of calcofluor white solution (fluorescent brightener 28, 300 mg L^{-1} , Sigma-Aldrich) was added and the sample

was incubated with shake for another 30 min to bind with β -linked polysaccharides. In extracellular PN staining, 100 μL of sodium bicarbonate buffer (0.1 M) was introduced to the sample to maintain the amine groups in non-protonated form. Subsequently, 100 μL of fluorescein isothiocyanate solution (FITC, 1 g L⁻¹, Fluka 46950) was supplemented and incubated with shake for 1 h to bind to proteins. Samples were washed three times with 1 \times PBS buffer after each staining stage to remove loosely bound and excess dyes. Finally, sectioned aerobic granule or biofloc samples were mounted onto the microscopic glass slides for observation of the distribution of extracellular PS and PN by a confocal laser scanning microscopy (CLSM; FV300, Olympus, Japan) equipped with an Ar-He-Ne laser unit and three barrier filters, i.e., BA510IF, BA530RIF and BA585-640. The image acquisition settings, such as laser intensity, numerical aperture, gain and offset settings, were adjusted according to Toh et al. (2003) and the levels were kept constant through observation. Samples were visualized with a 10 \times objective (UPlanApo NA 0.40, Olympus) and analyzed with the Fluoview FV300 confocal software. Signals from α -polysaccharides and β -polysaccharides were recorded separately by different channels. The corresponding excitation/emission wavelengths of the dyes were as follows: Con A, 555/580 nm; calcofluor white, 355/300-440 nm; and FITC, 494/518 nm.

4.2.3 HPSEC Analysis of EPS

The high performance size exclusion chromatography (HPSEC) analysis of extracted EPS was carried out with an HPLC system (Perkin Elmer Series 200, Waltham, MA, USA) equipped with a Series 200 LC quaternary pump, a Series 200 autosampler, a Perkin Elmer 600 interface and a BioSep-SEC-S2000 gel

filtration column (300×7.8 mm, Phenomenex, Torrance, CA) thermostated at 25°C. The mobile phase at the flow rate of 1.0 mL min⁻¹ consisted of 0.005 M NaCl and 0.005% NaN₃ with a pH of 7.2 and an ionic strength of 0.01 (Garnier et al. 2005). The detection was performed at 25°C with a diode array UV/Vis detector (785A) at 280 nm. All samples were filtered through 0.20-μm syringe filters (Minisart® NY 25, Germany) prior to injection (100 μL).

4.2.4 Biofilm Detachment Assay in 96-well Plates

Experiments were designed to investigate the effect of TCS on microbial detachment from 96-well plates. For this purpose, biofilms were pre-cultivated in flat-bottom 96-well tissue culture polystyrene microtiter plates (Iwaki, Japan) for 12 h following the procedure described in Chapter 3. Afterwards, 175 μL of TCS solution (2 mg L⁻¹ in 1× PBS buffer) was carefully added into each well, whereas control wells were treated with 175 μL of 1× PBS buffer without TCS. The plates were incubated at 30°C with shake (150 rpm) for 2 h. At the end of contact, the contents in respective wells were discarded and each well was gently rinsed with 1× PBS buffer for three times to remove detached cells. The remaining biomass in each well was stained with 175 μL of 1% (v/v) Gram's crystal violet (Fluka) for 2 min followed by three wash cycles with 1× PBS buffer. Each well of the stained plates was finally decolorized with 175 μL of 95% ethanol for 2 min and the absorbance of the eluted ethanol solution was measured at 600 nm with a UV-Vis spectrophotometer (UVmini-1240, Shimadzu, Japan) as described in Chapter 3.

4.2.5 Other Methods

The biomass mean size was determined by a laser particle size analysis system (Malvern Mastersizer 2000, Malvern Instruments) or an image analyzer (SZX-ILLK2000, Olympus) with Image Pro Plus software (Media Cybernetics, L.P.; version 4.0). One-way analysis of variance (ANOVA) was employed to evaluate if there was a significant difference between test groups with and without exposure to TCS, and the level of significance was set at 5%. Details of other analytical methods and procedure can be found in Chapter 3.

4.3 RESULTS

4.3.1 Effect of TCS on Substrate Removal

Figure 4.1 shows that TCS at the concentration studied had no negative impact on COD removal efficiency as compared with the control free of TCS (one-way ANOVA, $p > 0.05$). This result is consistent with those reported in Chapter 3 (Figure 3.7 and Table 3.1), which can also be explained by the fact that chemical uncouplers would not block electron transport along the respiratory chain to electron acceptor oxygen, during which process substrates are oxidized.

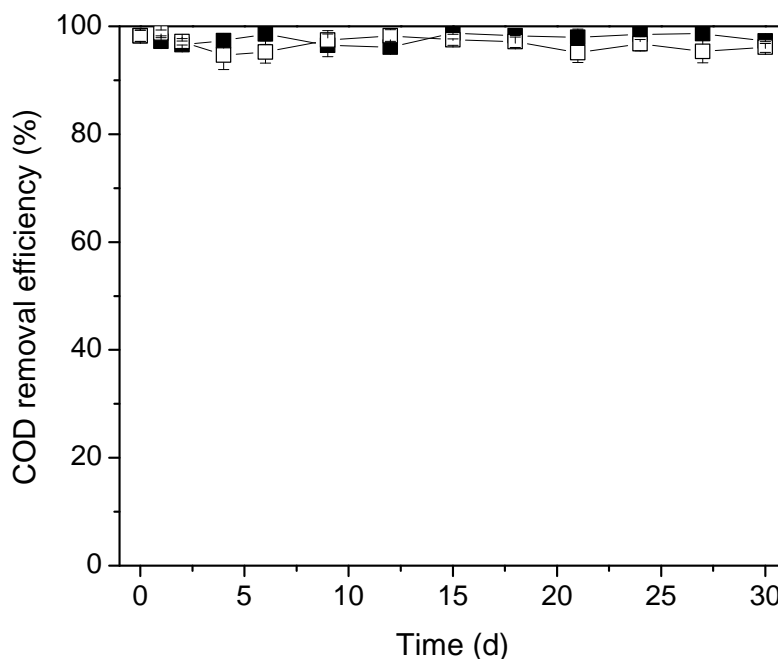


Figure 4.1 Profiles of COD removal efficiency in G1 and G2 during 30-d operation. ■: G1 free of TCS; □: G2 with 2 mg L⁻¹ TCS.

4.3.2 Effect of TCS on Granule Morphology and Structure

As discussed in Chapter 3, biomass size and density are two important parameters that have been frequently used to characterize aerobic granules. The seed aerobic granules used in this chapter had a mean size of 725 μm and a density of 1.017 g mL⁻¹. After 30 d of operation, the mean size and density of biomass in the control reactor without addition of TCS slightly increased to 950 μm and 1.025 g mL⁻¹, respectively. On the contrary, the biomass size and density in G2 supplemented with 2 mg L⁻¹ TCS dramatically decreased in the first 6 d and remained almost stable afterwards at around 300 μm and 1.005 g mL⁻¹, respectively (Figures 4.2 and 4.3), which were significantly lower than those observed in the control free of TCS (one-way ANOVA, $p < 0.05$).

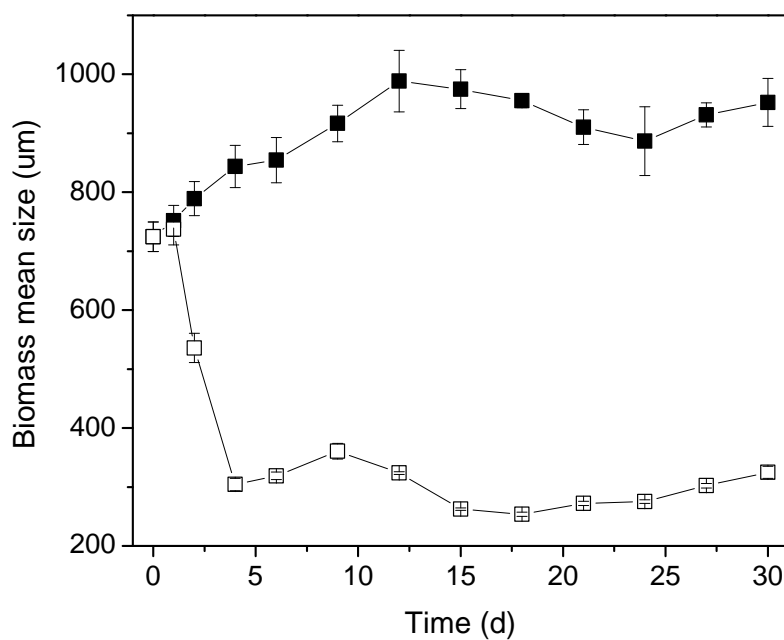


Figure 4.2 Profiles of biomass mean size in G1 and G2 during 30-d operation. ■: G1 free of TCS; □: G2 with 2 mg L⁻¹ TCS.

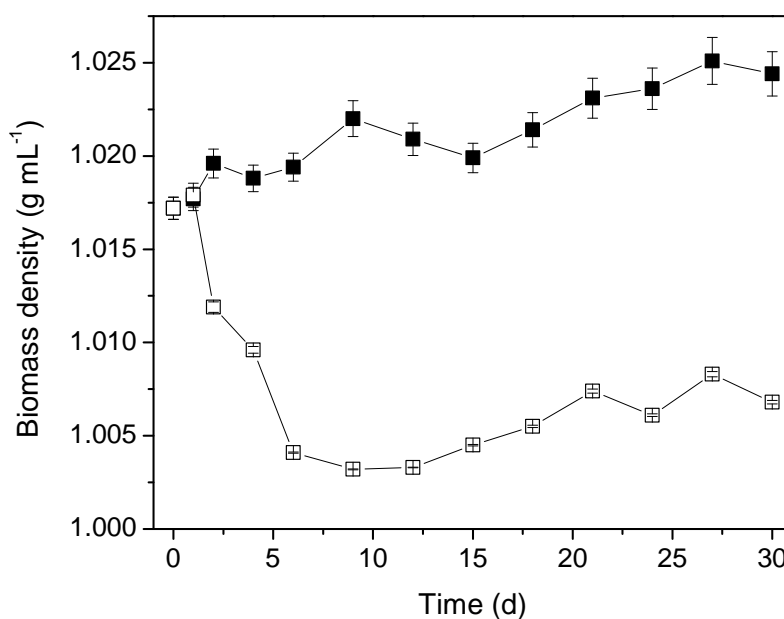


Figure 4.3 Profiles of biomass density in G1 and G2 during 30-d operation. ■: G1 free of TCS; □: G2 with 2 mg L⁻¹ TCS.

Figure 4.4 further shows the evolution of granule morphology with and without exposure to TCS. It can be seen that small aggregates gradually developed into relatively large granules in G1 free of TCS, and remained stable in terms of granule morphology and integrity over the entire operation period. Conversely, the seed aerobic granules in G2 began to disintegrate after the addition of TCS until a complete loss of granules was observed. As the consequence of granule disintegration, the suspended sludge flocs with a loose and irregular structure became the dominant form in G2 at the end of operation. The microscopic observations in Figure 4.4 are in good agreement with the changes in biomass mean size and density shown in Figures 4.2 and 4.3. These results imply that TCS as a typical chemical uncoupler can deteriorate the structure stability and integrity of pre-cultivated mature aerobic granules.

In addition, the SEM images of biomass sampled from G1 and G2 on day 30 were illustrated in Figure 4.5. It appears that non-filamentous bacteria resided in the aerobic granules and rod-like species were found to be predominant. The cells in G1-biomass were tightly linked and embedded in a filament-like EPS matrix, while no obvious EPS matrix could be observed in G2-biomass. Cavities or channels were also observed in aerobic granules, which may play an important role in mass transfer of substances between the bulk solution and the granules, that is, they would facilitate the transport of toxic metabolic by-products out of granules and the conveyance of nutrients and oxygen into the interior of granules (Liu and Tay 2004; Zhang et al. 2005b).

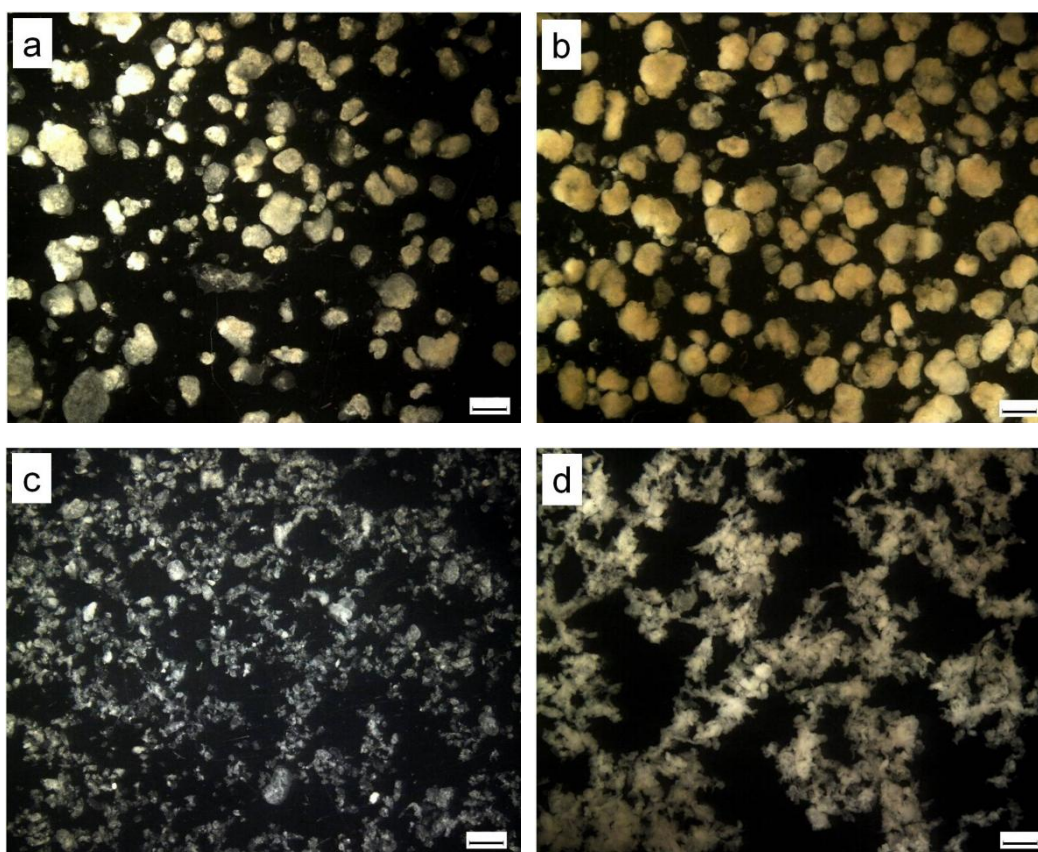


Figure 4.4 Sludge morphologies in G1 and G2. a: Seed aerobic granules; b: G1 free of TCS on day 30; c: G2 with 2 mg L⁻¹ TCS on day 4; d: G2 with 2 mg L⁻¹ TCS on day 30. Bar: 1 mm.

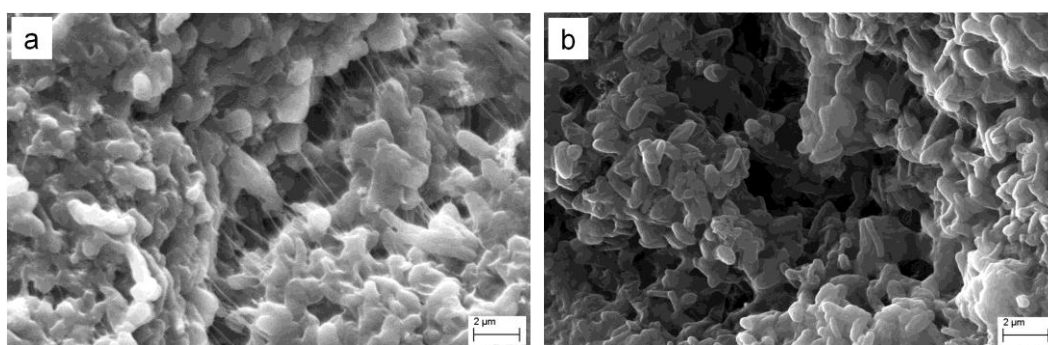


Figure 4.5 SEM images of biomass in G1 and G2 on day 30. a: G1 free of TCS; b: G2 with 2 mg L⁻¹ TCS. Bar: 2 μ m.

4.3.3 Effect of TCS on EPS

EPS attaches to the cell surface to form matrix structure which would facilitate cell-to-cell interaction and further strengthen microbial architecture (Sutherland 2001; Liu et al. 2004c; Flemming and Wingender 2010). Figure 4.6 shows the respective profiles of extracellular PS and PN contents in G1- and G2-biomass over 30-d operation. It appears that EPS content in G1-biomass remained nearly constant, i.e., 23 mg g⁻¹ MLVSS for extracellular PS and 55 mg g⁻¹ MLVSS for extracellular PN. However, EPS content in G2 fed with 2 mg L⁻¹ TCS was substantially reduced (one-way ANOVA, $p < 0.05$). For example, at the end of operation, respective extracellular PS and PN contents of G2-biomass were only about 7.6 and 21.9 mg g⁻¹ MLVSS, which were 3.1- and 2.5-fold lower than those of G1-granules.

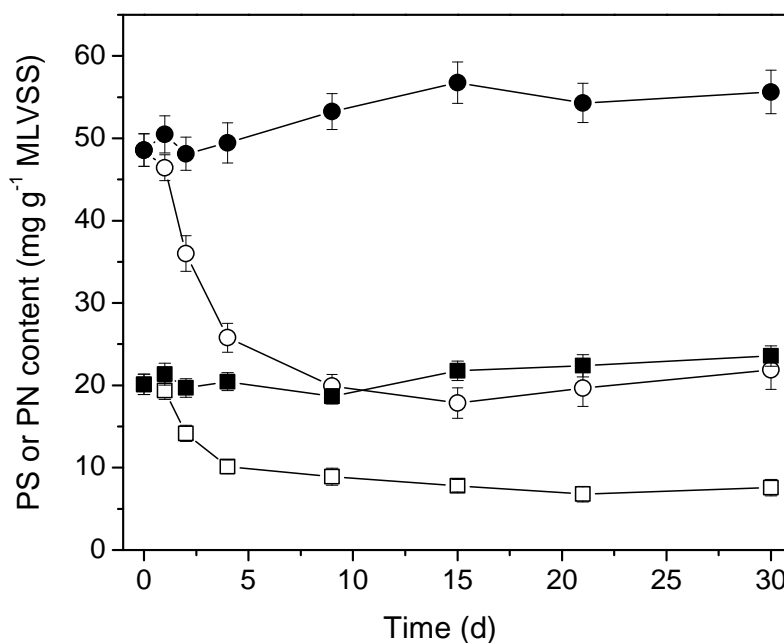


Figure 4.6 Changes of EPS content in G1- and G2-biomass during 30-d operation.

■: PS in G1; □: PS in G2; ●: PN in G1; ○: PN in G2.

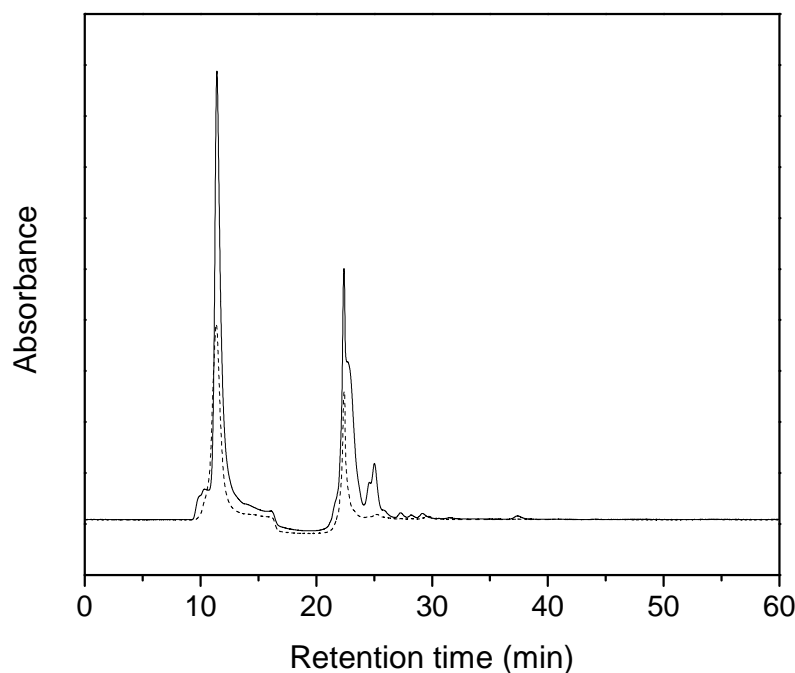


Figure 4.7 HPSEC chromatograms of EPS extracted from biomass in G1 (line) and G2 (dash) on day 30.

Figure 4.7 shows the HPSEC chromatographic profiles of the EPS extracted from G1- and G2-biomass on day 30. Generally, the EPS retention time in HPSEC spectrum is highly associated with the molecular weight, i.e., the peaks with low retention times correspond to high molecular weight molecules, whereas the peaks with high retention times represent low molecular weight molecules. Three main peaks appeared in Figure 4.7 for the EPS extracted from G1-granules, while the peak at the retention time of 25 min almost disappeared in the EPS extracted from G2-bioflocs. Such observations suggest that TCS can inhibit the production of certain type of EPS. Since the total area of the chromatogram reflects the total amount of exopolymers, Figure 4.7 also indicates that the amount of EPS extracted from G2-bioflocs exposed to TCS was much lower than that of the control granules. In fact, this is in good agreement with the results presented in Figure 4.6.

It appears from the HPSEC fingerprints that TCS can inhibit the EPS production, but also impacts on the chemical composition of EPS.

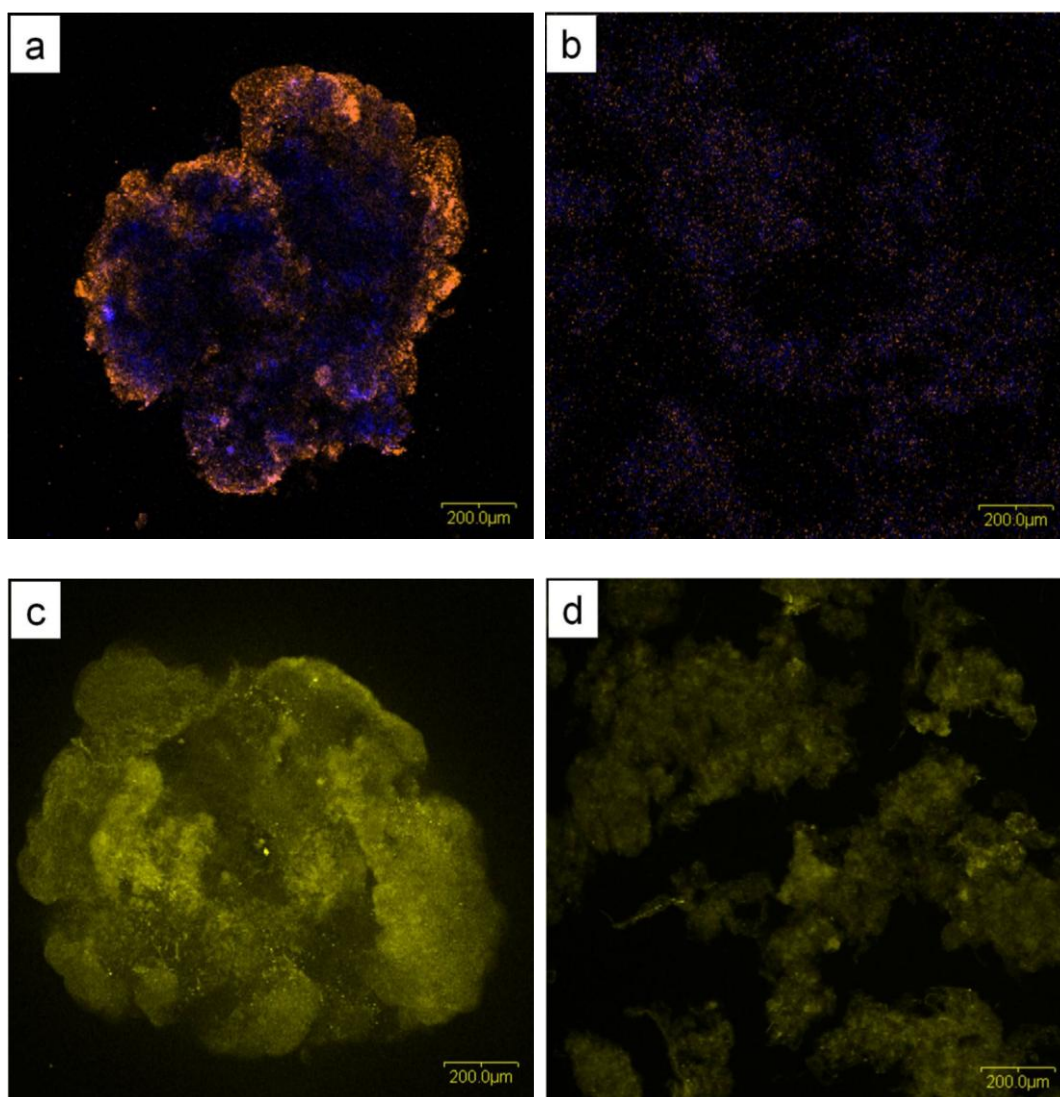


Figure 4.8 CLSM images of stained EPS in G1 and G2 on day 30. a: Extracellular PS in G1; b: extracellular PS in G2; c: extracellular PN in G1; d: extracellular PN in G2. Orange: α -polysaccharides stained by Con A. Blue: β -polysaccharides stained by calcofluor white. Yellow: proteins stained by FITC. Bar: 200 μ m.

Figure 4.8 further illustrates the fluorescent staining images of EPS distribution in G1- and G2-biomass on day 30. In G1 free of TCS, both proteins and β -polysaccharides were distributed throughout the entire granule, whereas α -polysaccharides were mainly found in the outer part of the granule. It seems that the EPS matrix would provide an architectural structure to enhance mechanical stability of aerobic granules. On the contrary, as discussed above, the aerobic granules in G2 subjected to 2 mg L^{-1} TCS disintegrated into bioflocs (Figure 4.4), thus, less EPS content and no clear EPS matrix were observed in G2-biomass. These observations provided visual evidence for Figures 4.6 and 4.7.

4.3.4 Effect of TCS on Cellular ATP Content

TCS is a typical chemical uncoupler which can effectively abolish the tight linkage between electron transport and oxidative phosphorylation, i.e., in the presence of TCS, electron transport continues, but oxidative phosphorylation is inhibited, as a result, PMF is dissipated and the efficiency of ATP synthesis would be reduced significantly (Mathews et al. 1999). Figure 4.9 shows the profiles of cellular ATP content in G1- and G2-biomass during 30-d operation. It can be seen that cellular ATP content in G1-granules remained at a relatively high and stable level of about $2 \times 10^{-6} \text{ mol g}^{-1} \text{ MLVSS}$, while ATP content in G2-biomass exposed to 2 mg L^{-1} TCS remarkably decreased (one-way ANOVA, $p < 0.05$). For instance, at the end of operation, ATP level in G2-biomass was about $1.27 \times 10^{-6} \text{ mol g}^{-1} \text{ MLVSS}$, which was 36.5% lower than that found in the control. Similarly, Figure 4.10 shows the cycle profiles of cellular ATP content in ethanol-fed aerobic granules with and without exposure to TCS. In the control reactor without addition of TCS, the cellular ATP content of ethanol-fed aerobic granules increased from 3.61×10^{-7} to

1.5×10^{-6} mol g^{-1} MLVSS, indicating a net ATP synthesis of 1.14×10^{-6} mol g^{-1} MLVSS. However, the cellular ATP content of biomass exposed to 4 mg L^{-1} TCS increased from 2.42×10^{-7} to only 5.24×10^{-7} mol g^{-1} MLVSS, i.e., a net ATP synthesis of 2.82×10^{-7} mol g^{-1} MLVSS was obtained, which was 4-fold lower than that observed in the control reactor, indicating that TCS can markedly inhibit ATP synthesis.

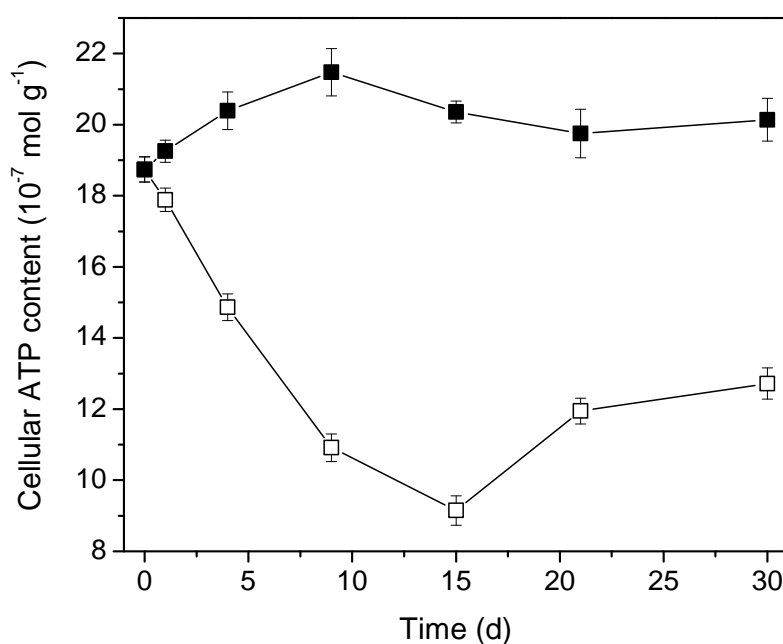


Figure 4.9 Profiles of cellular ATP content in G1- and G2-biomass during 30-d operation. ■: G1 free of TCS; □: G2 with 2 mg L^{-1} TCS.

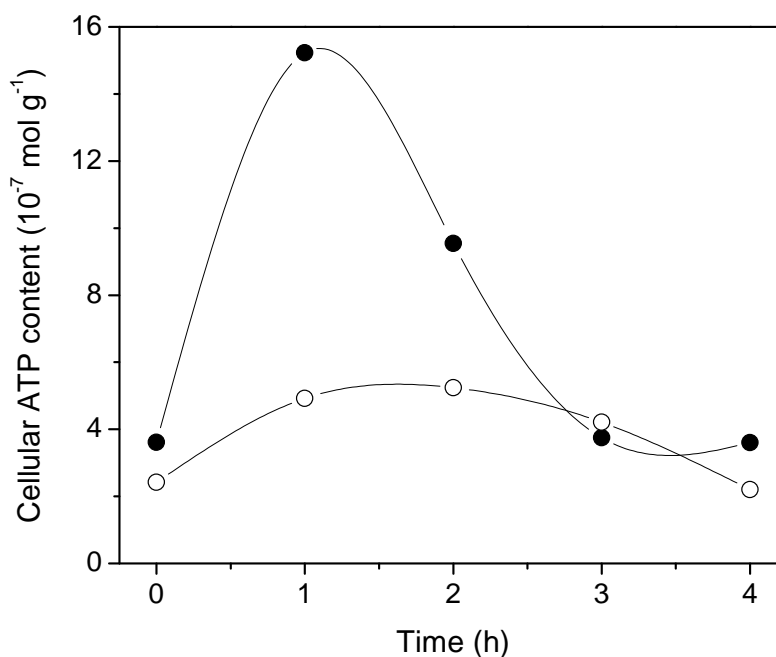


Figure 4.10 Cycle profiles of cellular ATP content in two SBRs inoculated with ethanol-fed aerobic granules. ●: SBR free of TCS; ○: SBR fed with 4 mg L⁻¹ TCS.

4.3.5 Effect of TCS on Relative AI-2 and AHL Contents

Quorum sensing through production, release and detection of signaling molecules can synchronize group behaviors of diverse bacterial species. Among various signaling molecules, AI-2 and AHLs have been recognized as two common types which can coordinate intra- and inter-species communication including biofilm formation (Rickard et al. 2006; Khajanchi et al. 2009). As discussed in Chapter 3, both AI-2 and AHLs are involved in the development of aerobic granules. However, their roles in maintaining the structure stability and integrity of aerobic granules are still unclear. As shown in Figure 4.11, Gram-negative bacteria were predominant in G1- and G2-biomass during the entire operation period, indicating AI-2- and AHL-mediated quorum sensing may be implicated in this system.

Figures 4.12 and 4.13 show the respective changes of relative AI-2 and AHL contents in G1- and G2-biomass during 30-d operation. It is obvious that both relative AI-2 and AHL contents remained at high levels in G1-granules, whereas significant reduction was observed in G2-biomass supplemented with 2 mg L⁻¹ TCS (one-way ANOVA, $p < 0.05$). For example, the relative AI-2 and AHL contents in G2-biomass were 2- and 5-time lower than those in G1-granules on day 30. Differences in AHL content between two reactors were further visualized by β -galactosidase bioassay as illustrated in Figure 4.14. It was found that intensive blue pigmentation was produced by G1-granules, while only little coloration appeared in G2-biomass, possibly suggesting that less AHL signals were produced by G2-biomass exposed to TCS. Indeed, these observations are consistent with the results presented in Figure 4.13. Consequently, TCS at the concentration studied likely can exert negative effect on the synthesis and secretion of AI-2 and AHLs.

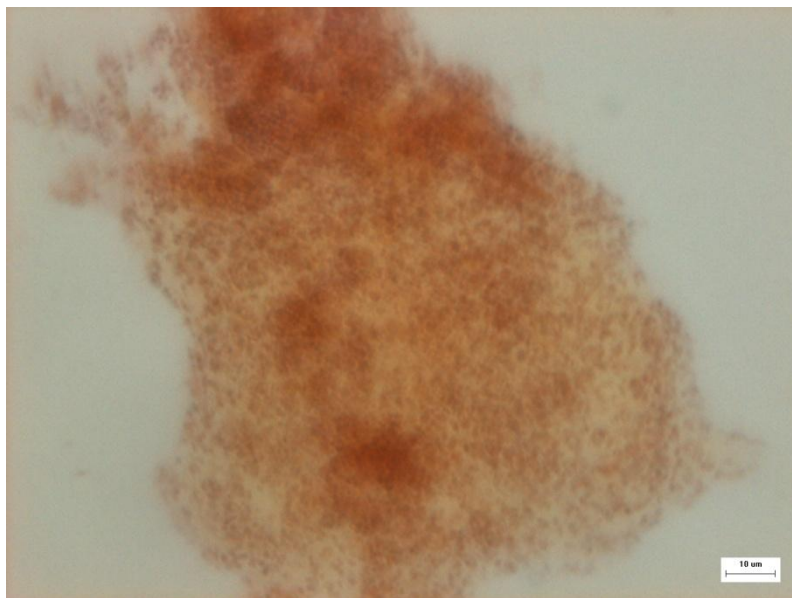


Figure 4.11 Gram-stained image of biomass. Red color represents Gram-negative bacteria. Bar: 10 μ m.

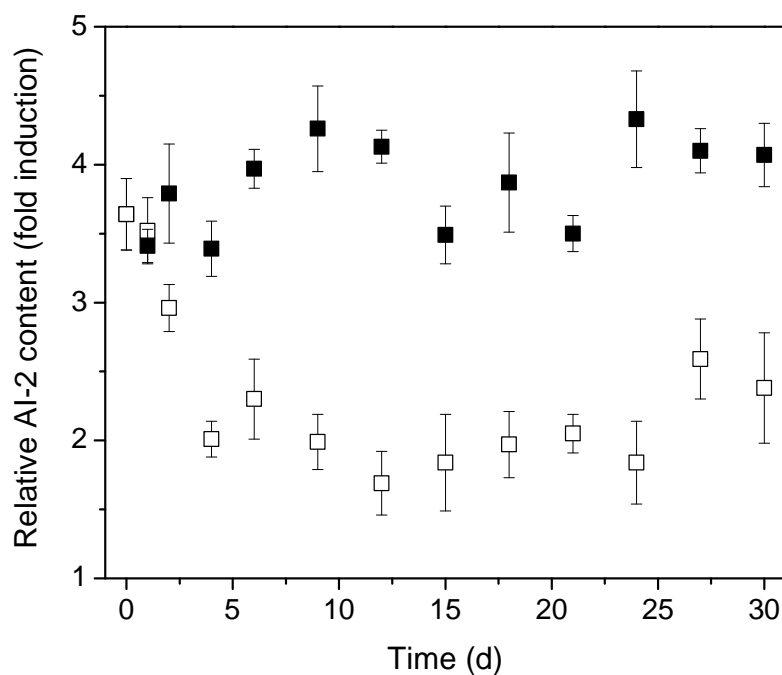


Figure 4.12 Changes of relative AI-2 content in G1- and G2-biomass during 30-d operation. ■: G1 free of TCS; □: G2 with 2 mg L⁻¹ TCS.

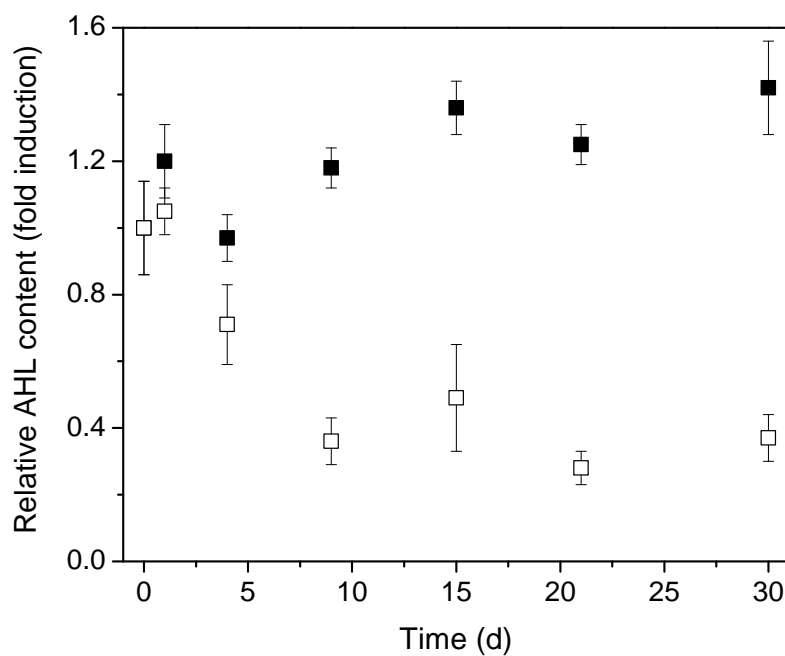


Figure 4.13 Changes of relative AHL content in G1- and G2-biomass during 30-d operation. ■: G1 free of TCS; □: G2 with 2 mg L⁻¹ TCS.

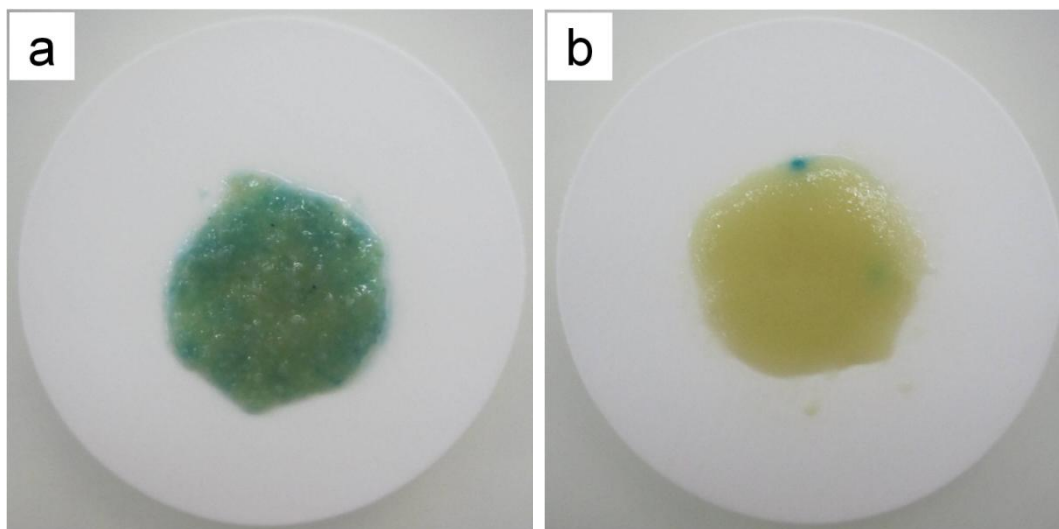


Figure 4.14 β -galactosidase bioassay of AHLs on day 30. a: G1 free of TCS; b: G2 with 2 mg L⁻¹ TCS. Blue color indicates the presence of AHLs.

4.3.6 Effect of TCS on Biofilm Stability

As discussed in Chapters 2 and 3, aerobic granules can be regarded as a special form of biofilms developed through cell-to-cell self-immobilization without addition of biocarriers. In order to further confirm the observations obtained from G1 and G2, the effect of TCS on biofilm stability was investigated by *in vitro* detachment assay in 96-well plates. For this purpose, 12-h old biofilms were pre-cultivated in flat-bottom 96-well tissue culture polystyrene microtiter plates and microbial detachment assay was subsequently carried out using these pre-cultured biofilms with and without exposure to TCS. As can be seen in Figure 4.15, the fixed biomass was reduced by 37.6% after 2-h contact with 2 mg L⁻¹ TCS, whereas the fixed biomass in the control wells was reduced only by 8.1%, i.e., the detachment of biofilms subjected to TCS was more profound than that observed in the control without exposure to TCS (one-way ANOVA, $p < 0.05$). These results

suggest that TCS at the concentration studied would effectively trigger the dispersal of biofilms, which in turn provided further support to TCS-induced disintegration of aerobic granules as shown in Figure 4.4.

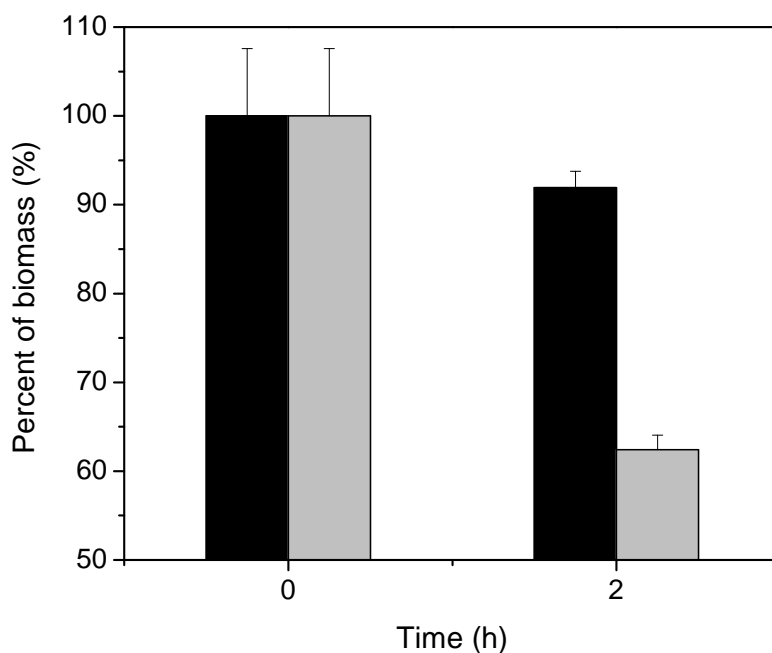


Figure 4.15 Effect of TCS on biofilm detachment from flat-bottom 96-well tissue culture polystyrene microtiter plates. Black: control wells free of TCS; grey: wells containing 2 mg L⁻¹ TCS. Each data point is the mean value of triplicate analyses and error bars represent one standard deviation.

4.4 DISCUSSION

In this chapter, the roles of ATP and cellular communication in maintaining the structure stability and integrity of aerobic granules were investigated. As discussed in Chapter 3, ATP, a principal bioenergy for living organisms, is synthesized via a chemiosmotic mechanism by coupling electron transport and oxidative

phosphorylation. TCS is a typical chemical uncoupler with the ability to collapse the chemiosmotic potential across the cellular membrane, thus inhibiting ATP generation (Mathews et al. 1999). In the control reactor (G1), cellular ATP content remained at a relatively high level, and G1-granules were found to be stable and intact throughout the entire operation period. On the contrary, cellular ATP content in G2-biomass exposed to 2 mg L⁻¹ TCS was substantially reduced (Figure 4.9), and the seed aerobic granules started to break up until complete disintegration was achieved (Figure 4.4). These seem to suggest that ATP is likely required for sustaining the structure stability and integrity of aerobic granules, and suppressed ATP synthesis by TCS would lead to the disintegration of aerobic granules. This conclusion indeed is supported by the biofilm detachment assay in 96-well plates, showing that TCS can trigger biofilm dispersal (Figure 4.15). Teo et al. (2000) studied the effect of chemical uncoupler CCCP on the strength of UASB granules, and found that the turbidity of the suspension increased by 41% when 100 µM of CCCP was added to the non-starved anaerobic granule suspension, indicating that CCCP could weaken the strength of anaerobic granules. In a study of the energetic and gene expression requirements for biofilm stability, Saville et al. (2011) reported that massive cell detachment from *Shewanella oneidensis* MR-1 biofilms occurred by the addition of oxidative phosphorylation inhibitors, such as CCCP and DNP, which are typical chemical uncouplers. It appears that cell energization would be essentially involved in maintaining the structure stability of biofilms and biogranules, while energy deprivation can trigger disintegration of microbial aggregates.

Population density-dependent quorum sensing has been believed to play a prominent role in the regulation of various microbial communal behaviors including biofilm formation (Davies et al. 1998; Surette et al. 1999). However,

little has been known about its possible involvement in maintaining the structure stability and integrity of aerobic granules. It can be seen from Figures 4.12 to 4.14 that the production of AI-2 and AHLs by microbes exposed to 2 mg L⁻¹ TCS in G2 dramatically decreased as compared with the control granules free of TCS. Moreover, positive correlations between cellular ATP and relative AI-2/AHL contents were established in Figures 4.16 and 4.17, i.e., less signaling molecules would be produced at lower cellular ATP content. Such observations can be explained by the fact that both AI-2 and AHLs are made from S-adenosylmethionine which is biosynthesized through the reaction between methionine and ATP by methionine adenosyltransferase (Bassler 2002; Chen et al. 2002; Dong et al. 2007). As such, it is reasonable to consider that the synthesis of signaling molecules is ATP-dependent. In fact, Keller and Surette (2006) have reported the metabolic costs associated with the production of signaling molecules in bacterial quorum sensing systems, e.g., 1 and 8 ATPs are required for producing one AI-2 and AHL molecules, respectively.

In addition, the PMF-associated RND efflux pumps are responsible for the transport of signaling molecules. As presented above, chemical uncouplers would result in the dissipation of PMF, which would in turn suppress the activity of the RND efflux pumps. As a consequence, signaling molecules would eventually be accumulated inside the bacterial cells rather than exported out of the membrane for cellular communication. It has been reported that PMF inhibitor CCCP caused increase in the cellular concentration of signaling molecules through inhibiting MexAB-OprM efflux system (Ikonomidis et al. 2008). Furthermore, the linkage between metabolic energy and quorum sensing has also been established in the study of quorum sensing-associated multidrug resistance and biofilm formation in *Bacteroides fragilis* with CCCP as the chemical uncoupler (Pumbwe et al. 2008).

Microscopic images in Figure 4.4 clearly showed the disintegration of aerobic granules in G2 with the addition of 2 mg L⁻¹ TCS. These observations together with Figures 4.12 to 4.14 suggest that the reduction of AI-2 and AHL contents in biomass, to some extent, would be responsible for the observed collapse of aerobic granules. In fact, decreased stability and resistance of fixed biomass due to the inactivation of quorum sensing systems were also observed in pure culture *Burkholderia cenocepacia* biofilms (Tomlin et al. 2005). Consequently, cellular communication mediated by AI-2 and AHLs is not only required in the formation of aerobic granules (Chapter 3), but also essential for sustaining the structure stability and integrity of aerobic granules.

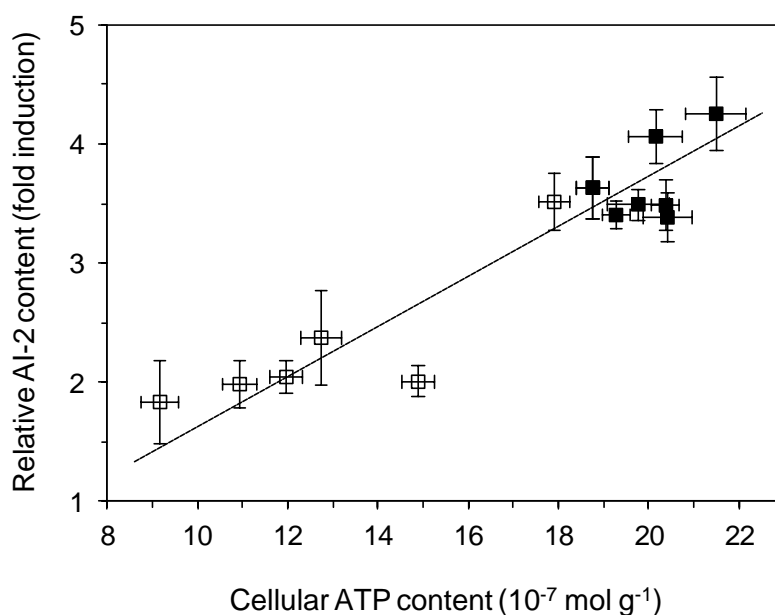


Figure 4.16 Relationship between cellular ATP and relative AI-2 contents. ■: G1 free of TCS; □: G2 with 2 mg L⁻¹ TCS.

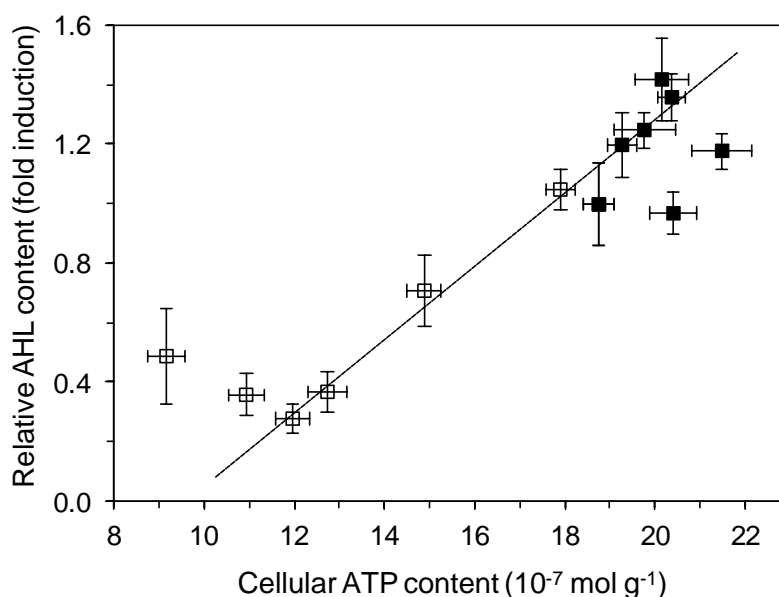


Figure 4.17 Relationship between cellular ATP and relative AHL contents. ■: G1 free of TCS; □: G2 with 2 mg L⁻¹ TCS.

EPS can facilitate microbial adhesion and aggregation through its matrix structure (Liu et al. 2004c; Flemming 2011). Figure 4.6 shows that both extracellular PS and PN contents tended to decrease in G2 supplemented with 2 mg L⁻¹ TCS as compared with the control. This is probably due to the fact that the synthesis of EPS is at the expense of consuming non-growth-associated energy, e.g., 12.6 and 36.4 mmol ATP are required for the synthesis of one gram of polysaccharides and proteins, respectively (Robinson et al. 1984; Russell 2007). In the presence of TCS, PMF is disrupted and ATP synthesis is inhibited thereafter, as a result, less energy would be available for EPS production. It has been reported that EPS deficiency either by inhibition of EPS production or by enzymatic hydrolysis of existing EPS would cause biofilm dispersal. For example, proteinase K, a wide-spectrum protease, triggered detachment in 52/53 (98%) isolates of *Staphylococcus haemolyticus* biofilms at the concentration of 0.1 mg mL⁻¹ (Fredheim et al. 2009). Similarly, *Staphylococcus epidermidis* biofilms on plastic surfaces were rapidly

and efficiently removed by *Actinobacillus actinomycetemcomitans* dispersin B, which can hydrolyze an *N*-acetylglucosamine-containing extracellular polysaccharide (Kaplan et al. 2004). It appears from this and previous studies that reduced EPS content would lead to dispersal of aerobic granules and biofilms. As can be seen in Figure 4.7, high molecular weight EPS at retention time of around 25 min disappeared in biomass exposed to TCS, indicating that TCS would inhibit the production of certain kind of EPS, i.e., TCS had effect on chemical composition and properties of EPS. In fact, Marino et al. (1985) has reported that uncouplers, e.g., DNP, CCCP, hindered the translocation of lipopolysaccharides to the outer membrane of pure culture *Salmonella typhimurium*. Microscopic images (Figure 4.4) together with Figures 4.6, 4.7 and 4.8 imply that the reduced EPS content and the destruction of EPS matrix would lead to the disintegration of aerobic granules.

Nowadays, accumulated evidence shows that EPS production is related to quorum sensing in many bacterial species and a number of quorum sensing-regulated genes involved in EPS synthesis have been identified (Marketon et al. 2003; Quiñones et al. 2005). Moreover, numerous mathematical models of quorum sensing-mediated EPS production in biofilm communities have also been developed (Anguige et al. 2006; Frederick et al. 2011). In the present study, ATP inhibition by TCS might affect the quorum sensing circuits including the production of transcription factor and gene expression required for EPS synthesis. This could partially explain the reduced EPS content in biomass exposed to TCS. On the other hand, with the reduction of EPS content and the disruption of EPS matrix, cells are prone to falling apart or detaching from granules. As a result, small nomadic bioflocs with lower biomass density were generated, eventually leading to the collapse of density-dependent quorum sensing. Conversely, biofilms or biogranules with a

stable EPS matrix would provide an ideal niche for commensal existence and efficient communication among bacterial species, which would contribute to their long-term stable mutualistic symbiosis even under some unfavourable growth conditions, such as the presence of antibiotics, limitation of nutrients, etc. (Shih and Huang 2002; Liu et al. 2010).

4.5 SUMMARY

The roles of ATP and cellular communication in sustaining the structure stability and integrity of mature aerobic granules were investigated in this chapter. The chemical uncoupler TCS, which can effectively dissipate PMF and subsequently inhibit cellular ATP synthesis was employed. Results showed that aerobic granules remained stable and intact during the whole operation period in the control reactor free of TCS, whereas aerobic granules exposed to 2 mg L⁻¹ TCS started to disintegrate until complete disappearance of aerobic granules was observed. In the presence of TCS, the production of signaling molecules (AI-2 and AHLs) was significantly suppressed, meanwhile, reduced EPS content and destructed EPS matrix were observed, leading to the collapse of aerobic granules. Furthermore, it was found that the chemical composition and properties of EPS were also altered by TCS. Consequently, this chapter for the first time clearly demonstrates that maintaining the structure stability and integrity of aerobic granules requires ATP and ATP-associated cellular communication.

CHAPTER 5

ANALYSIS OF CARBON FLOWS IN AEROBIC GRANULES

5.1 INTRODUCTION

According to microbial morphology and structure, microorganisms can be categorized into two types of growth mode, i.e., planktonic growth and immobilized growth (Dunne Jr 2002). Planktonic microorganisms, such as conventional activated sludge, have loose and nomadic structure, enabling individual cells to freely float in their environment. On the contrary, immobilized microorganisms (e.g., aerobic granules) usually exist in aggregated form and are embedded within the matrix of EPS, which results in highly compact structure. Such structural difference between planktonic and immobilized microorganisms would possibly lead to their different physiological behaviors, such as growth kinetics, energy metabolism, etc.

As discussed in Chapters 3 and 4, the development and maintenance of aerobic granules are ATP-dependent. However, some basic questions regarding the metabolic behaviors of aerobic granules are still unaddressed, e.g., (i) is there any difference in energy metabolism between aerobic granules and suspended sludge flocs? (ii) is the energy metabolism of aerobic granules biomass density-dependent? In order to answer these questions, this chapter aimed to look into the energy metabolism of highly structured and organized aerobic granules in comparison

with their counterparts, suspended bioflocs, which were produced from ground granules. For this purpose, a series of batch respiratory experiments with biomasses having different densities were carried out in a respirometric system and carbon flows into catabolism and anabolism were measured. In addition, the production of EPS and signaling molecules including AI-2 and AHLs was also investigated. This chapter is expected to offer useful information for better understanding the relationship between microbial structure and energy metabolism of aerobic granules.

5.2 MATERIALS AND METHODS

Figure 5.1 shows the respirometric system used in this chapter, which was equipped with a CO₂-free air supply unit, an air-tight bioreactor and a CO₂-trapping unit containing 1 mol L⁻¹ of sodium hydroxide solution. Mature acetate-fed aerobic granules with a mean size of 1185.6 µm and a density of 1.0257 g mL⁻¹ were pre-cultivated in an SBR. Part of the aerobic granules was gently washed and ground into suspended bioflocs which had a mean size of 130.7 µm and a density of 1.0086 g mL⁻¹. The respective morphologies of intact and ground aerobic granules are shown in Figure 5.2. It can be seen that intact granules had a regular and spherical outer shape, while ground granules had the appearance similar to the conventional activated sludge flocs. It should be noted that there was no difference in microbial population between intact and ground granules as the latter was physically produced from the former, whereas the major difference lay in the structure-associated biomass density.

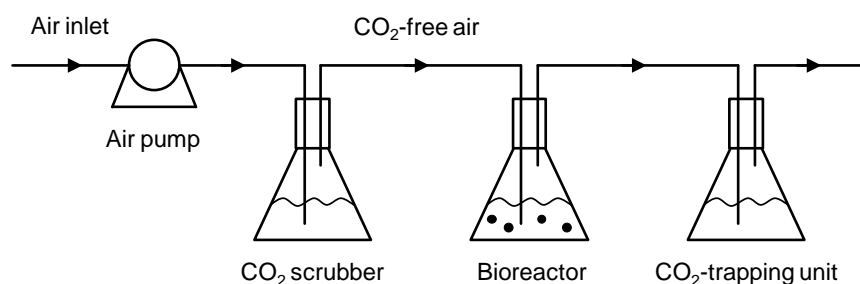


Figure 5.1 Schematic diagram of the respirometric system.

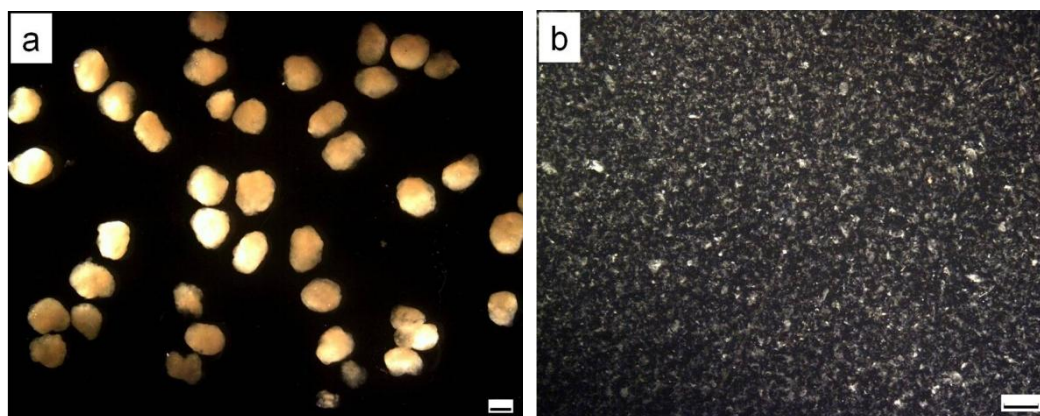


Figure 5.2 Biomass morphologies of (a) intact granules and (b) ground granules. Bar: 1 mm.

In order to investigate the relationship between biomass density and energy metabolism of aerobic granules, batch respiratory experiments were carried out with biomasses prepared by mixing intact and ground granules at five different ratios: 100% of ground granules (S1), 75% of ground granules plus 25% of intact granules (S2), 50% of ground granules plus 50% of intact granules (S3), 25% of ground granules plus 75% of intact granules (S4), and 100% of intact granules (S5). The biomass mixtures were inoculated into the bioreactor at the concentration of 1 g L^{-1} . The composition of synthetic substrate used in the batch experiments is presented in Table 5.1.

Table 5.1 The composition of synthetic substrate

Components	Concentration (mg L ⁻¹)
CH ₃ COONa	182.5 as TOC
NH ₄ Cl	100
K ₂ HPO ₄	15
KH ₂ PO ₄	15
CaCl ₂ ·2H ₂ O	15
MgSO ₄ ·7H ₂ O	12.5
FeSO ₄ ·7H ₂ O	10

After 2 h of reaction, biomass and supernatant samples were collected from the bioreactor and the CO₂-trapping unit for measurement of EPS, AI-2, AHLs, MLVSS, total organic carbon (TOC), total inorganic carbon (TIC), etc. TOC and TIC concentrations were determined by a TOC analyzer (ASI-V, TOC-V_{csb}, Shimadzu, Japan). In order to analyze the main elemental composition of biomass, intact and ground granules were washed twice with de-ionized water, dried to a constant weight at 105°C in an oven (Mettler, Germany) and then crushed into fine powder. 1.0 mg of dry biomass was used to determine the contents of carbon, hydrogen, nitrogen and sulphur by a CHNS analyzer (Perkin Elmer, 2400 II, USA). 0.1 g of dry biomass was concurrently digested with nitric acid according to Standard Method (APHA 2005) for analysis of trace elements using an inductively coupled plasma (ICP) emission spectrometer (Perkin Elmer Optima 2000 DV, USA). Analyses of other parameters were detailed in Chapters 3 and 4. One-way ANOVA at 95% confidence level was used to determine whether there were any significant differences among test groups.

5.3 RESULTS

5.3.1 Elemental Composition of Aerobic Granules

The elemental compositions of intact and ground granules were shown in Table 5.2. It is evident that there was no significant difference in elemental composition between intact and ground granules. Therefore, the average value of each element was used to compute the empirical formula of intact or ground aerobic granules. Since aerobic granules mainly consisted of C, H, O, N, S and P, the empirical formula was determined as $C_{5.87}H_{13.7}O_{3.44}NS_{0.11}P_{0.04}$.

Table 5.2 Elemental compositions of intact and ground granules

Elements	Composition (% by dry weight)	
	Intact granules	Ground granules
C	44.26	44.20
H	8.62	8.64
O	34.55	34.59
N	8.81	8.77
S	2.16	2.18
P	0.80	0.82
Ca	0.34	0.32
Na	0.10	0.10
K	0.17	0.15
Mg	0.11	0.12
Cu	0.05	0.06
Zn	0.02	0.03
Fe	0.01	0.02

5.3.2 Biomass Density and Substrate Removal

Biomass density is a vital indicator describing the compactness of a microbial community. As can be seen in Figure 5.3, the S1-biomass with 100% of ground granules had a density of around 1.0086 g mL^{-1} , which is comparable with that of conventional activated sludge. With increasing the mixing ratio of intact granules to ground granules, the biomass density gradually increased to 1.0257 g mL^{-1} for S5-biomass with 100% of intact granules. Figure 5.4 shows the profiles of TOC utilization in S1 to S5. After 2-h reaction, more than 50% of the input TOC still remained in the culture medium, implying that endogenous phase would not occur significantly.

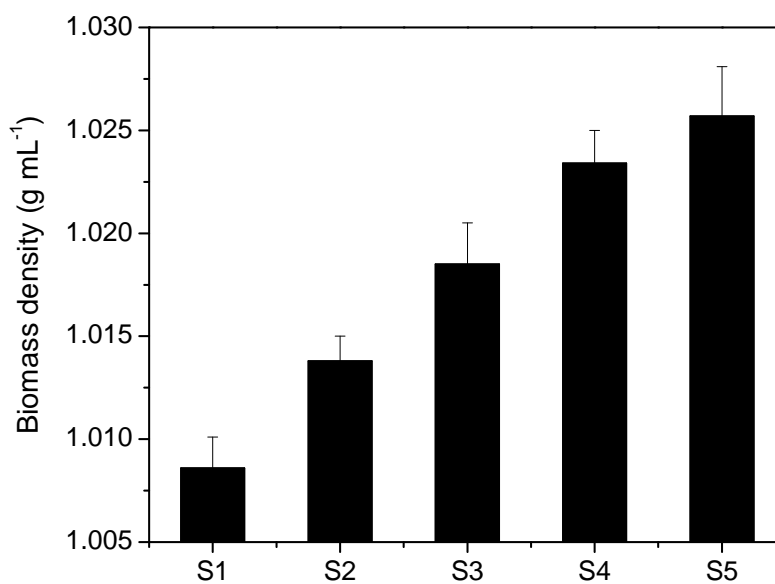


Figure 5.3 Respective densities of S1- to S5-biomass.

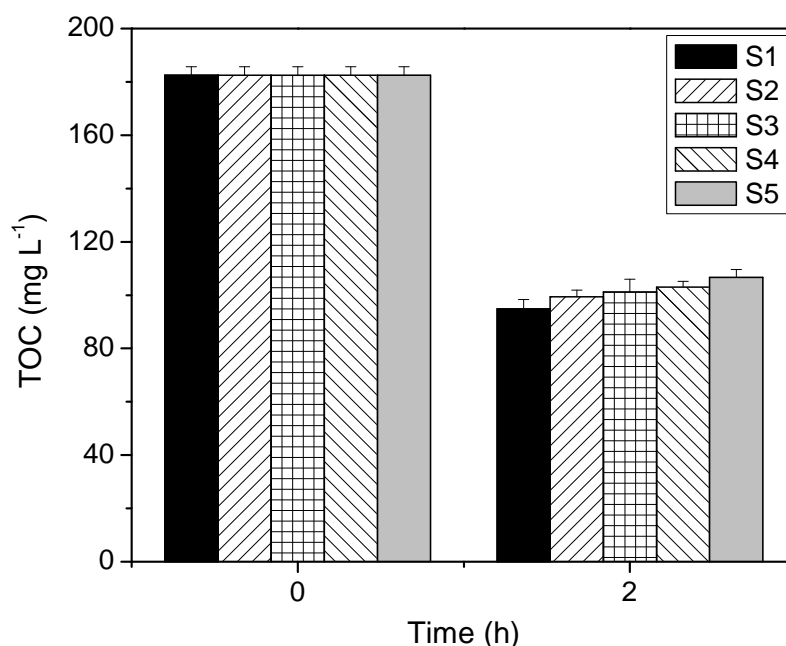


Figure 5.4 Profiles of TOC utilization by S1 to S5.

5.3.3 EPS Production and Distribution

Figures 5.5 and 5.6 illustrate the respective production profiles of extracellular PS and PN by S1 to S5 in batch cultures. It is obvious that intact granules produced more EPS than the mixtures of intact and ground granules (one-way ANOVA, $p < 0.05$). For example, the production of extracellular PS and PN by S5-biomass with 100% of intact granules was 4- and 5.7-fold of that by S1-biomass with 100% of ground granules. It appears from Figures 5.5 and 5.6 that the production of both extracellular PS and PN was positively related to the ratio of intact granules to ground granules. These results together with Figure 5.3 suggest that EPS production would be biomass density-dependent, i.e., a microbial community with a higher density would tend to produce more EPS in order to fulfill its structural requirements.

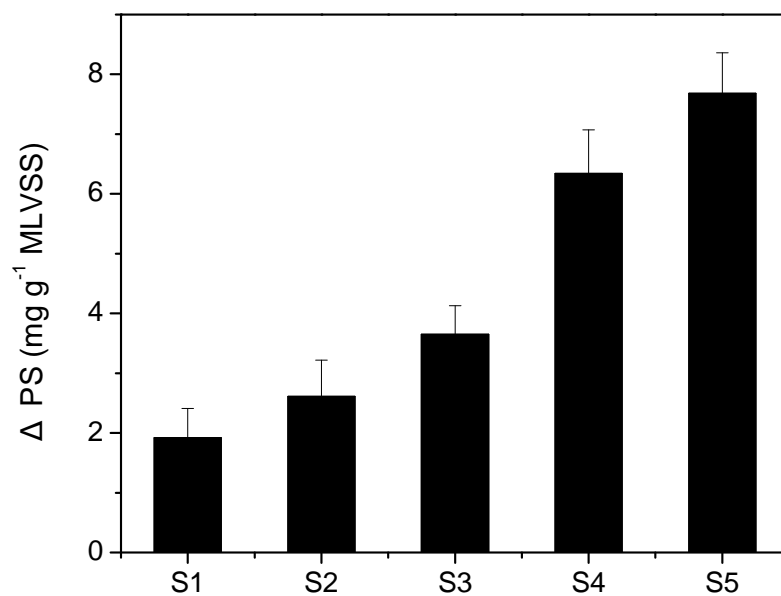


Figure 5.5 Production of extracellular PS by S1 to S5.

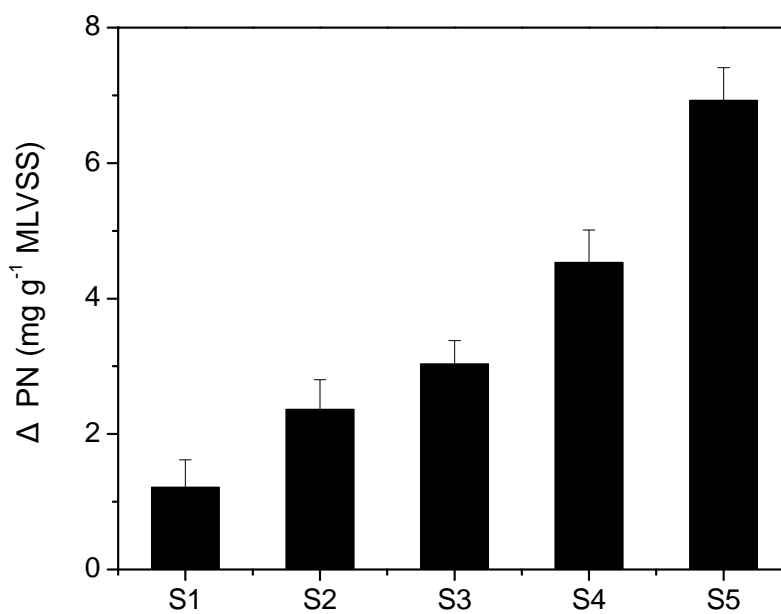


Figure 5.6 Production of extracellular PN by S1 to S5.

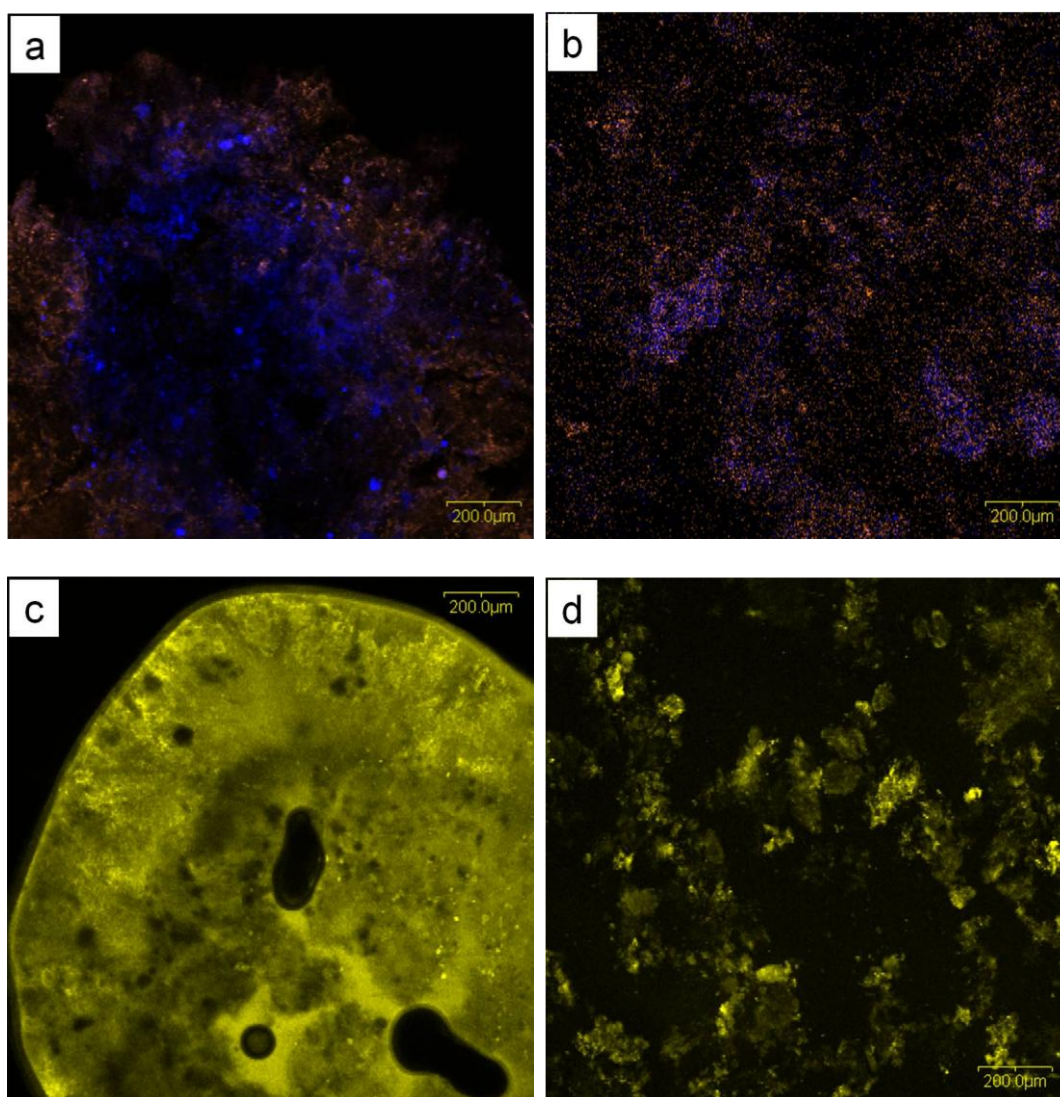


Figure 5.7 CLSM images of EPS distribution in intact and ground granules. a: Extracellular PS in intact granule; b: extracellular PS in ground granule; c: extracellular PN in intact granule; d: extracellular PN in ground granule. α -polysaccharides: orange (stained by Con A); β -polysaccharides: blue (stained by calcofluor white); proteins: yellow (stained by FITC). Bar: 200 μ m.

Figure 5.7 further reveals the differences in spatial distribution of EPS in intact and ground granules. For instance, β -polysaccharides, an important structural component of aerobic granules, were found to spread through the whole intact

granule, and a similar distribution was also observed for extracellular PN in intact granules. However, α -polysaccharides were primarily present in the outer part of intact granules. Such multiple-layered EPS matrix indeed is essential for sustaining the compact and highly organized architectural structure of aerobic granules. On the contrary, layered EPS matrix was not clearly observed in ground granules, i.e., extracellular PS and PN were distributed evenly over the biomass (Figure 5.7b and 5.7d).

5.3.4 Production of AI-2 and AHLs

AI-2 and AHLs as two predominant classes of signaling molecules have been commonly believed to coordinate biofilm formation. Figures 5.8 and 5.9 show that the production of AI-2 and AHLs was related to biomass density, i.e., more signaling molecules were produced by biomass with a higher density. For example, AI-2 and AHLs produced by intact granules were 6.3- and 3.4-time higher than those produced by ground granules. These results are in good agreement with the current understanding of that quorum sensing is regulated by biomass density, while also imply that AI-2 and AHLs would be necessarily required for maintaining the structure stability and integrity of aerobic granules.

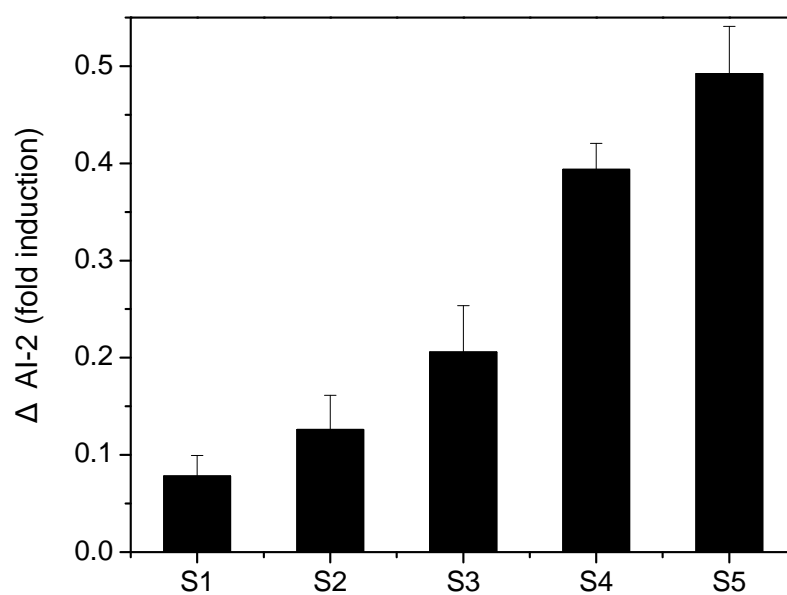


Figure 5.8 Production of AI-2 by S1 to S5.

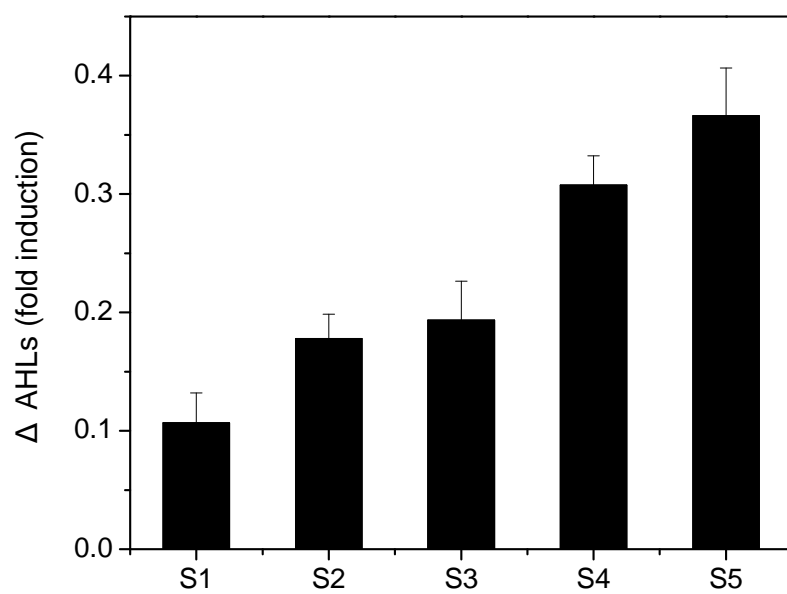


Figure 5.9 Production of AHLs by S1 to S5.

5.3.5 Carbon Flows

The metabolic network of microorganisms is the sum of biochemical transformations which basically include interrelated catabolic and anabolic reactions (Lehninger 1975). Under normal aerobic conditions, microorganisms utilize dissolved organic carbon (DOC) to form various intracellular metabolites and energy (ATP), which are then used for growth, maintenance and other energy-required activities. Thus, input DOC (C_0) can be converted to biomass-carbon (C_{biomass}), CO_2 -carbon (C_{CO_2}), soluble microbial products-carbon (C_{SMP}) and remaining original DOC (C_{ro}), i.e.,

$$C_0 = C_{\text{biomass}} + C_{\text{CO}_2} + C_{\text{SMP}} + C_{\text{ro}} \quad (5.1)$$

C_{SMP} and C_{ro} can be combined into the observed residual DOC (C_r), thus Eq. 5.1 reduces to

$$C_0 = C_{\text{biomass}} + C_{\text{CO}_2} + C_r \quad (5.2)$$

According to Eqs. 5.1 and 5.2, DOC removed by microorganisms (ΔC) can be expressed as:

$$\Delta C = C_0 - C_r = C_{\text{biomass}} + C_{\text{CO}_2} \quad (5.3)$$

The observed growth yield (Y_{obs}) is defined as the increase in biomass (ΔX) over removed DOC (ΔC):

$$Y_{\text{obs}} \text{ (g MLVSS g}^{-1} \text{ carbon)} = \frac{\Delta X}{\Delta C} \quad (5.4)$$

Similarly, the observed CO_2 production yield (Y_{CO_2}) is given by:

$$Y_{\text{CO}_2} \text{ (g carbon g}^{-1} \text{ carbon)} = \frac{C_{\text{CO}_2}}{\Delta C} \quad (5.5)$$

In fact, the observed microbial growth and CO_2 production yields reflect anabolic and catabolic activities, respectively (Burkhead and McKinney 1969).

According to the experimental data presented in Table 5.3, the observed growth and CO₂ production yields were calculated by Eqs. 5.4 and 5.5. It can be seen in Figure 5.10 that intact granules had the highest observed CO₂ production yield and the lowest observed growth yield as compared with the mixtures of intact and ground granules. For example, the observed CO₂ production yield of intact granules was 0.69 g C g⁻¹ C, i.e., 69% of consumed DOC was oxidized to CO₂. However, the observed CO₂ production yield of ground granules was about 0.45 g C g⁻¹ C, indicating that 45% of consumed DOC was transformed into CO₂. The observed growth yields of intact and ground granules were 0.66 and 1.14 g MLVSS g⁻¹ C, equivalent to 0.25 and 0.43 g MLVSS g⁻¹ COD, respectively, as 1 g DOC of acetate is equal to 2.67 g theoretical COD. It seems that the observed growth yield of ground granules is comparable with that of conventional activated sludge which has a typical growth yield of 0.4-0.6 g biomass g⁻¹ COD (Droste 1997). These results suggest that the observed growth and CO₂ production yields are biomass density-related, implying that metabolism of microorganisms would be dependent on the structural complexity and compactness of a microbial community. Elemental analysis of biomass showed that 1 g biomass contained 0.44 g carbon (Table 5.2), thus, the biomass-carbon (C_{biomass}) was calculated and presented in Table 5.3. As the input DOC concentration was 182.5 mg L⁻¹ (Table 5.1) and the working volume of the bioreactor was 60 mL, the input DOC was determined as 10.95 mg carbon. It can be seen from Table 5.3 that the carbon recoveries in S1 to S5 were greater than 97%.

Table 5.3 Carbon flows in batch respiratory experiments

	S1	S2	S3	S4	S5
Biomass density (g mL ⁻¹)	1.0086	1.0138	1.0185	1.0234	1.0257
ΔC (mg C)	5.26 \pm 0.29	4.99 \pm 0.24	4.88 \pm 0.34	4.77 \pm 0.23	4.55 \pm 0.26
C _{CO2} (mg C)	2.37 \pm 0.21	2.44 \pm 0.23	2.78 \pm 0.19	2.96 \pm 0.22	3.14 \pm 0.25
ΔX (mg MLVSS)	6.0 \pm 0.3	5.1 \pm 0.3	4.5 \pm 0.6	3.6 \pm 0.6	3.0 \pm 0.9
C _{biomass} (mg C)	2.64 \pm 0.13	2.24 \pm 0.13	1.98 \pm 0.26	1.58 \pm 0.26	1.32 \pm 0.40
Total carbon input (mg C)	10.95 \pm 0.2	10.95 \pm 0.2	10.95 \pm 0.2	10.95 \pm 0.2	10.95 \pm 0.2
Total carbon measured (mg C)	10.70 \pm 0.32	10.64 \pm 0.30	10.83 \pm 0.43	10.72 \pm 0.36	10.86 \pm 0.50
Carbon recovery (%)	97.7	97.2	98.9	97.9	99.2

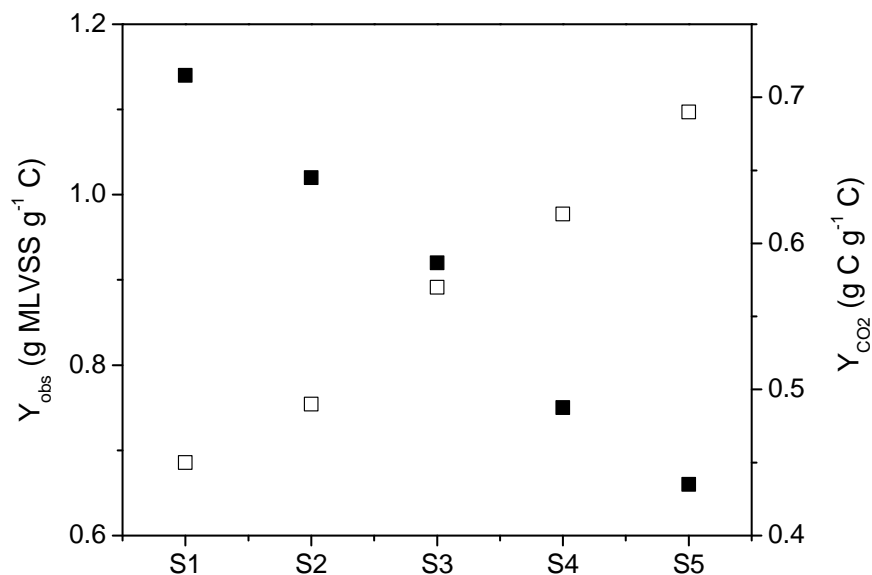


Figure 5.10 Carbon flows in the batch cultures of S1 to S5. ■: The observed growth yield (Y_{obs}); □: the observed CO₂ production yield (Y_{CO2}).

5.4 DISCUSSION

In steady state aerobic culture, removed DOC can be channeled into CO₂ by catabolism and new biomass through anabolism. As such, the physiological behaviors of a microbial culture are closely associated with the interaction between catabolism and anabolism (Liu et al. 2003b). It appears from Figure 5.10 that the observed growth yield was inversely related to catabolic activity described by the observed CO₂ production yield. This is within expectation because more carbon is utilized for CO₂ production, less carbon would be available for biomass synthesis. Figure 5.10 also shows that carbon flows between catabolism and anabolism were related to biomass density. The observed growth yield decreased with increasing biomass density, while the observed CO₂ production yield exhibited an increasing trend. Biomass density has been commonly used to describe the compactness of biofilms and biogranules, and a higher biomass density usually reflects a denser microbial community (Kwok et al. 1998; Kim et al. 2008), thus, biomass density could be regarded as an indicator of microbial structural characteristics. It seems a reasonable consideration that DOC flux between catabolism and anabolism would be biomass density-dependent and more DOC would be oxidized to CO₂ rather than used for biosynthesis by a microbial community with a higher biomass density, such as aerobic granules. In fact, high CO₂ production and low growth yields have also been observed in biofilms in a three-phase fluidized bed reactor (Vanderborght and Gilliard 1981).

The observed CO₂ production yield represents the catabolic activity of aerobic oxidation, i.e., it can indirectly reflect the energy generated from catabolism. Figure 5.11 further illustrates the relationship between biomass density and the

observed CO₂ production yield in S1 to S5. It is apparent that the observed CO₂ production yield quasi-linearly increased with the increase in biomass density, i.e., the catabolic activity or energy metabolism was positively correlated with biomass density. This means that extra energy derived from catabolism would be required to maintain the densely packed three-dimensional structure of aerobic granules. In fact, this viewpoint is supported by the results presented in Chapter 3 (Figure 3.10), showing that cellular ATP content of biomass increased along granulation process. In a study of biofilms, Liu and Tay (2001) found a correlation between catabolic activity and biofilm density, and further hypothesized that biofilm community was able to regulate its metabolic pathway via consuming non-growth-associated energy to maintain its mechanical stability.

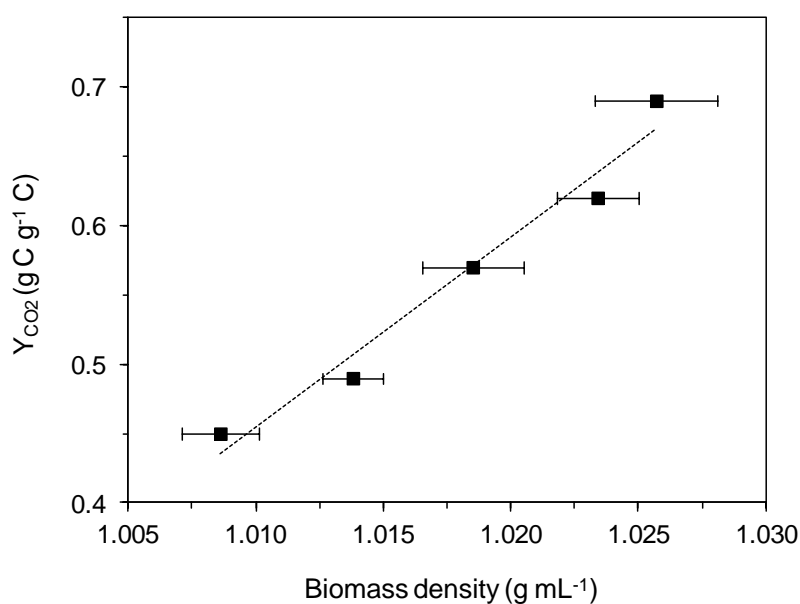


Figure 5.11 Relationship between biomass density and the observed CO₂ production yield.

EPS has been believed to be essential for maintaining the compact and stable microbial structure of aerobic granules through the formation of an interconnected

polymeric matrix. It can be seen from Figures 5.3, 5.5 and 5.6 that more EPS was produced by biomass with a higher density. Compared to suspended bioflocs, high EPS content in aerobic granules has often been reported in the literature. For example, Wang et al. (2006a) found that aerobic granules synthesized a great amount of polymers, while the EPS content in suspended sludge remained nearly unchanged. Vandevivere and Kirchman (1993) also observed that the amount of extracellular PS was 5-fold greater for attached cells than for their free-living counterparts. Furthermore, it appears from Figures 5.12 and 5.13 that the production of extracellular PS and PN was proportionally correlated to the observed CO₂ production yield, suggesting that EPS production would need energy input. Indeed, the synthesis of extracellular PS and PN is highly ATP-dependent, e.g., 12.6 and 36.4 mmol ATP is required to synthesize one gram of polysaccharides and proteins, respectively (Russell 2007). Reduced EPS production by suppressing catabolic activity was reported in the study of the inhibition of free ammonia to aerobic granulation (Yang et al. 2004c). Moreover, disappearance of aerobic granules due to lowered EPS content was also observed (Tay et al. 2001a), whereas EPS hydrolysis by enzymes resulted in collapse of structural integrity of aerobic granules (Adav et al. 2008b). For a highly compact microbial community, like aerobic granules, its structural stability essentially depends on EPS-associated polymeric matrix. This may provide an explanation for the observed biomass density-dependent EPS production.

It has been known that EPS production is a metabolic strategy for microbial community to protect fixed microorganisms from detachment from a solid surface or cell aggregate. For example, Tay et al. (2001b) found that when the shear force in term of superficial upflow air velocity exerted on granular sludge increased, much more energy generated by catabolism would be used for the production of

EPS rather than for microbial growth purpose, which in turn would help to maintain a balance with the external detachment forces. Similar phenomenon was observed in biofilms (Liu and Tay 2002; Ramasamy and Zhang 2005). It appears that microbial community can regulate its metabolic pathway through consuming non-growth-associated energy for EPS production in order to keep the microbial cells in immobilized form. Similarly, aerobic granules would also have to produce sufficient amount of EPS so as to maintain their structure stability and integrity. Thus, more non-growth-associated energy would be consumed, ultimately leading to a lower growth yield as observed in Figure 5.10. On the contrary, microorganisms in ground granules returned back to planktonic form with a weak and loose structure. As such, essentially there is no need for them to secrete excessive EPS to maintain their loose floc structure.

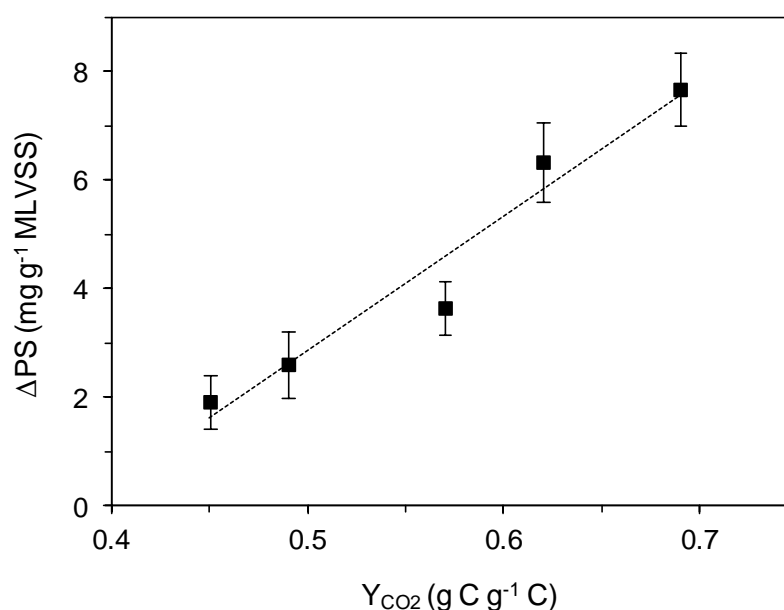


Figure 5.12 Dependence of extracellular PS production on the observed CO₂ production yield.

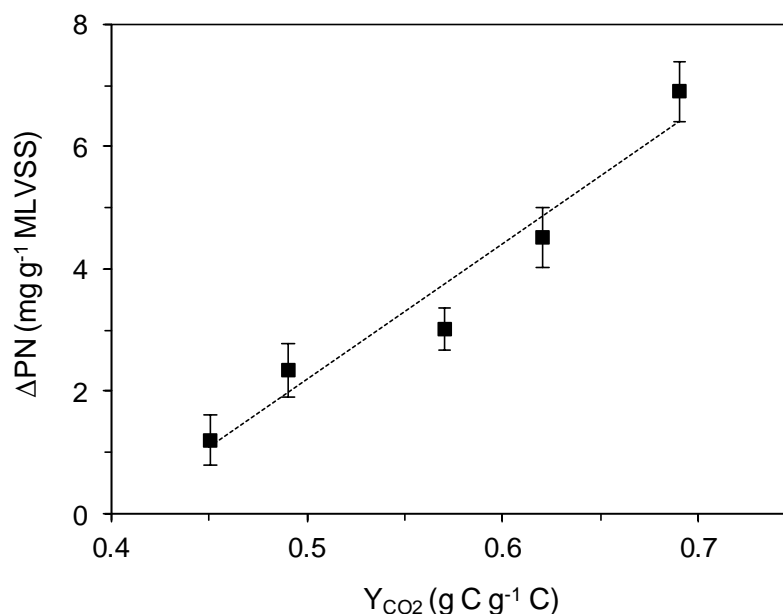


Figure 5.13 Dependence of extracellular PN production on the observed CO₂ production yield.

Similar to EPS production, Figures 5.3, 5.8 and 5.9 show that the production of AI-2 and AHLs was also biomass density-dependent, e.g., intact aerobic granules produced more signaling molecules than biomasses with lower densities. These results are in good agreement with the current understanding of biomass density-dependent quorum sensing. On the other hand, cellular communication appeared to be involved in maintaining the structure stability and integrity of aerobic granules. So far, cellular communication has been commonly recognized to mediate biofilm formation. For example, AHL-dependent quorum sensing systems have been identified to control biofilm formation between *Pseudomonas aeruginosa* and *Burkholderia cepacia* (Riedel et al. 2001). McNab et al. (2003) showed that *luxS* mutants of *Streptococcus gordonii* and *Porphyromonas gingivalis* could not form mixed-species biofilms, while complementation of the *luxS* mutation in either *S. gordonii* or *P. gingivalis* strain could reverse the defect. However, limited information is available for the post-role of cellular communication in mature

biofilms and aerobic granules. Existing evidence shows that bacteria in biofilm community are not randomly distributed, but highly organized to best satisfy the requirements of each individual cell and derive adaptive benefits from multicellular cooperation, such as efficient proliferation; effective metabolic interaction for exchange of nutrients and metabolites; decreased chance of dehydration through EPS matrix formation; collective defense against antimicrobial agents, biocides and stresses; gene transfer among microorganisms; etc. (Shapiro 1998; Davey and O'Toole 2000; Donlan 2002; Annous et al. 2009). Therefore, from an evolutionary perspective, bacteria in mature biofilms would still need continuous communication with their neighbors so as to coordinate synchronized microbial behaviors in the complex living environment (Hooshangi and Bentley 2008). In fact, some preliminary evidence has been documented. For instance, bacteria might use quorum sensing to regulate expression of extracellular enzymes to degrade macromolecules, which is advantageous to initiating catabolic production (Keller and Surette 2006). Similar to biofilm community, aerobic granules also have highly organized three-dimensional structure packed with millions of various bacteria. Thus, it is reasonable to consider that cellular communication would be essential for coordinating interactions among microorganisms living in a highly confined space of aerobic granules. The aggregated living mode of granule-associated bacteria allows all species to interact with the environment collectively which would benefit population survival. These are strongly evidenced by experimental findings showing that aerobic granules are much more tolerant than suspended sludge flocs toward the toxicity of wastewater containing heavy metals and xenobiotic pollutants (Tay et al. 2005a; Maszenan et al. 2011). In addition, EPS production was found to increase with the production of signaling molecules (Figures 5.5, 5.6, 5.8 and 5.9), suggesting that signaling molecules may play roles in mediating EPS synthesis. In fact, it has been reported

that reduced AI-2 activity by inactivation of *luxS* in *Erwinia amylovora* strain NCPPB1665 impaired the production of extracellular PS (Gao et al. 2009). Moreover, in comparison of the symbiotic process of wild type *Sinorhizobium meliloti* and the autoinducer synthase gene mutant, Marketon et al. (2003) found that exopolysaccharide production was controlled by AHL-mediated quorum sensing. Obviously, future study is strongly needed to illustrate possible linkage between EPS and signaling molecules.

Figures 5.14 and 5.15 further show the positive correlations of the observed CO₂ production yield with AI-2 and AHL production, indicating that the production of signaling molecules was energy-associated. Such observations are in accordance with the results presented in Chapter 3 (Figures 3.20 and 3.21) and Chapter 4 (Figures 4.16 and 4.17). These can also be indirectly supported by the findings of Surette and Bassler (1998), showing that signaling activity produced by *Salmonella typhimurium* LT2 reached maximum at exponential growth phase, while it was severely impaired at stationary phase when the glucose (substrate) was depleted from the medium. In fact, it has been known that S-adenosylmethionine, which serves as the substrate for *in vivo* production of both AI-2 and AHLs, is made from ATP and methionine by methionine adenosyltransferase (Bassler 2002; Dong et al. 2007), that is, the synthesis of AI-2 and AHLs requires energy. According to Keller and Surette (2006), the synthesis of each AI-2 and AHL molecule requires at least 1 and 8 ATPs, respectively. Consequently, more signaling molecules produced by intact granules would need more energy input, which, in turn, provided a plausible explanation for the higher observed CO₂ production yield and the lower observed growth yield as shown in Figure 5.10.

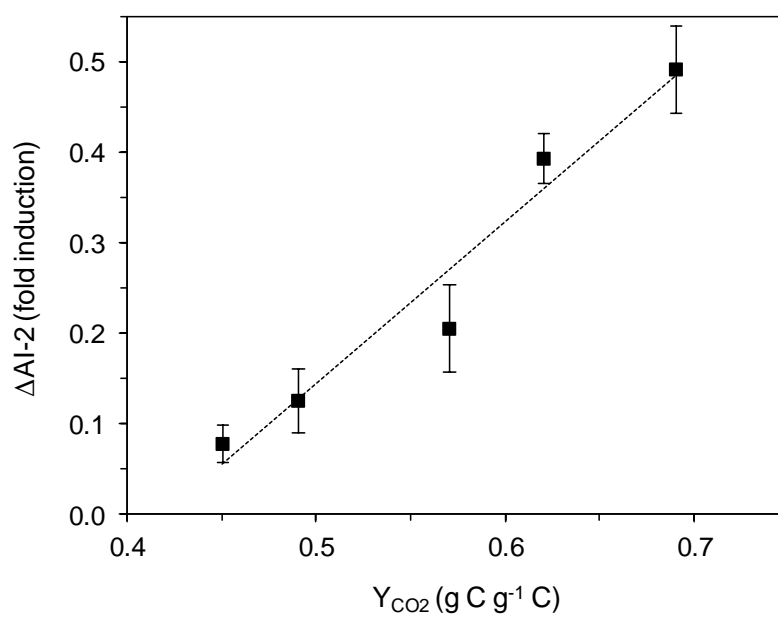


Figure 5.14 Dependence of AI-2 production on the observed CO₂ production yield.

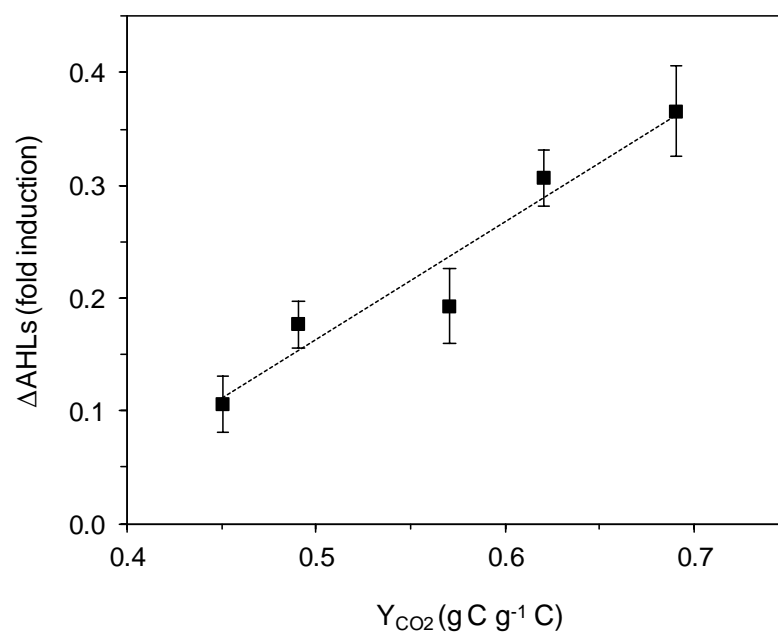


Figure 5.15 Dependence of AHL production on the observed CO₂ production yield.

5.5 SUMMARY

In order to investigate the relationship between microbial structure and energy metabolism of aerobic granules, a series of batch respiratory experiments were carried out with biomasses having different densities and carbon flows to catabolism and anabolism were measured. Results showed that intact aerobic granules with the most compact structure had the highest observed CO₂ production yield and the lowest observed growth yield as compared to the mixtures of intact and ground granules, i.e., more DOC was channeled into catabolism for energy production rather than diverted into anabolism for biomass synthesis in intact aerobic granules. In order to maintain their compact and highly organized three-dimensional structure, aerobic granules would have to produce more EPS and signaling molecules (e.g., AI-2 and AHLs), but at the cost of consuming more non-growth-associated energy. The results presented in this chapter provided direct experimental evidence that the energy metabolism of microbial community would be structure-related.

CHAPTER 6

CONCLUSIONS AND RECOMMENDATIONS

6.1 CONCLUSIONS

This study investigated the possible roles of ATP and ATP-associated cellular communication in the formation and maintenance of aerobic granules. Following conclusions can be drawn from this study.

1. The formation of aerobic granules required ATP and ATP-associated cellular communication

Results showed that the development of aerobic granules was completely inhibited by a typical chemical uncoupler TCS, which can effectively dissipate the PMF and subsequently inhibit ATP synthesis. On the contrary, aerobic granules were successfully cultivated in the control reactor free of TCS. In the absence of TCS, cellular ATP content increased along aerobic granulation process, meanwhile, the increase in the production of signaling molecules, e.g., AI-2 and AHLs, as well as EPS was also observed. Conversely, the production of AI-2, AHLs and EPS was significantly suppressed when the energy was deprived of by supplement of 2 and 4 mg L⁻¹ TCS, which was responsible for the failure of aerobic granulation. These results demonstrated that ATP and ATP-associated cellular communication were essential in the formation of aerobic granules. Moreover, two AHL molecules were found to be primarily present in mature aerobic granules, i.e., HHL and OHL, indicating they may play important roles in aerobic granulation. In addition, TCS

at the concentrations studied did not show significant influence on substrate removal efficiency.

2. ATP and ATP-associated cellular communication were essentially involved in maintaining the structure stability and integrity of aerobic granules

Results showed that mature aerobic granules remained stable and integral during the whole operation period in the control reactor free of chemical uncoupler TCS. However, aerobic granules disintegrated due to energy uncoupling by the addition of 2 mg L⁻¹ TCS. In the absence of TCS, cellular ATP, AI-2, AHLs and EPS contents kept nearly constant in aerobic granules in the control reactor, while ATP synthesis was dramatically inhibited after exposure to 2 mg L⁻¹ TCS which subsequently resulted in reduced production of signaling molecules (AI-2 and AHLs) for cellular communication. Meanwhile, decreased EPS content and destructed EPS matrix were also observed after the addition of TCS. These led to the collapse of aerobic granules. Experimental results revealed that ATP and ATP-associated cellular communication played indispensable roles in sustaining the structure stability and integrity of aerobic granules.

3. The energy metabolism of aerobic granules was structure-related

Batch respiratory experiments showed that aerobic granules had the highest observed CO₂ production yield and the lowest observed growth yield as compared to biomasses with lower densities. Aerobic granules have highly organized three-dimensional structure embedded with various bacterial species. In order to maintain such compact and complex structure, microorganisms in aerobic granules would have to produce more EPS to form polymeric matrix and more signaling molecules (e.g., AI-2 and AHLs) for microbial communication. As a result, more

non-growth-associated energy would be consumed. Thus, more DOC in the substrate would be diverted into catabolism for energy production and less carbon would be channeled into anabolism for growth, which was responsible for the enhanced CO₂ production yield and lowered growth yield as observed in aerobic granules. Consequently, the energy metabolism of aerobic granules appeared to be structure-related.

6.2 RECOMMENDATIONS

This study provided deeper insights into the mechanisms of aerobic granulation at levels of energy metabolism and cellular communication. In order to fundamentally understand this biotechnology and put it into practice for full-scale wastewater treatment, future study should look into the following aspects:

- The possibility of expediting the development of aerobic granules in SBRs by enhancing energy metabolism or cellular communication of microorganisms needs to be examined.
- The relationship between aerobic granulation and microbial community dynamics should be investigated. The physiological behaviors of aerobic granule-associated bacteria, such as quorum sensing-controlled gene expression and gene transfer, also need further examination.

- It is desirable to study the feasibility of cultivation of aerobic granules with genetically engineered species for treating multiple toxicants in wastewater.
- It would be interesting to look into the feasibility of coupling aerobic granule-based biotechnology with other treatment units, such as membrane bioreactor (MBR), to complement advantages from both processes for efficient wastewater treatment.

REFERENCES

- Adav, S. S., Lee, D. J. and Lai, J. Y. (2007a) Effects of aeration intensity on formation of phenol-fed aerobic granules and extracellular polymeric substances. *Applied Microbiology and Biotechnology* **77**(1): 175-182.
- Adav, S. S., Lee, D. J. and Ren, N. Q. (2007b) Biodegradation of pyridine using aerobic granules in the presence of phenol. *Water Research* **41**(13): 2903-2910.
- Adav, S. S. and Lee, D. J. (2008a) Extraction of extracellular polymeric substances from aerobic granule with compact interior structure. *Journal of Hazardous Materials* **154**(1-3): 1120-1126.
- Adav, S. S. and Lee, D. J. (2008b) Single-culture aerobic granules with *Acinetobacter calcoaceticus*. *Applied Microbiology and Biotechnology* **78**(3): 551-557.
- Adav, S. S., Lee, D. J., Show, K. Y. and Tay, J. H. (2008a) Aerobic granular sludge: Recent advances. *Biotechnology Advances* **26**(5): 411-423.
- Adav, S. S., Lee, D. J. and Tay, J. H. (2008b) Extracellular polymeric substances and structural stability of aerobic granule. *Water Research* **42**(6-7): 1644-1650.
- Allison, D. G. and Sutherland, I. W. (1987) The role of exopolysaccharides in adhesion of fresh-water bacteria. *Journal of General Microbiology* **133**: 1319-1327.
- Anguige, K., King, J. R. and Ward, J. P. (2006) A multi-phase mathematical model of quorum sensing in a maturing *Pseudomonas aeruginosa* biofilm. *Mathematical Biosciences* **203**(2): 240-276.

- Annous, B. A., Fratafico, P. M. and Smith, J. L. (2009) Quorum sensing in biofilms: Why bacteria behave the way they do. *Journal of Food Science* **74**(1): R24-R37.
- APHA (2005) Standard Methods for the Examination of Water and Wastewater. American Public Health Association, Washington, D. C., USA.
- Arrojo, B., Mosquera-Corral, A., Garrido, J. M. and Mendez, R. (2004) Aerobic granulation with industrial wastewater in sequencing batch reactors. *Water Research* **38**(14-15): 3389-3399.
- Asahi, Y., Noiri, Y., Igarashi, J., Asai, H., Suga, H. and Ebisu, S. (2010) Effects of *N*-acyl homoserine lactone analogues on *Porphyromonas gingivalis* biofilm formation. *Journal of Periodontal Research* **45**(2): 255-261.
- Bassler, B. L., Wright, M. and Silverman, M. R. (1994) Multiple signalling systems controlling expression of luminescence in *Vibrio harveyi*: sequence and function of genes encoding a second sensory pathway. *Molecular Microbiology* **13**(2): 273-286.
- Bassler, B. L. (2002) Small talk: cell-to-cell communication in bacteria. *Cell* **109**(4): 421-424.
- Black, J. G. (1993) Microbiology: Principles and Applications. Prentice-Hall, Englewood Cliffs, NJ.
- Brown, V. M., Jordan, D. H. M. and Tiller, B. A. (1967) The effect of temperature on the acute toxicity of phenol to rainbow trout in hard water. *Water Research* **1**(8-9): 587-594.
- Burkhead, C. E. and McKinney, R. E. (1969) Energy concepts of aerobic microbial metabolism. *Journal of the Sanitary Engineering Division* **95**(2): 253-268.
- Calleja, G. B. (1984) Microbial Aggregation. CRC Press, Florida.
- Camilli, A. and Bassler, B. L. (2006) Bacterial small-molecule signaling pathways. *Science* **311**(5764): 1113-1116.

- Cammarota, M. C. and Sant'Anna Jr., G. L. (1998) Metabolic blocking of exopolysaccharides synthesis: effects on microbial adhesion and biofilm accumulation. *Biotechnology Letters* **20**(1): 1-4.
- Carucci, A., Milia, S., De Gioannis, G. and Piredda, M. (2008) Acetate-fed aerobic granular sludge for the degradation of chlorinated phenols. *Water Science and Technology* **58**(2): 309-315.
- Carucci, A., Milia, S., De Gioannis, G. and Piredda, M. (2009) Acetate-fed aerobic granular sludge for the degradation of 4-chlorophenol. *Journal of Hazardous Materials* **166**(1): 483-490.
- Cassidy, D. P. and Belia, E. (2005) Nitrogen and phosphorus removal from an abattoir wastewater in a SBR with aerobic granular sludge. *Water Research* **39**(19): 4817-4823.
- Chandler, J. R., Duerkop, B. A., Hinz, A., West, T. E., Herman, J. P., Churchill, M. E. A., Skerrett, S. J. and Greenberg, E. P. (2009) Mutational analysis of *Burkholderia thailandensis* quorum sensing and self-aggregation. *Journal of Bacteriology* **191**(19): 5901-5909.
- Chen, G. H. and Leung, D. H. W. (2000) Utilization of oxygen in a sanitary gravity sewer. *Water Research* **34**(15): 3813-3821.
- Chen, M. Y., Lee, D. J., Tay, J. H. and Show, K. Y. (2007a) Staining of extracellular polymeric substances and cells in bioaggregates. *Applied Microbiology and Biotechnology* **75**(2): 467-474.
- Chen, X., Schauder, S., Potier, N., Van Dorsselaer, A., Pelczer, I., Bassler, B. L. and Hughson, F. M. (2002) Structural identification of a bacterial quorum-sensing signal containing boron. *Nature* **415**(6871): 545-549.
- Chen, Y., Jiang, W., Liang, D. T. and Tay, J. H. (2007b) Structure and stability of aerobic granules cultivated under different shear force in sequencing batch reactors. *Applied Microbiology and Biotechnology* **76**(5): 1199-1208.

- Chen, Y., Jiang, W. J., Liang, D. T. and Tay, J. H. (2008) Biodegradation and kinetics of aerobic granules under high organic loading rates in sequencing batch reactor. *Applied Microbiology and Biotechnology* **79**(2): 301-308.
- Cook, G. M. and Russell, J. B. (1994) Energy-spilling reactions of *Streptococcus bovis* and resistance of its membrane to proton conductance. *Applied and Environmental Microbiology* **60**(6): 1942-1948.
- Daniels, R., Vanderleyden, J. and Michiels, J. (2004) Quorum sensing and swarming migration in bacteria. *FEMS Microbiology Reviews* **28**(3): 261-289.
- Davey, M. E. and O'Toole, G. A. (2000) Microbial biofilms: From ecology to molecular genetics. *Microbiology and Molecular Biology Reviews* **64**(4): 847-867.
- Davies, D. G., Parsek, M. R., Pearson, J. P., Iglewski, B. H., Costerton, J. W. and Greenberg, E. P. (1998) The involvement of cell-to-cell signals in the development of a bacterial biofilm. *Science* **280**(5361): 295-298.
- de Kreuk, M. K., Pronk, M. and van Loosdrecht, M. C. M. (2005) Formation of aerobic granules and conversion processes in an aerobic granular sludge reactor at moderate and low temperatures. *Water Research* **39**(18): 4476-4484.
- de Kreuk, M. K., Picioreanu, C., Hosseini, M., Xavier, J. B. and van Loosdrecht, M. C. M. (2007) Kinetic model of a granular sludge SBR: Influences on nutrient removal. *Biotechnology and Bioengineering* **97**(4): 801-815.
- Dong, Y. H., Wang, L. H. and Zhang, L. H. (2007) Quorum-quenching microbial infections: mechanisms and implications. *Philosophical Transactions of the Royal Society B: Biological Sciences* **362**(1483): 1201-1211.
- Donlan, R. M. (2002) Biofilms: Microbial life on surfaces. *Emerging Infectious Diseases* **8**(9): 881-890.

- Droste, R. L. (1997) Theory and practice of water and wastewater treatment. Wiley, New York.
- Dubois, M., Gilles, K. A., Hamilton, J. K., Rebers, P. A. and Smith, F. (1956) Colorimetric method for determination of sugars and related substances. *Analytical Chemistry* **28**(3): 350-356.
- Dufrene, Y. F., Vermeiren, H., Vanderleyden, J. and Rouxhet, P. G. (1996) Direct evidence for the involvement of extracellular proteins in the adhesion of *Azospirillum brasilense*. *Microbiology-UK* **142**: 855-865.
- Dulekgurgen, E., Ovez, S., Artan, N. and Orhon, D. (2003) Enhanced biological phosphate removal by granular sludge in a sequencing batch reactor. *Biotechnology Letters* **25**(9): 687-693.
- Dunne Jr, W. M. (2002) Bacterial adhesion: Seen any good biofilms lately? *Clinical Microbiology Reviews* **15**(2): 155-166.
- Ellwood, D. C., Keevil, C. W., Marsh, P. D., Brown, C. M. and Wardell, J. N. (1982) Surface-associated growth. *Philosophical Transactions of the Royal Society of London. Series B: Biological Sciences* **297**(1088): 517-532.
- Farooqi, I. H., Basheer, F. and Ahmad, T. (2008) Studies on biodegradation of phenols and m-cresols by upflow anaerobic sludge blanket and aerobic sequential batch reactor. *Global Nest Journal* **10**(1): 39-46.
- Flemming, H. C. and Wingender, J. (2010) The biofilm matrix. *Nature Reviews Microbiology* **8**(9): 623-633.
- Flemming, H. C. (2011) The perfect slime. *Colloids and Surfaces B: Biointerfaces* **86**(2): 251-259.
- Flint, S. H., Brooks, J. D. and Bremer, P. J. (1997) The influence of cell surface properties of thermophilic streptococci on attachment to stainless steel. *Journal of Applied Microbiology* **83**(4): 508-517.

- Frederick, M. R., Kuttler, C., Hense, B. A. and Eberl, H. J. (2011) A mathematical model of quorum sensing regulated EPS production in biofilm communities. *Theoretical Biology and Medical Modelling* **8**(1): 1-29.
- Fredheim, E. G. A., Klingenberg, C., Rohde, H., Frankenberger, S., Gaustad, P., Flægstad, T. and Sollid, J. E. (2009) Biofilm formation by *Staphylococcus haemolyticus*. *Journal of Clinical Microbiology* **47**(4): 1172-1180.
- Fuqua, C. and Greenberg, E. P. (2002) Listening in on bacteria: acyl-homoserine lactone signalling. *Nature Reviews Molecular Cell Biology* **3**(9): 685-695.
- Gai, L. H., Wang, S. G., Gong, W. X., Liu, X. W., Gao, B. Y. and Zhang, H. Y. (2008) Influence of pH and ionic strength on Cu(II) biosorption by aerobic granular sludge and biosorption mechanism. *Journal of Chemical Technology and Biotechnology* **83**(6): 806-813.
- Gao, D., Liu, L., Liang, H. and Wu, W. M. (2011a) Aerobic granular sludge: characterization, mechanism of granulation and application to wastewater treatment. *Critical Reviews in Biotechnology* **31**(2): 137-152.
- Gao, J. F., Zhang, Q. A., Wang, J. H., Wu, X. L., Wang, S. Y. and Peng, Y. Z. (2011b) Contributions of functional groups and extracellular polymeric substances on the biosorption of dyes by aerobic granules. *Bioresource Technology* **102**(2): 805-813.
- Gao, Y., Song, J. X., Hu, B. S., Zhang, L., Liu, Q. Q. and Liu, F. Q. (2009) The *luxS* gene is involved in AI-2 production, pathogenicity, and some phenotypes in *Erwinia amylovora*. *Current Microbiology* **58**(1): 1-10.
- García, M. A., Alonso, J. and Melgar, M. J. (2005) *Agaricus macrosporus* as a potential bioremediation agent for substrates contaminated with heavy metals. *Journal of Chemical Technology and Biotechnology* **80**(3): 325-330.
- Garnier, C., Gärner, T., Lartiges, B. S., Abdelouhab, S. and de Donato, P. (2005) Characterization of activated sludge exopolymers from various origins: A

- combined size-exclusion chromatography and infrared microscopy study. *Water Research* **39**(13): 3044-3054.
- Ghisalba, O. (1983) Microbial degradation of chemical waste, an alternative to physical methods of waste disposal. Chemical wastes and their biodegradation-an overview. *Experientia* **39**(11): 1247-1257.
- Göksungur, Y., Üren, S. and Güvenç, U. (2005) Biosorption of cadmium and lead ions by ethanol treated waste baker's yeast biomass. *Bioresource Technology* **96**(1): 103-109.
- Gupta, V. K., Ali, I., Suhas and Mohan, D. (2003) Equilibrium uptake and sorption dynamics for the removal of a basic dye (basic red) using low-cost adsorbents. *Journal of Colloid and Interface Science* **265**(2): 257-264.
- Hardie, K. R. and Heurlier, K. (2008) Establishing bacterial communities by 'word of mouth': LuxS and autoinducer 2 in biofilm development. *Nature Reviews Microbiology* **6**(8): 635-643.
- Ho, K. L., Chen, Y. Y., Lin, B. and Lee, D. J. (2010) Degrading high-strength phenol using aerobic granular sludge. *Applied Microbiology and Biotechnology* **85**(6): 2009-2015.
- Hong, Y. S. and Brown, D. G. (2009) Variation in bacterial ATP level and proton motive force due to adhesion to a solid surface. *Applied and Environmental Microbiology* **75**(8): 2346-2353.
- Hooshangi, S. and Bentley, W. E. (2008) From unicellular properties to multicellular behavior: bacteria quorum sensing circuitry and applications. *Current Opinion in Biotechnology* **19**(6): 550-555.
- Hu, J. Y., Fan, Y., Lin, Y. H., Zhang, H. B., Ong, S. L., Dong, N., Xu, J. L., Ng, W. J. and Zhang, L. H. (2003) Microbial diversity and prevalence of virulent pathogens in biofilms developed in a water reclamation system. *Research in Microbiology* **154**(9): 623-629.

- Ikonomidis, A., Tsakris, A., Kanellopoulou, M., Maniatis, A. N. and Pournaras, S. (2008) Effect of the proton motive force inhibitor carbonyl cyanide-*m*-chlorophenylhydrazone (CCCP) on *Pseudomonas aeruginosa* biofilm development. *Letters in Applied Microbiology* **47**(4): 298-302.
- Jain, A., Nishad, K. K. and Bhosle, N. B. (2007) Effects of DNP on the cell surface properties of marine bacteria and its implication for adhesion to surfaces. *Biofouling* **23**(3): 171-177.
- Jang, A., Yoon, Y. H., Kim, I. S., Kim, K. S. and Bishop, P. L. (2003) Characterization and evaluation of aerobic granules in sequencing batch reactor. *Journal of Biotechnology* **105**(1-2): 71-82.
- Jia, X. S., Furumai, H. and Fang, H. H. P. (1996) Yields of biomass and extracellular polymers in four anaerobic sludges. *Environmental Technology* **17**(3): 283-291.
- Jiang, B. and Liu, Y. (2010) Energy uncoupling inhibits aerobic granulation. *Applied Microbiology and Biotechnology* **85**(3): 589-595.
- Jiang, H. L., Tay, J. H. and Tay, S. T. L. (2002) Aggregation of immobilized activated sludge cells into aerobically grown microbial granules for the aerobic biodegradation of phenol. *Letters in Applied Microbiology* **35**(5): 439-445.
- Jiang, H. L., Tay, J. H., Liu, Y. and Tay, S. T. L. (2003) Ca²⁺ augmentation for enhancement of aerobically grown microbial granules in sludge blanket reactors. *Biotechnology Letters* **25**(2): 95-99.
- Jiang, H. L., Tay, J. H., Maszenan, A. M. and Tay, S. T. L. (2004) Bacterial diversity and function of aerobic granules engineered in a sequencing batch reactor for phenol degradation. *Applied and Environmental Microbiology* **70**(11): 6767-6775.

- Kang, S. Y., Lee, J. U. and Kim, K. W. (2007) Biosorption of Cr(III) and Cr(VI) onto the cell surface of *Pseudomonas aeruginosa*. *Biochemical Engineering Journal* **36**(1): 54-58.
- Kaplan, J. B., Ragunath, C., Velliyagounder, K., Fine, D. H. and Ramasubbu, N. (2004) Enzymatic detachment of *Staphylococcus epidermidis* biofilms. *Antimicrobial Agents and Chemotherapy* **48**(7): 2633-2636.
- Keller, L. and Surette, M. G. (2006) Communication in bacteria: an ecological and evolutionary perspective. *Nature Reviews Microbiology* **4**(4): 249-258.
- Keweloh, H., Heipieper, H. J. and Rehm, H. J. (1989) Protection of bacteria against toxicity of phenol by immobilization in calcium alginate. *Applied Microbiology and Biotechnology* **31**(4): 383-389.
- Khajanchi, B. K., Sha, J., Kozlova, E. V., Erova, T. E., Suarez, G., Sierra, J. C., Popov, V. L., Horneman, A. J. and Chopra, A. K. (2009) *N*-acylhomoserine lactones involved in quorum sensing control the type VI secretion system, biofilm formation, protease production, and in vivo virulence in a clinical isolate of *Aeromonas hydrophila*. *Microbiology* **155**(11): 3518-3531.
- Kim, I. S., Kim, S. M. and Jang, A. (2008) Characterization of aerobic granules by microbial density at different COD loading rates. *Bioresource Technology* **99**(1): 18-25.
- Klebensberger, J., Rui, O., Fritz, E., Schink, B. and Philipp, B. (2006) Cell aggregation of *Pseudomonas aeruginosa* strain PAO1 as an energy-dependent stress response during growth with sodium dodecyl sulfate. *Archives of Microbiology* **185**(6): 417-427.
- Kogure, K., Ikemoto, E. and Morisaki, H. (1998) Attachment of *Vibrio alginolyticus* to glass surfaces is dependent on swimming speed. *Journal of Bacteriology* **180**(4): 932-937.

- Kwok, W. K., Picioreanu, C., Ong, S. L., van Loosdrecht, M. C. M., Ng, W. J. and Heijnen, J. J. (1998) Influence of biomass production and detachment forces on biofilm structures in a biofilm airlift suspension reactor. *Biotechnology and Bioengineering* **58**(4): 400-407.
- Lehninger, A. L. (1975) Biochemistry. Worth Publishers, New York.
- Lemaire, R., Yuan, Z., Blackall, L. L. and Crocetti, G. R. (2008) Microbial distribution of *Accumulibacter* spp. and *Competibacter* spp. in aerobic granules from a lab-scale biological nutrient removal system. *Environmental Microbiology* **10**(2): 354-363.
- Lemon, K. P., Higgins, D. E. and Kolter, R. (2007) Flagellar motility is critical for *Listeria monocytogenes* biofilm formation. *Journal of Bacteriology* **189**(12): 4418-4424.
- Li, A. J., Yang, S. F., Li, X. Y. and Gu, J. D. (2008) Microbial population dynamics during aerobic sludge granulation at different organic loading rates. *Water Research* **42**(13): 3552-3560.
- Li, A. J. and Li, X. Y. (2009) Selective sludge discharge as the determining factor in SBR aerobic granulation: Numerical modelling and experimental verification. *Water Research* **43**(14): 3387-3396.
- Li, X. M., Liu, Q. Q., Yang, Q., Guo, L., Zeng, G. M., Hu, J. M. and Zheng, W. (2009) Enhanced aerobic sludge granulation in sequencing batch reactor by Mg^{2+} augmentation. *Bioresource Technology* **100**(1): 64-67.
- Liao, B. Q., Allen, D. G., Droppo, I. G., Leppard, G. G. and Liss, S. N. (2001) Surface properties of sludge and their role in bioflocculation and settleability. *Water Research* **35**(2): 339-350.
- Lin, Y. M., Liu, Y. and Tay, J. H. (2003) Development and characteristics of phosphorous-accumulating granules in sequencing batch reactor. *Applied Microbiology and Biotechnology* **62**(4): 430-435.

- Liu, J., Nguyen, D. and Paice, M. (2010) Aerobic granule formation in a sequencing batch reactor treating newsprint effluent under low phosphate conditions. *Water Science and Technology* **62**(11): 2571-2578.
- Liu, Q. S., Tay, J. H. and Liu, Y. (2003a) Substrate concentration-independent aerobic granulation in sequential aerobic sludge blanket reactor. *Environmental Technology* **24**(10): 1235-1242.
- Liu, X., Bimerew, M., Ma, Y., Müller, H., Ovadis, M., Eberl, L., Berg, G. and Chernin, L. (2007) Quorum-sensing signaling is required for production of the antibiotic pyrrolnitrin in a rhizospheric biocontrol strain of *Serratia plymuthica*. *FEMS Microbiology Letters* **270**(2): 299-305.
- Liu, Y. and Tay, J. H. (2001) Metabolic response of biofilm to shear stress in fixed-film culture. *Journal of Applied Microbiology* **90**(3): 337-342.
- Liu, Y. and Tay, J. H. (2002) The essential role of hydrodynamic shear force in the formation of biofilm and granular sludge. *Water Research* **36**(7): 1653-1665.
- Liu, Y. and Wang, Z. W. (2007) Selection pressure theory for aerobic granulation in sequencing batch reactor. In: Liu, Y. (Ed.), *Wastewater Purification: Aerobic Granulation in Sequencing Batch Reactors*. CRC Press, Florida. pp. 85-110.
- Liu, Y., Yang, S. F., Tan, S. F., Lin, Y. M. and Tay, J. H. (2002) Aerobic granules: a novel zinc biosorbent. *Letters in Applied Microbiology* **35**(6): 548-551.
- Liu, Y., Lin, Y. M., Yang, S. F. and Tay, J. H. (2003b) A balanced model for biofilms developed at different growth and detachment forces. *Process Biochemistry* **38**(12): 1761-1765.
- Liu, Y., Xu, H., Yang, S. F. and Tay, J. H. (2003c) A general model for biosorption of Cd^{2+} , Cu^{2+} and Zn^{2+} by aerobic granules. *Journal of Biotechnology* **102**(3): 233-239.

- Liu, Y., Yang, S. F., Liu, Q. S. and Tay, J. H. (2003d) The role of cell hydrophobicity in the formation of aerobic granules. *Current Microbiology* **46**(4): 270-274.
- Liu, Y., Yang, S. F., Xu, H., Woon, K. H., Lin, Y. M. and Tay, J. H. (2003e) Biosorption kinetics of cadmium(II) on aerobic granular sludge. *Process Biochemistry* **38**(7): 997-1001.
- Liu, Y. and Tay, J. H. (2004) State of the art of biogranulation technology for wastewater treatment. *Biotechnology Advances* **22**(7): 533-563.
- Liu, Y., Xu, H., Yang, S. F. and Tay, J. H. (2004a) A theoretical model for biosorption of cadmium, zinc and copper by aerobic granules based on initial conditions. *Journal of Chemical Technology and Biotechnology* **79**(9): 982-986.
- Liu, Y., Yang, S. F., Tay, J. H., Liu, Q. S., Qin, L. and Li, Y. (2004b) Cell hydrophobicity is a triggering force of biogranulation. *Enzyme and Microbial Technology* **34**(5): 371-379.
- Liu, Y., Liu, Y. Q., Wang, Z. W., Yang, S. F. and Tay, J. H. (2005a) Influence of substrate surface loading on the kinetic behaviour of aerobic granules. *Applied Microbiology and Biotechnology* **67**(4): 484-488.
- Liu, Y., Wang, Z. W., Liu, Y. Q., Qin, L. and Tay, J. H. (2005b) A generalized model for settling velocity of aerobic granular sludge. *Biotechnology Progress* **21**(2): 621-626.
- Liu, Y., Wang, Z. W., Qin, L., Liu, Y. Q. and Tay, J. H. (2005c) Selection pressure-driven aerobic granulation in a sequencing batch reactor. *Applied Microbiology and Biotechnology* **67**(1): 26-32.
- Liu, Y., Wang, Z. W. and Tay, J. H. (2005d) A unified theory for upscaling aerobic granular sludge sequencing batch reactors. *Biotechnology Advances* **23**(5): 335-344.

- Liu, Y., Wang, F., Xia, S. Q. and Zhao, J. F. (2008) Study of 4-*t*-octylphenol degradation and microbial community in granular sludge. *Journal of Environmental Sciences-China* **20**(2): 167-171.
- Liu, Y. Q., Liu, Y. and Tay, J. H. (2004c) The effects of extracellular polymeric substances on the formation and stability of biogranules. *Applied Microbiology and Biotechnology* **65**(2): 143-148.
- Lowry, O. H., Rosebrough, N. J., Farr, A. L. and Randall, R. J. (1951) Protein measurement with the folin phenol reagent. *Journal of Biological Chemistry* **193**(1): 265-275.
- Ma, D. Y., Wang, X. H., Song, C., Wang, S. G., Fan, M. H. and Li, X. M. (2011) Aerobic granulation for methylene blue biodegradation in a sequencing batch reactor. *Desalination* **276**(1-3): 233-238.
- Mahoney, E. M., Varangu, L. K., Cairns, W. L., Kosaric, N. and Murray, R. G. E. (1987) The effect of calcium on microbial aggregation during UASB reactor start-up. *Water Science and Technology* **19**(1-2): 249-260.
- Marino, P. A., Phan, K. A. and Osborn, M. J. (1985) Energy dependence of lipopolysaccharide translocation in *Salmonella typhimurium*. *Journal of Biological Chemistry* **260**(28): 4965-4970.
- Marketon, M. M., Glenn, S. A., Eberhard, A. and González, J. E. (2003) Quorum sensing controls exopolysaccharide production in *Sinorhizobium meliloti*. *Journal of Bacteriology* **185**(1): 325-331.
- Maszenan, A. M., Liu, Y. and Ng, W. J. (2011) Bioremediation of wastewaters with recalcitrant organic compounds and metals by aerobic granules. *Biotechnology Advances* **29**(1): 111-123.
- Mathews, C. K., van Holde, K. E. and Ahern, K. G. (1999) Biochemistry. Addison Wesley Longman, San Francisco.

- McNab, R., Ford, S. K., El-Sabaeny, A., Barbieri, B., Cook, G. S. and Lamont, R. J. (2003) LuxS-based signaling in *Streptococcus gordonii*: autoinducer 2 controls carbohydrate metabolism and biofilm formation with *Porphyromonas gingivalis*. *Journal of Bacteriology* **185**(1): 274-284.
- McSwain, B. S., Irvine, R. L. and Wilderer, P. A. (2004) The influence of settling time on the formation of aerobic granules. 3rd IWA Conference on Sequencing Batch Reactor Technology, Noosa, Australia.
- McSwain, B. S., Irvine, R. L., Hausner, M. and Wilderer, P. A. (2005) Composition and distribution of extracellular polymeric substances in aerobic flocs and granular sludge. *Applied and Environmental Microbiology* **71**(2): 1051-1057.
- McSwain, B. S. and Irvine, R. L. (2008) Dissolved oxygen as a key parameter to aerobic granule formation. *Water Science and Technology* **58**(4): 781-787.
- Mishima, K. and Nakamura, M. (1991) Self-immobilization of aerobic activated sludge-a pilot study of the aerobic upflow sludge blanket process in municipal sewage treatment. *Water Science and Technology* **23**(4-6): 981-990.
- Mitchell, P. (1961) Coupling of phosphorylation to electron and hydrogen transfer by a chemi-osmotic type of mechanism. *Nature* **191**: 144-148.
- Moy, B. Y. P., Tay, J. H., Toh, S. K., Liu, Y. and Tay, S. T. L. (2002) High organic loading influences the physical characteristics of aerobic sludge granules. *Letters in Applied Microbiology* **34**(6): 407-412.
- Nancharaiah, Y. V., Joshi, H. M., Mohan, T. V. K., Venugopalan, V. P. and Narasimhan, S. V. (2006) Aerobic granular biomass: A novel biomaterial for efficient uranium removal. *Current Science* **91**(4): 503-509.

- Nancharaiah, Y. V., Joshi, H. M., Mohan, T. V. K., Venugopalan, V. P. and Narasimban, S. V. (2008) Formation of aerobic granules in the presence of a synthetic chelating agent. *Environmental Pollution* **153**(1): 37-43.
- Ni, B. J., Yu, H. Q. and Sun, Y. J. (2008) Modeling simultaneous autotrophic and heterotrophic growth in aerobic granules. *Water Research* **42**(6-7): 1583-1594.
- O'Toole, G. A., Gibbs, K. A., Hager, P. W., Phibbs, P. V. and Kolter, R. (2000) The global carbon metabolism regulator Crc is a component of a signal transduction pathway required for biofilm development by *Pseudomonas aeruginosa*. *Journal of Bacteriology* **182**(2): 425-431.
- Pan, S., Tay, J. H., He, Y. X. and Tay, S. T. L. (2004) The effect of hydraulic retention time on the stability of aerobically grown microbial granules. *Letters in Applied Microbiology* **38**(2): 158-163.
- Pearson, J. P., Van Delden, C. and Iglewski, B. H. (1999) Active efflux and diffusion are involved in transport of *Pseudomonas aeruginosa* cell-to-cell signals. *Journal of Bacteriology* **181**(4): 1203-1210.
- Peng, D. C., Bernet, N., Delgenes, J. P. and Moletta, R. (1999) Aerobic granular sludge-A case report. *Water Research* **33**(3): 890-893.
- Petersen, F. C., Ahmed, N. A. A. M., Naemi, A. and Scheie, A. A. (2006) LuxS-mediated signalling in *Streptococcus anginosus* and its role in biofilm formation. *Antonie van Leeuwenhoek, International Journal of General and Molecular Microbiology* **90**(2): 109-121.
- Pumbwe, L., Skilbeck, C. A. and Wexler, H. M. (2008) Presence of quorum-sensing systems associated with multidrug resistance and biofilm formation in *Bacteroides fragilis*. *Microbial Ecology* **56**(3): 412-419.
- Qin, L., Liu, Y. and Tay, J. H. (2004a) Effect of settling time on aerobic granulation in sequencing batch reactor. *Biochemical Engineering Journal* **21**(1): 47-52.

- Qin, L., Tay, J. H. and Liu, Y. (2004b) Selection pressure is a driving force of aerobic granulation in sequencing batch reactors. *Process Biochemistry* **39**(5): 579-584.
- Quiñones, B., Dulla, G. and Lindow, S. E. (2005) Quorum sensing regulates exopolysaccharide production, motility, and virulence in *Pseudomonas syringae*. *Molecular Plant-Microbe Interactions* **18**(7): 682-693.
- Ramasamy, P. and Zhang, X. (2005) Effects of shear stress on the secretion of extracellular polymeric substances in biofilms. *Water Science and Technology* **52**(7): 217-223.
- Ren, T. T., Liu, L., Sheng, G. P., Liu, X. W., Yu, H. Q., Zhang, M. C. and Zhu, J. R. (2008) Calcium spatial distribution in aerobic granules and its effects on granule structure, strength and bioactivity. *Water Research* **42**(13): 3343-3352.
- Rickard, A. H., Palmer Jr, R. J., Blehert, D. S., Campagna, S. R., Semmelhack, M. F., Eglund, P. G., Bassler, B. L. and Kolenbrander, P. E. (2006) Autoinducer 2: a concentration-dependent signal for mutualistic bacterial biofilm growth. *Molecular Microbiology* **60**(6): 1446-1456.
- Riedel, K., Hentzer, M., Geisenberger, O., Huber, B., Steidle, A., Wu, H., Hoiby, N., Givskov, M., Molin, S. and Eberl, L. (2001) *N*-acylhomoserine-lactone-mediated communication between *Pseudomonas aeruginosa* and *Burkholderia cepacia* in mixed biofilms. *Microbiology-Sgm* **147**: 3249-3262.
- Robinson, J. A., Trulear, M. G. and Characklis, W. G. (1984) Cellular reproduction and extracellular polymer formation by *Pseudomonas aeruginosa* in continuous culture. *Biotechnology and Bioengineering* **26**(12): 1409-1417.
- Russell, J. B. and Cook, G. M. (1995) Energetics of bacterial growth: Balance of anabolic and catabolic reactions. *Microbiological Reviews* **59**(1): 48-62.

- Russell, J. B. (2007) The energy spilling reactions of bacteria and other organisms. *Journal of Molecular Microbiology and Biotechnology* **13**(1-3): 1-11.
- Saville, R. M., Rakshe, S., Haagenen, J. A. J., Shukla, S. and Spormann, A. M. (2011) Energy-dependent stability of *Shewanella oneidensis* MR-1 biofilms. *Journal of Bacteriology* **193**(13): 3257-3264.
- Schauder, S. and Bassler, B. L. (2001) The languages of bacteria. *Genes and Development* **15**(12): 1468-1480.
- Schwarzenbeck, N., Erley, R. and Wilderer, P. A. (2004) Aerobic granular sludge in an SBR-system treating wastewater rich in particulate matter. *Water Science and Technology* **49**(11-12): 41-46.
- Schwarzenbeck, N., Borges, J. M. and Wilderer, P. A. (2005) Treatment of dairy effluents in an aerobic granular sludge sequencing batch reactor. *Applied Microbiology and Biotechnology* **66**(6): 711-718.
- Shao, H. J., Lamont, R. J. and Demuth, D. R. (2007) Autoinducer 2 is required for biofilm growth of *Aggregatibacter* (*Actinobacillus*) *actinomycetemcomitans*. *Infection and Immunity* **75**(9): 4211-4218.
- Shapiro, J. A. (1998) Thinking about bacterial populations as multicellular organisms. *Annual Review of Microbiology* **52**: 81-104.
- Shaw, P. D., Ping, G., Daly, S. L., Cha, C., Cronan, J. E., Rinehart, K. L. and Farrand, S. K. (1997) Detecting and characterizing *N*-acyl-homoserine lactone signal molecules by thin-layer chromatography. *Proceedings of the National Academy of Sciences of the United States of America* **94**(12): 6036-6041.
- Sheng, P. X., Ting, Y. P., Chen, J. P. and Hong, L. (2004) Sorption of lead, copper, cadmium, zinc, and nickel by marine algal biomass: characterization of biosorptive capacity and investigation of mechanisms. *Journal of Colloid and Interface Science* **275**(1): 131-141.

- Shih, P. C. and Huang, C. T. (2002) Effects of quorum-sensing deficiency on *Pseudomonas aeruginosa* biofilm formation and antibiotic resistance. *Journal of Antimicrobial Chemotherapy* **49**(2): 309-314.
- Singh, M. P. and Greenstein, M. (2006) A simple, rapid, sensitive method detecting homoserine lactone (HSL)-related compounds in microbial extracts. *Journal of Microbiological Methods* **65**(1): 32-37.
- Song, Z., Ren, N., Zhang, K. and Tong, L. (2009) Influence of temperature on the characteristics of aerobic granulation in sequencing batch airlift reactors. *Journal of Environmental Sciences* **21**(3): 273-278.
- Srivastava, N. K. and Majumder, C. B. (2008) Novel biofiltration methods for the treatment of heavy metals from industrial wastewater. *Journal of Hazardous Materials* **151**(1): 1-8.
- Sun, X. F., Wang, S. G., Liu, X. W., Gong, W. X., Bao, N., Gao, B. Y. and Zhang, H. Y. (2008) Biosorption of Malachite Green from aqueous solutions onto aerobic granules: Kinetic and equilibrium studies. *Bioresource Technology* **99**(9): 3475-3483.
- Surette, M. G. and Bassler, B. L. (1998) Quorum sensing in *Escherichia coli* and *Salmonella typhimurium*. *Proceedings of the National Academy of Sciences of the United States of America* **95**(12): 7046-7050.
- Surette, M. G., Miller, M. B. and Bassler, B. L. (1999) Quorum sensing in *Escherichia coli*, *Salmonella typhimurium*, and *Vibrio harveyi*: A new family of genes responsible for autoinducer production. *Proceedings of the National Academy of Sciences of the United States of America* **96**(4): 1639-1644.
- Sutherland, I. W. (2001) Biofilm exopolysaccharides: A strong and sticky framework. *Microbiology* **147**(1): 3-9.

- Tay, J. H., Xu, H. L. and Teo, K. C. (2000) Molecular mechanism of granulation. I: H^+ translocation-dehydration theory. *Journal of Environmental Engineering* **126**(5): 403-410.
- Tay, J. H., Liu, Q. S. and Liu, Y. (2001a) The role of cellular polysaccharides in the formation and stability of aerobic granules. *Letters in Applied Microbiology* **33**(3): 222-226.
- Tay, J. H., Liu, Q. S. and Liu, Y. (2001b) The effects of shear force on the formation, structure and metabolism of aerobic granules. *Applied Microbiology and Biotechnology* **57**(1-2): 227-233.
- Tay, J. H., Liu, Q. S. and Liu, Y. (2001c) Microscopic observation of aerobic granulation in sequential aerobic sludge blanket reactor. *Journal of Applied Microbiology* **91**(1): 168-175.
- Tay, J. H., Liu, Q. S. and Liu, Y. (2002a) Characteristics of aerobic granules grown on glucose and acetate in sequential aerobic sludge blanket reactors. *Environmental Technology* **23**(8): 931-936.
- Tay, J. H., Pan, S., Tay, S. T. L., Ivanov, V. and Liu, Y. (2002b) The effect of organic loading rate on the aerobic granulation: the development of shear force theory. 3rd World Water Congress of the International-Water-Association, Melbourne, Australia.
- Tay, J. H., Yang, S. F. and Liu, Y. (2002c) Hydraulic selection pressure-induced nitrifying granulation in sequencing batch reactors. *Applied Microbiology and Biotechnology* **59**(2-3): 332-337.
- Tay, J. H., Pan, S., He, Y. and Tay, S. T. L. (2004a) Effect of organic loading rate on aerobic granulation. I: Reactor performance. *Journal of Environmental Engineering* **130**(10): 1094-1101.

- Tay, J. H., Pan, S., He, Y. X. and Tay, S. T. L. (2004b) Effect of organic loading rate on aerobic granulation. II: Characteristics of aerobic granules. *Journal of Environmental Engineering-Asce* **130**(10): 1102-1109.
- Tay, S. T. L., Moy, B. Y. P., Maszenan, A. M. and Tay, J. H. (2005a) Comparing activated sludge and aerobic granules as microbial inocula for phenol biodegradation. *Applied Microbiology and Biotechnology* **67**(5): 708-713.
- Tay, S. T. L., Zhuang, W. Q. and Tay, J. H. (2005b) Start-up, microbial community analysis and formation of aerobic granules in a *tert*-butyl alcohol degrading sequencing batch reactor. *Environmental Science & Technology* **39**(15): 5774-5780.
- Teo, K. C., Xu, H. L. and Tay, J. H. (2000) Molecular mechanism of granulation. II: Proton translocating activity. *Journal of Environmental Engineering* **126**(5): 411-418.
- Toh, S. K., Tay, J. H., Moy, B. Y. P., Ivanov, V. and Tay, S. T. L. (2003) Size-effect on the physical characteristics of the aerobic granule in a SBR. *Applied Microbiology and Biotechnology* **60**(6): 687-695.
- Tomlin, K. L., Malott, R. J., Ramage, G., Storey, D. G., Sokol, P. A. and Ceri, H. (2005) Quorum-sensing mutations affect attachment and stability of *Burkholderia cenocepacia* biofilms. *Applied and Environmental Microbiology* **71**(9): 5208-5218.
- Vanderborght, J. P. and Gilliard, C. (1981) BOD removal in fluidized beds: high biomass concentration or high oxygen transfer. In: Cooper, P. F. and Atkinson, B. (Ed.), *Biological Fluidized Bed Treatment of Water and Wastewater*. Ellis Horwood, Chichester. pp. 383-389.
- Vandevivere, P. and Kirchman, D. L. (1993) Attachment stimulates exopolysaccharide synthesis by a bacterium. *Applied and Environmental Microbiology* **59**(10): 3280-3286.

- Wang, S. G., Liu, X. W., Zhang, H. Y., Gong, W. X., Sun, X. F. and Gao, B. Y. (2007a) Aerobic granulation for 2,4-dichlorophenol biodegradation in a sequencing batch reactor. *Chemosphere* **69**(5): 769-775.
- Wang, S. G., Lu, X. W., Gong, W. X., Gao, B. Y., Zhang, D. H. and Yu, H. Q. (2007b) Aerobic granulation with brewery wastewater in a sequencing batch reactor. *Bioresource Technology* **98**(11): 2142-2147.
- Wang, Z. P., Liu, L. L., Yao, H. and Cai, W. M. (2006a) Effects of extracellular polymeric substances on aerobic granulation in sequencing batch reactors. *Chemosphere* **63**(10): 1728-1735.
- Wang, Z. W., Liu, Y. and Tay, J. H. (2006b) The role of SBR mixed liquor volume exchange ratio in aerobic granulation. *Chemosphere* **62**(5): 767-771.
- Watanabe, K., Teramoto, M. and Harayama, S. (1999) An outbreak of nonflocculating catabolic populations caused the breakdown of a phenol-digesting activated-sludge process. *Applied and Environmental Microbiology* **65**(7): 2813-2819.
- Whiteley, A. S. and Bailey, M. J. (2000) Bacterial community structure and physiological state within an industrial phenol bioremediation system. *Applied and Environmental Microbiology* **66**(6): 2400-2407.
- Wolfe, S. L. (1993) Molecular and Cellular Biology. Wadsworth Publications Co. Belmont, California, USA.
- Xavier, J. B., de Kreuk, M. K., Picioreanu, C. and van Loosdrecht, M. C. M. (2007) Multi-scale individual-based model of microbial and bioconversion dynamics in aerobic granular sludge. *Environmental Science & Technology* **41**(18): 6410-6417.
- Xu, H., Liu, Y. and Tay, J. H. (2006) Effect of pH on nickel biosorption by aerobic granular sludge. *Bioresource Technology* **97**(3): 359-363.

- Xu, H. and Liu, Y. (2008) Mechanisms of Cd^{2+} , Cu^{2+} and Ni^{2+} biosorption by aerobic granules. *Separation and Purification Technology* **58**(3): 400-411.
- Yang, S. F., Tay, J. H. and Liu, Y. (2003) A novel granular sludge sequencing batch reactor for removal of organic and nitrogen from wastewater. *Journal of Biotechnology* **106**(1): 77-86.
- Yang, S. F., Liu, Q. S., Tay, J. H. and Liu, Y. (2004a) Growth kinetics of aerobic granules developed in sequencing batch reactors. *Letters in Applied Microbiology* **38**(2): 106-112.
- Yang, S. F., Tay, J. H. and Liu, Y. (2004b) Respirometric activities of heterotrophic and nitrifying populations in aerobic granules developed at different substrate N/COD ratios. *Current Microbiology* **49**(1): 42-46.
- Yang, S. F., Tay, J. H. and Liu, Y. (2004c) Inhibition of free ammonia to the formation of aerobic granules. *Biochemical Engineering Journal* **17**(1): 41-48.
- Yang, S. F., Tay, J. H. and Liu, Y. (2005) Effect of substrate nitrogen/chemical oxygen demand ratio on the formation of aerobic granules. *Journal of Environmental Engineering-Asce* **131**(1): 86-92.
- Yeon, K. M., Cheong, W. S., Oh, H. S., Lee, W. N., Hwang, B. K., Lee, C. H., Beyenal, H. and Lewandowski, Z. (2008) Quorum sensing: a new biofouling control paradigm in a membrane bioreactor for advanced wastewater treatment. *Environmental Science & Technology* **43**(2): 380-385.
- Yi, S., Zhuang, W. Q., Wu, B., Tay, S. T. L. and Tay, J. H. (2006) Biodegradation of *p*-nitrophenol by aerobic granules in a sequencing batch reactor. *Environmental Science and Technology* **40**(7): 2396-2401.
- Yoshida, A., Ansai, T., Takehara, T. and Kuramitsu, H. K. (2005) LuxS-based signaling affects *Streptococcus mutans* biofilm formation. *Applied and Environmental Microbiology* **71**(5): 2372-2380.

- Zeng, P., Zhuang, W. Q., Tay, S. T. L. and Tay, J. H. (2007) The influence of storage on the morphology and physiology of phthalic acid-degrading aerobic granules. *Chemosphere* **69**(11): 1751-1757.
- Zeng, P., Moy, B. Y. P., Song, Y. H. and Tay, J. H. (2008) Biodegradation of dimethyl phthalate by *Sphingomonas* sp. isolated from phthalic-acid-degrading aerobic granules. *Applied Microbiology and Biotechnology* **80**(5): 899-905.
- Zhang, H. B., Wang, L. H. and Zhang, L. H. (2002) Genetic control of quorum-sensing signal turnover in *Agrobacterium tumefaciens*. *Proceedings of the National Academy of Sciences of the United States of America* **99**(7): 4638-4643.
- Zhang, L. L., Feng, X. X., Xu, F., Xu, S. and Cai, W. M. (2005a) Biosorption of rare earth metal ion on aerobic granules. *Journal of Environmental Science and Health - Part A Toxic/Hazardous Substances and Environmental Engineering* **40**(4): 857-867.
- Zhang, L. L., Zhang, B., Huang, Y. F. and Cai, W. M. (2005b) Application of aerobic granular sludge in polishing the UASB effluent. *Environmental Technology* **26**(12): 1327-1334.
- Zhang, L. L., Feng, X. X., Zhu, N. W. and Chen, J. M. (2007) Role of extracellular protein in the formation and stability of aerobic granules. *Enzyme and Microbial Technology* **41**(5): 551-557.
- Zhang, L. L., Chen, J. M. and Fang, F. (2008a) Biodegradation of methyl *t*-butyl ether by aerobic granules under a cosubstrate condition. *Applied Microbiology and Biotechnology* **78**(3): 543-550.
- Zhang, L. L., Zhu, R. Y., Chen, J. M. and Cai, W. M. (2008b) Biodegradation of methyl *tert*-butyl ether as a sole carbon source by aerobic granules

- cultivated in a sequencing batch reactor. *Bioprocess and Biosystems Engineering* **31**(6): 527-534.
- Zheng, Y. M., Yu, H. Q. and Sheng, G. P. (2005) Physical and chemical characteristics of granular activated sludge from a sequencing batch airlift reactor. *Process Biochemistry* **40**(2): 645-650.
- Zhu, L., Xu, X., Luo, W., Cao, D. and Yang, Y. (2008) Formation and microbial community analysis of chloroanilines-degrading aerobic granules in the sequencing airlift bioreactor. *Journal of Applied Microbiology* **104**(1): 152-160.
- Zhuang, W. Q., Tay, J. H., Yi, S. and Tay, S. T. L. (2005) Microbial adaptation to biodegradation of *tert*-butyl alcohol in a sequencing batch reactor. *Journal of Biotechnology* **118**(1): 45-53.
- Zitomer, D. H., Duran, M., Albert, R. and Guven, E. (2007) Thermophilic aerobic granular biomass for enhanced settleability. *Water Research* **41**(4): 819-825.